SIMPLIFIED MULTIUSER DETECTION FOR CDMA SYSTEMS

A DISSERTATION

SUBMITTED TO THE DEPARTMENT OF ELECTRICAL ENGINEERING

AND THE COMMITTEE ON GRADUATE STUDIES

OF STANFORD UNIVERSITY

IN PARTIAL FULFILLMENT OF THE REQUIREMENTS

FOR THE DEGREE OF

DOCTOR OF PHILOSOPHY

Zartash Afzal Uzmi

September 2002

I certify that I have read this dissertation and that in my opinion it is fully adequate, in scope and quality, as a dissertation for the degree of Doctor of Philosophy.

G. L. Tyler
(Principal Adviser)

I certify that I have read this dissertation and that in my opinion it is fully adequate, in scope and quality, as a dissertation for the degree of Doctor of Philosophy.

M. J. Narasimha

I certify that I have read this dissertation and that in my opinion it is fully adequate, in scope and quality, as a dissertation for the degree of Doctor of Philosophy.

M. G. Baker

Approved for the University Committee on Graduate Studies:

Abstract

The capacity of Direct Sequence Code Division Multiple Access (DS-CDMA) systems is limited by multiple access interference (MAI) instead of thermal noise. Commercial CDMA systems, such as the ones based on the IS-95 standard, regard MAI as additive noise and employ matched filter detectors. This technique limits the number of users that can be supported in a DS-CDMA system to less than 10% of the spreading gain. Moreover, the bit error rates for individual users degrade rapidly with an increase in the number of users.

A new sub-symbol based multiuser detection technique addresses the two major concerns in DS-CDMA systems: high bit error rates and low system capacity. The two filters in traditional multiuser detectors—a code-matched and a multiuser linear filter—are designed independently, resulting in an increase in system complexity due to asynchronous operation. Multiuser detection based on sub-symbols is a joint optimization of the code-matched filter and the linear multiuser detection filter. This design approach drastically reduces the implementation complexity while asymptotically approaching the ideal performance exhibited by the zero-forcing multiuser detector.

In the sub-symbol scheme, data symbols of users are partitioned into sub-symbols such that the resulting sub-symbols from different users are time-aligned at the receiver. Simplified optimal linear filters operate in each sub-symbol interval, and the filtered outputs are processed using various diversity combining algorithms. Simulation results indicate that a condition number based combining algorithm approaches

the ideal bit error rate performance. Other combining schemes, such as simple accumulation, select-best, and maximal ratio, demonstrate immunity to the near-far effect but do not perform as well overall.

Although the sub-symbol scheme in conjunction with the diversity combining algorithms yields lower bit error rates, it does not guarantee a significant increase in the number of simultaneous users. Assuming that the system can be made to operate in a quasi-synchronous mode, two specific thresholds, the chip threshold and the condition number threshold, are introduced to improve the system capacity. Increasing the condition number threshold allows the use of more sub-symbols in the combining algorithms, and hence an increase in the number of simultaneous users for a fixed bit error rate. By dynamically adjusting the chip threshold, the system capacity can be increased to the number of chips in the longest sub-symbol.

While multiuser detectors perform well in the reduction of MAI that arises from the local cell, they fail to suppress the MAI contributed from other cells. Suppression of other cell MAI is accomplished using multiple antenna systems. These systems, however, are not robust against near-far effect. But the use of multiple antennas in conjunction with linear multiuser detectors conveys both near-far resistance and immunity to inter-cell MAI. Simulations of the resulting system indicates an improved overall performance.

To my parents

Afzal Ahmad and Nasreen Afzal

and to my wife and children

Arshia, Ali Shan, and Alizay

Acknowledgments

I would like to thank Allah Almighty who gave me the ability and bestowed me with perseverance to write this thesis. He is the one I always looked to in the face of trouble and He always created a way for me out of the trouble. I would not be what I am today if He did not want me to be.

My sincere thanks to my advisors, Professor Len Tyler and Professor Madihally Narasimha. I recall the days of kindergarten when my teachers taught me how to write. It is Len and Sim, however, who taught me how to write well and how to write for others. While Sim guided me throughout my graduate studies in learning how to solve technical problems, Len taught me how to tell others what problems have been solved. Every time I got the draft of this thesis revised, I felt significant improvement in my thought process and in my writing skills. I am thankful to both of them for their patience during the writing process. I admit that there were stylistic errors that occurred repeatedly but they always took time to point those out. I promise Len not to attenuate or decorrelate any more users!

I would like to thank Professor Mary Baker who agreed to not only serve as the Chair of my oral defense examination committee but also be a reader of this thesis. I am thankful to Professor Donald Cox from whom I learned the ABCs of wireless communications. He was kind enough to let me attend his group meetings and also served on my oral defense committee.

My longtime neighbor, Robert Scafe, proofread the draft of this thesis and provided comments and feedback that were extremely useful to me. I would like to thank Robert for his efforts and help. My interest in the problem addressed in this thesis

was sparked when I was at Bell Laboratories in 1998 as a student intern. I would like to thank my friend Syed Aon Mujtaba who arranged that internship and spent long nights of technical discussion in the Murray Hill facility of Bell Laboratories.

During my stay at Stanford as a graduate student, I had the opportunity to get advice and answers to my questions from a number of people. Professor Tobagi has always been very kind and responsive to my requests whether it's a question on LAN bridges or writing a reference letter for a job. Professor John Cioffi has also been extremely helpful throughout my graduate studies. He provided useful advice at a time when I had not taken my qualifying examinations and did not know how to start researching technical problems.

I had the opportunity to make a number of friends from various labs within the department. I changed offices twice and enjoyed the company of all my past and current officemates. Shahriyar and Dana always cheered me up whether we are discussing a puzzle, jogging along the campus drive loop, or playing the "SET" game.

Outside the department, I enjoyed the company of numerous friends during my graduate studies at Stanford. First name to be mentioned is Syed Akbar Ali who, on May 05, 2001, left us in deep pain and sorrow after being hit by a drunk driver. He will never be forgotten. I would like to thank the following people, whom I met at Stanford, for their sincere friendship: Asad, Atif, Bilal, Faraz, Jawad, Khurram, Mike, Mustafa, Nabeel, Naeem, Nauman, Shabnam, Shehzaad, Travis, and others. I have been blessed by so many good friends that these pages are too short to name them all.

I also made friends outside Stanford and during the period when I was working. All of these friends have been extremely kind to me and simply saying thanks wouldn't do justice to their sincerity. These include Aurangzeb, Hashim, Hamid, Kamran, Mudassir, and Noman.

A number of people have impacted my studies and career and my life in general. Rehan and Atif, who are my oldest friends, always provided me support when it was needed. My parents and siblings have been extremely supportive of me throughout

my life. It is the desire to see them happy that keeps me motivated. I want to thank them and my wife and kids. These are the people who make a difference in my life.

Zartash A. Uzmi

Stanford, California
June 28, 2002

This work was supported by the Ministry of Science and Technology, Government of Pakistan, and by the Electrical Engineering Department at Stanford University, Stanford, CA.

Contents

List of Acronyms and Abbreviations

AMPS Advanced Mobile Phone System

AOA Angle of Arrival

AWGN Additive White Gaussian Noise

AWN Additive White Noise

BER Bit Error Rate

BF Beamforming

BPSK Binary Phase Shift Keying

CCI Co-channel Interference

CDM Code Division Multiplexing

CDMA Code Division Multiple Access

DAMA Demand Assigned Multiaccess

DAMPS Digital AMPS

DS Direct Sequence

DS-CDMA Direct Sequence Code Division Multiple Access

DSSS Direct Sequence Spread Spectrum

EDGE Enhanced Data Rates for Global Evolution

ETSI European Telecommunications Standards Institute

FCFS First-come First-serve

FDM Frequency Division Multiplexing

FDMA Frequency Division Multiple Access

FH Frequency Hopping

FM Frequency Modulation

GPRS Generalized Packet Radio Service

GSM Global System for Mobile

IBI Isolation Bit Insertion

ISI Inter-Symbol Interference

LAN Local Area Network

LFSR Linear Feedback Shift Register

MAC Media Access Control

MAI Multiple Access Interference

MIMO Multiple Input Multiple Output

ML Maximum Likelihood

MLSE Maximum Likelihood Sequence Estimation

MMSE Minimum Mean Squared Error

MRC Maximal Ratio Combining

MTSO Mobile Telephone Switching Office

MUD Multiuser Detector

NAMPS Narrowband Analog Mobile Phone Service

PM Phase Modulation

PN Pseudo Noise

PSK Phase Shift Keying

PSTN Public Switched Telephone Network

QAM Quadrature Amplitude Modulation

QPSK Quadrature Phase Shift Keying

QS-CDMA Quasi-synchronous CDMA

SINR Signal-to-Interference-Plus-Noise Ratio

SNR Signal-to-Noise Ratio

SQM Signal Quality Measurement

SS Spread Spectrum

ST Space-Time

SUMF Single User Matched Filter

TDM Time Division Multiplexing

TDMA Time Division Multiple Access

VD Viterbi Decoder

WCDMA Wideband Code Division Multiple Access

ZF Zero Forcing

List of Tables

List of Figures

Chapter 1

Introduction

The use of radio waves to transmit information from one point to another was discovered over a century ago. While commercial and military radio communication systems have been deployed for many decades, the last decade has seen an unprecedented surge in demand for personal wireless devices. Extensive penetration of the end user market is a direct result of advances in circuit design and chip manufacturing technologies that have enabled a complete wireless transmitter and receiver to be packaged in a pocket-sized device. With the recent advent of low power circuit design and miniaturization technologies, more versatile wireless devices that run data hungry applications such as browsing the Internet are appearing on the market.

The popularity of handheld personal wireless devices has created a need for wireless communication systems that can accommodate many users simultaneously. It is also required that such systems provide high data rates and on-demand data transfers. An efficient multiaccess scheme can satisfy both of these requirements.

Transmitting information through a wireless channel is more challenging than through a wireline channel. This is principally because the wireless environment has problems not encountered in wireline systems including multipath propagation and near-far interference.

This chapter introduces some fundamental concepts of wireless communications and multiaccess techniques related to issues above. An understanding of these concepts is necessary for the development of the rest of the chapters.

1.1 Cellular Systems

If the frequency spectrum available to run a mobile system were infinite and regulatory authorities set no limit on the power transmitted within that frequency band, the simplest wireless system would have a centralized base station serving a large geographical area with all the users in the area communicating directly with the base station. Such a system would not be practical or efficient for various reasons. First, the users far away from the base station would have to transmit at higher power signals, which would decrease the battery life of their devices. Second, there would be a single point of failure, since there is only one base station.

The total bandwidth utilized in an area increases with the number of users communicating in that area. If a single base station were to cover the entire geographical area and serve all the users, the total bandwidth required would be enormous. Since the regulatory authorities allocate frequency bands for different communication applications in any given area, the number of users that can be supported without exceeding the frequency limitations is limited. Furthermore, a single base station covering the entire area would require transmission at higher power levels to communicate with distant users. Transmission at higher power levels may also not be permitted by the regulatory authorities in order to avoid interference with other applications. Thus, in practical systems, power and bandwidth constraints limit the service areas to the vicinity of base stations.

1.1.1 Cellular Concept

Cellular communication involves dividing a large geographical area into smaller sized areas called cells. The basic concept for such a system was developed in 1970's as a result of extensive research in wireless communications [1–7]. Instead of using one high-power transmitter for the entire area to be covered, many low power base stations are placed within cells at approximately their centers [8]. Using this cellular concept, the allocated frequency band can be reused by cells that are separated sufficiently.

The "cellularization" of a geographical region is flexible in nature in that the size of the cell can be determined according to the population density or subscriber density, and can be changed at a later stage when additional customers subscribe to the system. The size of the cell is controlled primarily by the following factors:

- Power transmitted by the base station belonging to the cell.
- Terrain within the region of the cell.
- Presence of man-made features such as buildings and other structures.
- Siting and sizing of adjacent cells.

These factors also determine the shape of the cell, which is rarely regular [9]. Choosing a cell size and shape involves determining two necessary parameters: the location available for siting the base station relative to terrain and man-made features, and the maximum power practically available to be transmitted by the base station.

In the cellular systems, a user belonging to a particular cell communicates with the base station of that cell while all other base stations neglect the signal received from this user. When the user moves from one cell to another, the communication link to the new cell base station becomes more reliable[1] than the communication link to the old cell base station. The new base station then becomes responsible for all the communications to and from the user. The process in which a user moves from one cell to the other and establishes a communication link with the base station in the new cell is called *handoff* [11]. When a handoff occurs, the new base station starts and the old base station ceases to interpret the signal from the user. Handoffs create challenges that are unique to cellular wireless systems.

In a cellular system, users typically communicate with the base stations by means of handsets. The base stations not only provide a communication link to and from the handset, they also provide connectivity to the public switched telephone network

[1]Reliability of radio signals in a cellular environment is generally determined by means of SQM techniques. See [10] for details.

(PSTN) or a gateway for voice and data access. Each base station is connected to a mobile telephone switching office (MTSO) which provides connectivity between the wired and wireless networks. Depending upon the cellular system, the MTSOs can provide a variety of supporting functions, ranging from simple interfacing to complex protocol translation (see [12] and the references therein).

1.1.2 Frequency Reuse

Use of the same frequencies for communications within different cells is called frequency reuse. Mutual interference usually prohibits frequency reuse in cells that are close to each other. A *cluster* is defined as a group of cells in which frequencies are not reused. For example, the number of cells in an FDMA cluster vary, with 3 and 7 as the typical values. Clusters with fewer cells generally require fewer handoffs [13, 14]. Each cell within a cluster is assigned a group of frequencies which can be reused in cells in other clusters. There are systems, for example CDMA systems, that allow single cell clusters. In single cell cluster systems, same frequency band is reused in every cell. Frequency reuse is one of the major benefits of cellular systems as it significantly increases the capacity of the system while using only a limited number of frequencies [3, 13].

All modern wireless cellular communication systems are interference limited and are designed to take maximum benefit of frequency reuse. If these systems are noise-limited, where noise refers to the the thermal noise, then generally the cells are probably too far apart and frequency reuse is not being exploited efficiently. When the cells are too far apart, the interference from users of other cells is smaller compared to the additive noise, and the capacity of a cell is determined by the additive noise. For this reason, noise-limited systems have a lower capacity than do interference-limited systems.

1.2 Multiaccess Systems

Communication systems can be classified as either point-to-point, where two entities communicate over an isolated link, or multipoint-to-multipoint, where more than two entities can simultaneously communicate with each other through a communication channel.[2] When a multitude of users wish to communicate, it is more economical to share link resources than it is to have an isolated link for each pair of users [15]. For example, in local area networks (LANs) and cellular systems, users share the communication channel. All practical multipoint-to-multipoint networks employ link sharing. When the communication channel is shared, users can communicate with each other either directly, as in a multiuser system, or indirectly through a single entity, as in a multiaccess system.[3]

In a multiuser system, direct communication between two stations does not require that each pair of users has a separate channel. Instead, some kind of sharing protocol is used that allows pairs of users to share the communication medium. Similarly, multiaccess systems provide channel sharing by means of some multiaccess protocol. Both of these paradigms are used in present day communication systems [16–19]; the choice of one over the other is dictated by the application environment. For example, a LAN environment, in which stations have high processing power and are generally connected through physical lines, reflects a multiuser system in which each user has the responsibility of filtering out the undesired data. On the other hand, cellular systems are designed to be multiaccess because the handsets are mobile with limited processing capabilities so the computation burden is vested in a single element, the base station. Both multiuser and multiaccess systems pose two basic problems: identification of the intended receiver, and sharing of the communication channel. The former is solved by means of addressing and the latter by means of media access control (MAC) protocols.

All cellular networks use a central base station, as discussed in Sec. 1.1. A link

[2]The terms "link" and "channel" are used interchangeably.

[3]In the literature, multiaccess systems are also referred to as multiple access systems.

between two users in the same cell can be considered as a concatenation of two separate links, one each from both users to the base station. A link from the base station to the handset is called a downlink or forward link while a link from the handset to the base station is referred to as an uplink or reverse link. Downlink poses the handset identification problem that is solved by addressing. Uplink, on the other hand, poses the channel sharing problem that is solved by MAC protocols.

In cellular systems, the downlink is a broadcast channel in which the addressing is provided by assigning a unique frequency, a unique time slot, or a unique code to each intended receiver. A transmitter at the base station addresses a multitude of receivers over a broadcast channel by using a technique called multiplexing. Use of a unique frequency assignment to each receiver is referred to as frequency division multiplexing (FDM), use of unique time slot for each receiver is referred to as time division multiplexing (TDM), and use of unique code assignment to each receiver is referred to as code division multiplexing (CDM).

The uplink in cellular systems is a multiple access channel in which several transmitters address a single base station. The transmitters use a media access control (MAC) protocol or a multiaccess protocol to address a single base station. In a single cell environment, however, there is only one base station and there is no need of addressing. Commercial systems employ a number of cells serving a large geographical area so that addressing in the uplink is generally required. As with the downlink, uplink also assigns unique frequencies (FDMA), time slots (TDMA), or codes (CDMA) to individual transmitters. Sharing of the uplink channel can be provided by one or more of the following multiaccess protocols [20, 21]:

i) Static Multiaccess

ii) Demand Assigned Multiaccess

iii) Random Multiaccess

The choice of a multiaccess protocol depends upon the traffic characteristics of the network. Demand assigned multiaccess and random multiaccess are usually grouped

under *dynamic multiaccess*. Dynamic multiaccess methods are differentiated from the static multiaccess methods by virtue of their ability to allocate channels and channel resources to individual users "on demand."

A description of the multiaccess methods commonly used in practice is given below.

1.2.1 Static Multiaccess

In static multiaccess, a channel's capacity is divided into fixed portions, one or more of which is allocated to a specific user depending on traffic demand. The fixed or static portions can be realized on the basis basis of time, frequency, or code separations. The channels allocated to individual users are, by design, orthogonal or nearly orthogonal to each other. If a user has no traffic to use in the allocated portion, then that portion just goes unused, thereby decreasing the overall efficiency of the system. There is no concept of shared resources at any given time. Generally, a static allocation of channels performs better when the traffic is predictable and the set of active terminals in the network does not vary with time [20]. The main examples of static multiaccess—FDMA and TDMA—are described below.

1.2.1.1 FDMA

In a simple FDMA system, channels comprise different frequency bands; each user is allocated one frequency band for transmission in the uplink. The Advanced Mobile Phone System (AMPS) was the first standardized cellular system and belongs to this class; it uses the 800 MHz to 900 MHz band and allocates 30 kHz for each channel [2,4]. The modulation scheme used by AMPS is analog frequency modulation (FM).

An AMPS-based system design is simpler than that of other cellular systems and can be based on analog modulation for its continuous transmission properties. The AMPS system has several drawbacks, though. An AMPS handset may need to change transmission frequency during the handoff (as the user moves from one cell to the other). Furthermore, static channel sharing of AMPS leaves the idle channels

unused while making it difficult to allocate multiple channels per user. The most serious disadvantage of the AMPS system, however, is the limitation that it places on system capacity [8]. Narrowband analog mobile phone service (NAMPS) was proposed as an interim solution to address the capacity limitations of AMPS. In NAMPS, each 30 kHz channel that previously carried a single voice conversation in AMPS, is utilized to carry three conversations by dividing the 30 kHz channel into three 10 kHz channels. Although capacity is increased, the channels in NAMPS remain statically shared and the idle channels remain unused.

1.2.1.2 TDMA

Time Division Multiple Access (TDMA) systems provide multiple access by sharing the same transmission resource at different times. Thus, end users take turns and transmit in sequence one after the other. The non-continuous nature of transmissions makes it easier to implement handoff in a TDMA system as compared to an FDMA system. Because the channels are typically wideband, inter-symbol interference (ISI) occurs. Required compensation for ISI generally is achieved by means of an equalizer [22].

In FDMA, the difficulty of allocating multiple frequency bands to a single user poses a limitation on bandwidth. Because it is easier to combine time slots than it is to combine frequency bands, TDMA systems are superior to FDMA systems in achieving high bandwidth links. In fact, the recent evolution of the Global System for Mobile (GSM) [23] for general packet radio service (GPRS) [24, 25] and enhanced data rates for global evolution (EDGE) [26] capabilities makes use of this particular feature. If, for these reasons, time division multiple access is superior to FDMA, it also has its own disadvantages: TDMA systems have more stringent synchronization requirements and are less robust to multipath effects. Once again, channel sharing is static in nature while unused time slots are wasted unless dynamic access is introduced.

To enjoy benefits of TDMA without putting the AMPS infrastructure out of service, digital AMPS (DAMPS) was proposed in the United States as a TDMA

"overlay" on the AMPS network [17]. DAMPS is one of the first digital cellular standards and uses the same channel bandwidth as AMPS but it time multiplexes multiple channels on each available frequency band.[4] Other possible combinations of FDMA and TDMA are similar to NAMPS with TDMA overlays [27]. GSM [23, 28] standard, which is quite popular in Europe, uses a hybrid TDMA and FDMA system. These systems use different techniques to increase the system capacity, but all FDMA and TDMA systems and their hybrids rely on static sharing of the channel in one way or the other.

1.2.2 Demand Assigned Multiaccess (DAMA)

When the traffic sent by users is bursty, i.e., transmission occur at a rate which varies significantly, then, under a static allocation, a user's portion of the channel may be idle when another user could use it. In such instances, a dynamic allocation strategy is desirable. Furthermore, when the set of active users changes with time, some method is needed to dynamically reallocate the channels to the various users as they come and go [20]. Ideally, a first-come first-serve (FCFS) strategy with some "policing" would be most efficient [29]. In practice, however, it is not possible to implement FCFS in a multiaccess channel since the uplink data are buffered at the transmitters and not at the base station.

When users originate bursty traffic and the set of active users changes with time, it is desirable to assign channel capacity to users "on demand" by using a DAMA architecture. In a DAMA system, a separate channel, called the *request channel*, is used to allocate a portion of the channel to active users. At the same time, actual data from users are communicated over a *data channel*. The data channel in DAMA systems is divided into as many portions as the number of active users in the system, while the request channel is shared by all users, active or inactive. Thus, using DAMA systems, the multiaccess problem is shifted from data channel to request channel.

There are two versions of DAMA systems: DAMA with a static request channel,

[4]DAMPS uses digital phase modulation (PM) in contrast to analog FM used in AMPS.

and DAMA with a random access request channel. In the former case, the data channel is statically divided among active users and the request channel is statically divided among all the users. User handsets initiate a 'request' for allocation of data channel which is sent over the request channel. This means that some control overhead is required for DAMA with the static request channel. In a DAMA system with a random access request channel, the data channel remains statically shared by active users, while the request channel uses random multiaccess to allocate portions of data channel to the active users.

1.2.3 Random Multiaccess

Random multiaccess methods allow users to transmit whenever they want without considering orthogonality with other users. The need for random multiaccess arises in various scenarios, two of which are as follows:

i) In a DAMA system, if the number of potential users is much larger than the number of active users, it is impractical to use static sharing in the request channel because static sharing requires allocation of a portion of the channel to each user, active or inactive. In such a case, it becomes necessary to allow random access in the request channel. The data channel in DAMA systems always uses static sharing.

ii) When data from individual users are so bursty that the control overhead of the DAMA protocol is unacceptable [20], the practical alternative is to use random access for user transmissions in the data channel rather than using a request channel.

Users transmit simultaneously and at the same frequency in random multiaccess. This results in collisions and possible retransmissions that limit the efficiency of the overall system [29,30]. Various random access protocols have been devised and extensively studied to improve system efficiency while allowing random (or semi-random) access [31]. From a wireless communication perspective, code division multiple access

(CDMA) systems can provide inherent random access capability more readily than DAMA systems.

1.2.4 Code Division Multiple Access (CDMA)

A CDMA system is a multiuser spread spectrum system that eliminates the frequency reuse problem in cellular systems. The following outline of multiaccess mechanism in CDMA systems will be expanded to a more detailed description in the subsequent chapters.

Unlike TDMA and FDMA systems, where user signals never overlap in either the time or the frequency domains, respectively, a CDMA system allows transmissions at the same time while using the same frequency. For example, in the first widespread commercial CDMA system, deployed by Sprint in the USA, based on the IS-95 standard [18], users transmit simultaneously using a 1.25 MHz frequency band. The mechanism separating the users in a CDMA system consists of assigning a unique code that modulates the signal from each user; the number of unique codes in a CDMA link is equal to the number of active users. The code modulating the user's signal is also called a spreading code, spreading sequence, or chip sequence. A CDMA system can have:

- Orthogonal codes which may make the system appear as an FDMA or a TDMA system. The users are non-interfering in this case and a hard capacity limit can be obtained for the system.

- Semi-orthogonal codes which result in interfering users, but pose no hard limit on the capacity. In this case, the number of semi-orthogonal codes for a given spreading depends upon the degree of orthogonality and is generally larger than the number of orthogonal codes [32, 33].

A CDMA system with orthogonal codes is an example of static channel sharing. That is, the user signals are completely separated by orthogonal codes as they are separated in frequency and time in FDMA and TDMA systems, respectively. When

semi-orthogonal codes are used in a CDMA system, interference occurs among active users just as collision occurs in a random multiaccess channel. Thus a CDMA system has some characteristics of a random multiaccess channel.

While random multiaccess channels generally require retransmission in case of collisions, CDMA systems allow detection of individual users even in the presence of multiaccess interference without necessitating retransmission. Consequently, a larger number of users can be accommodated in a CDMA system by allowing multiple access interference (MAI) in the uplink channel. Since the number of semi-orthogonal codes is not fixed, CDMA systems are said to have soft capacity.

In addition to random multiaccess, other important benefits of CDMA systems include narrowband interference mitigation and multipath rejection [33]. Due to multipath rejection property, equalizers are not needed at a CDMA receiver. This doesn't necessarily result in a simplified receiver design, however. Despite the complexity of receiver design and the stringent power control requirements [34], the CDMA system provides a natural mechanism for dynamic channel sharing [33]. This, combined with the soft capacity feature, can provide a significant increase in the maximum number of allowable users within a cell. These benefits render the CDMA systems an attractive choice for cellular communications.

1.3 Problem Statement

In a Direct Sequence CDMA system, the signals on all the links are transmitted simultaneously. Further, all uplink signals are transmitted in one frequency band and all downlink signals in another frequency band. The individual signals are separated by using spreading codes, with one or more spreading signals embedded within the desired signal.[5] Because of the propagation environment, such codes are only

[5]Many CDMA systems use two levels of spreading. For example, channelization codes are used to separate intra-cell users, and scrambling codes are used to separate the inter-cell users. The combination of channelization code and scrambling code makes up the actual spreading code, also termed the channel code. For examples of channelization and scrambling codes, see [35].

semi-orthogonal,[6] especially in the uplink direction where the signals originate from disparate geographical locations. The result is that the desired signal for each user is contaminated not only by the thermal noise but also by the signals from other users. This interference from other users, or multiple access interference (MAI), is a limiting factor in the capacity of CDMA systems. In simple CDMA receivers, MAI is regarded as additive noise and detection is based on the assumption that additive noise due to MAI is gaussian [37, 38].

In IS-95 cellular phones, a signal quality indicator depicts the strength of the desired signal that "includes" the interference from other users. This is why the call quality often does not correspond closely to the readout of the signal quality indicator.[7] The amount of multiple access interference (MAI) in a CDMA system depends upon two factors: relative signal strength from individual transmitters, and the cross-correlation properties of the spreading sequences. The relative signal strengths, in turn, depend upon the transmitted power from each user in the uplink and upon their relative distances from the base station. The amount of MAI for each user may be so large that it renders the system unusable due to excessive bit error rates. Most of the undesired signal is due to MAI and very little due to thermal noise.

The signal received at the front end of a receiver is the sum of the desired signal, the thermal noise, and the MAI. In a conventional CDMA receiver, the signal from each user is demodulated and detected independently while regarding the MAI in the demodulated signal as noise. This limits the capacity of a CDMA system [36]. It is important to note that the MAI from signals within the cell under consideration has a known structure, as compared to the interference from other cells, or "unknown" MAI [39] where the codes are generally different. It was mentioned in Sec. 1.1 that, for efficiency reasons, the cellular systems should be interference-limited rather than

[6] Time-shifted versions of the orthogonal codes are not orthogonal in general. It is, therefore, impossible to maintain the code orthogonality conditions in the presence of multipath [36, 37].

[7] Most commercial cellular handsets come with a feature that allows viewing the received signal strength by means of a signal quality indicator. For the IS-95 based CDMA systems currently used in practice, this signal indicator merely indicates the radio signal strength *including* the interference from other users as obtained by using signal quality measurement (SQM) techniques.

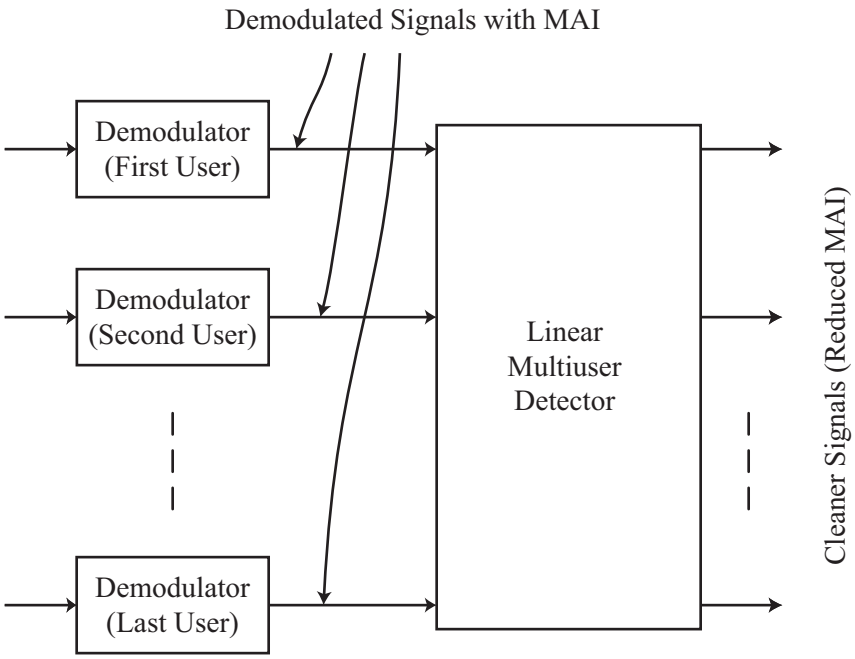

Figure 1.1: Multiuser Detection. Demonstration of a linear multiuser detector in a DS-CDMA system. Existing systems make decisions on individually demodulated signals which contain MAI. Linear multiuser detectors reduce the MAI and allow more users within a given cell.

noise-limited.[8] IS-95 systems, by virtue of regarding MAI as additive noise, are clearly interference-limited.

Multiuser detection is largely the process of mitigating the multiple access interference (MAI). Several different multiuser detection paradigms have been developed by previous researchers [36]. In this thesis, we consider linear multiuser detection schemes as depicted in Fig. 1.1. As this figure illustrates, signals from individual users, in the uplink, are first demodulated without any knowledge of other users. For each user, the demodulated signal contains MAI that, in current CDMA systems, is regarded as added noise. Linear multiuser detection is a standard approach that involves passing the demodulated signals for all users through a linear filter which generates cleaner signals for the users with minimal or no MAI. The design of the linear filter dictates the extent of MAI reduction.

Decoding decisions made on processed signals from multiuser detectors generate

[8]Interference referred to in this statement corresponds to other-cell interference or unknown MAI.

significantly lower bit error rates for individual users. Furthermore, the reduction in MAI allows more active users within a given cell, thus boosting the capacity of the system. Thus, multiuser detection brings lower bit error rates and a higher number of users, both of which account for a capacity increase in a cellular system.

This thesis is concerned with the design of the linear multiuser detector that is depicted in Fig. 1.1. We consider the design of a system in which a linear multiuser detector operates on signals from single as well as multiple antennas. Furthermore, we consider the joint design of the demodulator and the linear multiuser detector. This approach allows extra flexibility in receiver design and results in significant performance improvements.

1.4 Contributions

The principal contributions of the research presented in this thesis are:

i) Proposal for a simplified multiuser detector using sub-symbols.

ii) Proposal for diversity combining algorithms for the sub-symbol scheme.

iii) Demonstration by simulation that the bit error rates of condition number based combining algorithms outperform all other combining algorithms.

iv) Rules for maximizing the number of users in the sub-symbol scheme using proper thresholds.

v) Discovery that a single sub-symbol is sufficient to outperform the conventional detector when the sub-symbol scheme is employed for a large number of users in a quasi-synchronous system.

vi) Demonstration that the performance difference between “zero forcing” and “minimum mean squared error” multiuser detectors for a synchronous CDMA system depends on the condition number of the correlation matrices of spreading sequences.

vii) Design for combining linear multiuser detectors with multiple antennas which outperforms each of these systems considered alone.

Chapters 2–5 and the appendices develop and demonstrate the points above.

Chapter 2

System Model

This chapter introduces the wireless communication model and the direct sequence code division multiple access (DS-CDMA) transmission environment, and develops models of different components in a generic DS-CDMA system. The actual models used for applying specific techniques and algorithms presented in this thesis are discussed in later chapters.

A mathematical basis for understanding the communications of signals in a wireless DS-CDMA communication system is provided in this chapter. The single user direct sequence spread spectrum communication system is described as a basis for understanding of multiuser direct sequence spread spectrum communication system.[1] Single user end-to-end systems consist of three components: a spread spectrum transmitter, a spread spectrum receiver, and a communication channel through which the spread spectrum signal propagates. These components of the system are formulated in Secs. 2.1 and 2.3. A multiuser system is introduced as a superposition of multiple single user systems in Sec. 2.2 and the uplink in a multiuser system is described in detail in Sec. 2.5. Section 2.4 describes the spreading sequences for DS-CDMA system simulations presented in this thesis.

[1] A multiuser direct sequence spread spectrum system is also known as direct sequence code division multiple access or (DS-CDMA) system.

2.1 Single User DS Spread Spectrum System

Spread spectrum (SS) systems are broadly classified as direct sequence (DS) SS systems and frequency hopped (FH) SS systems. In either case, the generation of a pseudo noise (PN) signal is required. Most commercial spread spectrum systems use direct sequence spreading, and these are the systems that are considered in this thesis.

In a SS system, the digital data signal is processed before transmission in such a way that the processed signal "spreads" over a wider range of frequencies. That is, the frequency spectrum is widened relative to that with the user signal alone. This technique has been used by the military for decades and has significant advantages over non-spread systems: it provides better security, reduces the susceptibility to jamming, and mitigates interference.[2]

2.1.1 Spread Spectrum Transmitter

A spread spectrum transmitter generates a spread spectrum signal from a binary information signal. The binary information signal, represented as a sequence, is usually obtained from a physical phenomenon. For example, in cellular handsets, sampling and quantization of a voice signal generates a digital signal that can be represented as a binary signal [41]. The bit duration of the binary signal depends upon the source of generation of the binary signal.

Each of the many possible methods [22] of generating a direct sequence spread spectrum signal requires a pseudo noise sequence or spreading sequence.[3] Two methods of generating the DSSS signal are as follows:

- Mapping the original binary information signal into a binary phase shift keying (BPSK) signal [42], and then taking the product of the resulting signal and

[2]The interference mitigated by the use of spread spectrum transmission can either be external, as generated by a jamming device, or it can be internal resulting from the multipath propagation of the signal in a wireless environment [22, 34, 40].

[3]The terms PN sequence and spreading sequence are used interchangeably. The spreading signal additionally includes the timing information usually given by the chip duration. "Rate" of the spreading sequence refers to the rate of the corresponding spreading signal.

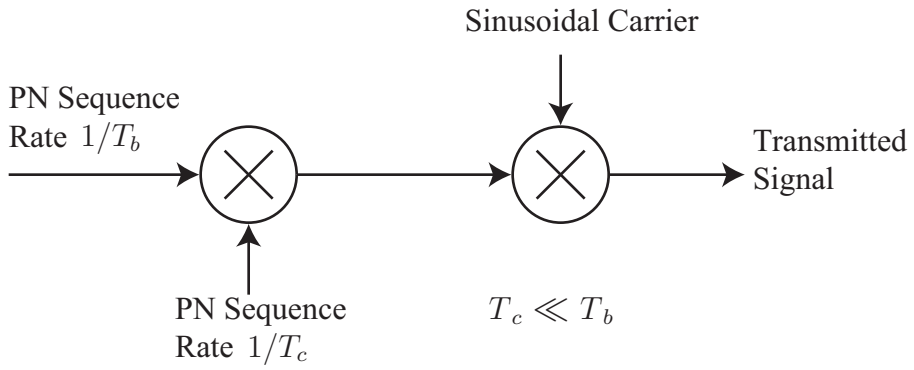

Figure 2.1: Spread Spectrum Modulation. A basic direct sequence spread spectrum transmitter that uses binary phase shift keying (BPSK) modulation.

the spreading signal where the spreading signal is a series of unit amplitude rectangular pulses each of duration equal to the duration of one chip and of polarity as determined by the value in the PN sequence.

- XORing the original binary sequence with the spreading sequence preserving the timing information, and then mapping the resulting sequence into a BPSK signal.

In practice, channel coding is employed in which the original binary sequence is replaced by a coded sequence of higher rate. The channel code rate [22] is usually selected such that the rate of the coded sequence is the same as the rate of the spreading sequence. Construction of a simple spread spectrum transmitter using direct sequence spreading is shown in Fig. 2.1. This construction uses the first method of implementing the spread spectrum transmitter.

Spreading Gain: The spreading gain or the spreading factor, at a spread spectrum transmitter, is defined as the ratio of the signal bandwidth after spreading to the original binary information signal bandwidth. The spreading gain is approximately equal to the number of chips in one bit duration of the binary information signal [43].

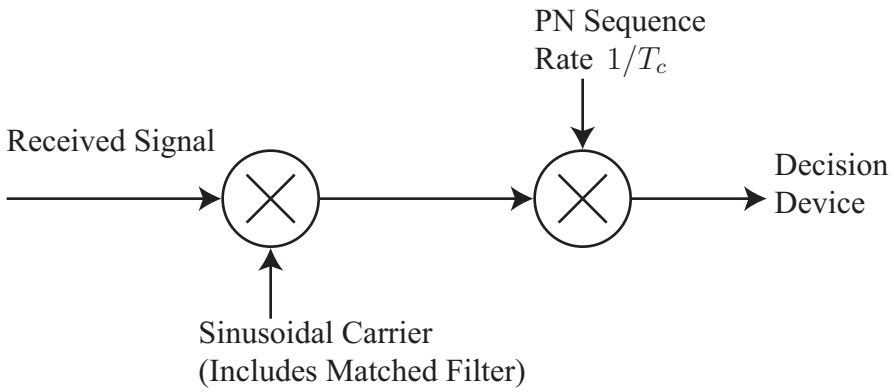

Figure 2.2: Spread Spectrum Demodulation. A basic direct sequence spread spectrum receiver that assumes BPSK modulated received signal.

2.1.2 Spread Spectrum Receiver

A direct sequence spread spectrum receiver requires knowledge of the spreading sequence used at the transmitter. For a single user spread spectrum system, the only undesired signal is the additive white gaussian noise, in addition to any interfering signal.[4] When the undesired signal follows the Gaussian distribution, the optimal receiver for the received signal can be implemented as either a correlator or a matched filter. The two implementations are functionally equivalent and yield the same output signal. Proakis [22] discusses a somewhat detailed construction of such receiver implementations. A simplified form of a spread spectrum receiver is shown in Fig. 2.2.

Processing Gain: Processing gain at a spread spectrum demodulator is defined as the number of chip periods over which the matched filtering or the correlation is carried out. Usually, the correlation is performed over the bit period or the symbol period of the binary information signal and processing gain is equal to the number of chips per bit of the binary information signal. Processing gain signifies the relative gain of the desired signal compared to the undesired signal [22].

[4]Historically, a jamming signal, used in military application, is regarded as the interfering signal. In commercial systems, however, the interfering signal is the multiple access interference.

2.2 Multiuser DS Spread Spectrum System

A single user DS spread spectrum system can be extended to a multiuser system. In fact, both single user and multiuser spread spectrum systems have similar transmitter and receiver structures,[5] and the multiuser channel is just the superposition of many single user channels [22].

At the base station, detection of a particular user's signal assumes that signals from the other users can be regarded as additive noise. This assumption is based on the fact that direct sequence spreading results in frequency components with diminished amplitudes [34], and that the spectrum of a spread spectrum signal resembles that of additive noise.

Commercial CDMA systems are multiuser DS spread spectrum systems [18]. Since the multiuser detectors developed in this thesis are designed for DS-CDMA systems, detailed construction of the transmitter and the receiver for such systems is described in later sections. Section 2.5 is dedicated to the description of a DS-CDMA transmitter and DS-CDMA channel while later chapters will describe a variety of DS-CDMA receivers.

2.3 Wireless Communications Model

Wireless cellular communication using DS-CDMA requires understanding not only the DS-CDMA transmitter and receiver models but also the wireless channel through which the transmitted signal propagates. In this section, a wireless communication channel model is developed for performance analysis of various DS-CDMA receivers described in this thesis.

The channel model is best understood by considering a radio signal propagating through the channel. It is then used with DS-CDMA transmitter and receiver models to evaluate the performance of the complete DS-CDMA wireless communication

[5] In a multiuser system, signal transmitted from a single base station is the sum of signals intended for each individual user; the signal received at the base station is the sum of signals individually transmitted from users at disparate locations.

system. The essential parameter of a radio channel is the variation in radio signal level [11]. The radio signal suffers variations due to many reasons including the mobile user movement, terrain, and building structures [44]. The strength of a received radio signal is segregated into three main components, each of which is characterized separately [45, 46]. Thus complete characterization of the radio signal is given by considering the following three parameters:

i) Path loss resulting from destructive interference of large scale multipath.

ii) Long-term fading distribution considering the attenuation of each path in a large scale propagation environment.

iii) Short-term fading distribution taking into account the local multipath caused by objects in the vicinity of transmitter and receiver.

Each of these components of a radio signal model is described in detail in the following sections:

2.3.1 Path Loss

Path loss is the decrease in radio signal strength as the signal propagates through space. It is defined as the ratio of transmitted power to received power of a radio signal. Power in a radio signal decreases as the signal moves away from the transmitter. For a radio signal propagating through free space, the average received power is given by Friis formula [43, 45, 47]:

$$P_r = P_t G_r G_t \left(\frac{\lambda}{4\pi d}\right)^2 \tag{2.1}$$

where P_r is the received power, P_t is the transmitted power, G_r is the gain for receive antenna, G_t is the gain for transmit antenna, d is the distance from the transmitter, and λ is the wavelength of the transmitted signal. Equation 2.1 describes the relation between the transmitted and received powers of a radio signal as the radio

signal propagates through the free space. A decrease in the strength of a signal as it propagates through free space is called free space loss.

Path loss accounts for free space loss and for interference that may occur due to large scale reflections from static objects. In a typical urban environment, the propagation of a radio signal is accomplished via direct path, reflection, scattering and diffraction [44]. Thus the propagating signal suffers not only from variations in amplitude and phase but also from a spread in the received signal. The temporal spread in received signal relative to the transmitted signal is called delay spread, and the inverse delay spread is called coherence bandwidth [43, 46]. For narrowband channels,[6] the received signal can be regarded as multiple copies of the transmitted signal, received one after the other, and typically decreasing in amplitude [11, 46].

Of the models used to characterize the path loss in a radio channel, the 2-ray and the 10-ray models are the most popular [43, 48]. These models take into account the free space loss and the interference that occurs as a result of large scale reflection. Ray tracing techniques are used as a design tool for such models [49–51]. Although ray tracing models are only approximate, yet they are complex to develop. Analysis of ray tracing models results in power fall-off rates that are generally higher than those given by free space path loss [43, 52]. Simplification of ray tracing models results in received power that can be expressed as a function of distance from the transmitter. A simplified model can be expressed in the following equation:

$$P_r = P_{r_0}\left[\frac{d_0}{d}\right]^n \tag{2.2}$$

where P_{r_0} is the power received at a distance d_0 from the transmitter, and n is the propagation index typically ranging from 2 to 5 [53]. The above model is valid for distances $d > d_0$, where d_0 is the reference distance for the antenna far-field. The distance d_0 is usually determined by propagation measurements [52].

The propagation index depends on the environment as well as the distance from

[6] A channel is regarded as narrowband if the coherence bandwidth is greater than the signal bandwidth; otherwise, the channel is regarded as wideband.

the transmitter. Thus, there are models (see [53] and the references therein) that specify a value of propagation index based on the distance from the transmitter. For distances less than d_0, the propagation index is usually taken as 2, corresponding to free space, while for distances greater than d_0, the propagation index usually lies between 2 and 5 as dictated by the propagation measurements. References [52] and [54] report propagation measurements at 800 MHz, for example. In summary, these measurements indicate that path loss falls off approximately as d^2 up to a critical distance d_0 and sharply increases with distance beyond the critical distance.

2.3.2 Lognormal Fading

The path loss described in Sec. 2.3.1 is the result of free space loss plus the destructive combination of different replicas of the transmitted signal. Each replica of the transmitted signal also fades individually as it passes through various obstacles and structures [45, 46]. Thus, the received signal, given by the combination of such replicas, exhibits fluctuations in the amplitude in addition to the path loss. The random fluctuation in the received signal due to large scale objects is termed long-term fading or shadowing, and has been characterized as following a lognormal distribution [45].

Shadowing is the fluctuation in the received signal superimposed over the path loss. Therefore, shadowing distribution has a mean that is equal to the path loss. The standard deviation of the lognormal shadowing distribution typically ranges from 5–12 dB [11]. Thus the received signal power exhibits a 5–12 dB variation around a signal power that would be expected if only path loss were taken into account.

Lognormal shadowing is completely characterized by the mean and standard deviation of the distribution [55] which are usually obtained through empirical data [56, 57]. The autocorrelation of the lognormal shadowing depends upon the surrounding building sizes. Measurement data, reported by Gudmundson in [58], address the autocorrelation properties of the lognormal shadowing.

2.3.3 Short-Term Fading

Variation in signal due to local multipath is referred to as short-term fading. Local multipath or short-range multipath, a result of presence of objects in close vicinity to the transmitter and the receiver, imparts additional statistical characteristics to the radio signal. Short-term fading has a distribution whose *local* mean is given by the lognormal distribution. Of the several short-term statistical fading models that have been developed in the literature [44, 46, 59], the most widely accepted is developed in the following and used for simulations in later chapters.

Complete characterization of the channel consists of considering a few dominant large-scale multiple paths, where each of these paths is comprised of short-range multipath component waves, and is characterized independently [11]. To derive the expression for one dominant path, let $x(t)$ be the transmitted signal given by:

$$x(t) = \Re\left\{s(t)e^{j(2\pi f_c t+\phi_0)}\right\} \tag{2.3}$$

where $s(t)$ is the complex baseband signal, f_c is the carrier frequency, and ϕ_0 is an arbitrary initial phase that can be considered as zero for further analysis. Now, consider a particular large-scale path consisting of N_0 short-range multipath components. The short-range multipath components are generated by reflection and scattering from local scatterers. The received signal can, therefore, be expressed as:

$$r(t) = \Re\left\{\sum_{n=1}^{N_0} \alpha_n(t)s(t-\tau_n(t))e^{j2\pi(f_c+\Delta f_n(t))(t-\tau_n(t))}\right\} \tag{2.4}$$

where N_0 is the total number of multipaths, τ_n is the delay of the *n-th* multipath component, and Δf_n designates the doppler shift of that component. Path loss, lognormal shadowing, and antenna gain are factored into α_n, which designates the net amplitude gain for the large-scale path given by Eq. 2.4. Defining the parameter $\phi_n(t) = (f_c+\Delta f_n(t))\tau_n(t)-t\Delta f_n(t)$ which indicates the phase imparted by the channel

to the *n-th* multipath component, the above expression can also be written as:

$$r(t) = \Re\Big\{ \Big[\sum_{n=1}^{N_0} \alpha_n(t) e^{-j\phi_n(t)} s(t - \tau_n(t))\Big] e^{j2\pi f_c t} \Big\} \tag{2.5}$$

We define the *multipath delay spread* as the maximum difference in arrival times of any two multipath components. The relative values of the signal bandwidth and inverse delay spread classify the channel as a narrowband or wideband. Modelling of narrowband channels is relatively simple because relative delays for individual multipath components are assumed to be negligible [11,43], and $s(t-\tau_n(t))$ is approximated by $s(t)$ [46]. Therefore, for a narrowband channel, a received path can be written as:

$$r(t) = \Re\Big\{ s(t) e^{j2\pi f_c t} \Big(\sum_{n=1}^{N_0} \alpha_n(t) e^{-j\phi_n(t)} \Big) \Big\} \tag{2.6}$$

which contains an additional complex scaling factor in parentheses as compared to the original signal. To characterize the scale factor, let[7] $s(t) = 1$, which results in:

$$r(t) = \Re\Big\{ \Big(\sum_{n=1}^{N_0} \alpha_n(t) e^{-j\phi_n(t)} \Big) e^{j2\pi f_c t} \Big\} \tag{2.7}$$

$$r(t) = r_I(t) \cos 2\pi f_c t + r_Q(t) \sin 2\pi f_c t \tag{2.8}$$

where $r_I(t)$ is the in-phase and $r_Q(t)$ is the quadrature component of $r(t)$. The components of $r(t)$ are given by:

$$r_I(t) = \sum_{n=0}^{N_0} \alpha_n(t) \cos \phi_n(t) \tag{2.9}$$

$$r_Q(t) = \sum_{n=0}^{N_0} \alpha_n(t) \sin \phi_n(t) \tag{2.10}$$

It should be noted that the number of short-range local multipath components, N_0,

[7] As seen from Eq. 2.3, taking $s(t) = 1$ yields a single tone, and hence renders the transmitted signal narrowband. This is necessary for proper characterization of the scale factor.

also depends on position, and hence on time for a user in motion. The value of N_0 is generally very large for typical environments, such that the central limit theorem is applicable [55], rendering the in-phase and quadrature components as Gaussian random processes. The envelope of each path of the received signal $|r(t)| = \sqrt{r_I^2(t) + r_Q^2(t)}$, therefore, follows a Rayleigh distribution[8] assuming no line-of-sight path exists. If a line-of-sight path is present, then the in-phase and quadrature components of the received signal are not zero-mean [60, 61]. In such a case, the signal envelope has a Rician distribution [46, 61].

2.4 Spreading Sequences

All spread spectrum systems use one or more spreading codes[9] to achieve spreading of the desired signal prior to transmission. Selection of spreading codes for a typical application depends on the application itself and on the specific properties of the spreading codes. For single user communications in a multipath environment the most important factor is to achieve the ability to resolve the multipath. To do this effectively, the spreading codes must have excellent autocorrelation properties, ideally a delta function. Similarly, for a multiuser system in a non-multipath environment the most important factor in selecting the spreading sequences is the ability to minimize the multiaccess interference. The multiaccess problem can be addressed if the spreading sequences are selected such that the maximum value of cross-correlation is minimized [22, 36].

Commercial CDMA systems are multiuser systems in multipath environment. Therefore, the spreading sequences for CDMA systems are selected by considering both their autocorrelation and cross-correlation properties. Furthermore, CDMA systems are cellular and require separation of intra-cell as well as inter-cell users. This requires two levels of spreading achieved by a combination of two spreading codes,

[8] This also implies that the received power in this signal path follows an exponential distribution.

[9] Spreading codes are generated from pseudo random or pseudo noise (PN) sequences. This is because PN sequences exhibit such statistical properties that are desired of spreading codes.

referred to as channelization codes and scrambling codes. Multiple spreading is described in detail elsewhere [35]. Subsequent sections discuss the spreading sequences commonly used in commercial DS-CDMA systems and in our simulations as well.

2.4.1 Maximal Length Sequences

Maximal length sequences or m-sequences are the most widely recognized and used pseudo noise (PN) sequences; they can be generated by two methods by using a linear feedback shift register (LFSR). The first using *simple* LFSR and the other using *modular* LFSR. Each of the LFSR, either simple or modular, can be represented by means of a polynomial [22].

A sequence, generated by an LFSR with m registers, is said to be a maximal length sequence or an m-sequence if its length is $L = 2^m - 1$. An m-sequence is generated when the LFSR structure represents a primitive polynomial [32, 62]. The length of the m-sequence is the possible number of states an LFSR can take,[10] except for an all zero state. For an LFSR, an m-sequence of length L provides the best autocorrelation properties [22, 32], as follows:

$$R(n) = \begin{cases} L & n = 0, L, 2L, \cdots \\ -1 & \text{otherwise} \end{cases} \tag{2.11}$$

An example generation of an m-sequence using a simple LFSR is shown in Fig. 2.3. The same m-sequence can also be generated by a modular LFSR as shown in Fig. 2.4. The constructions in Fig. 2.3 and Fig. 2.4 are equivalent: they generate the same m-sequence, represent the same polynomial $1 + x^2 + x^5$, and implement the same difference equation $x[i] = x[i-2] \oplus x[i-5]$.

Another representation of both constructions is written as $[2 \quad 5]_S \equiv [3 \quad 5]_M$. It should be noted that $[\quad]_S$ notation indicates the quotients of the primitive polynomial

[10] Each register in an LFSR is a binary register and has two possible states. The state of an LFSR with r binary registers is an r-tuple where each element indicates the state of one distinct binary register.

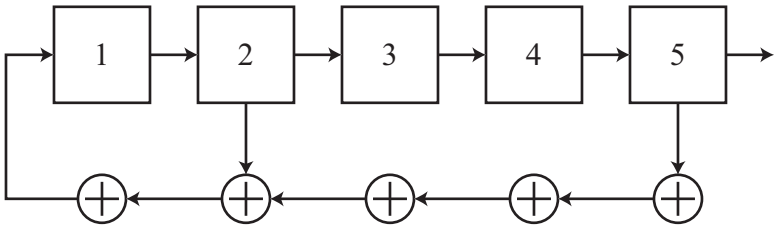

Figure 2.3: Simple LFSR. Simple linear feedback shift register realization of a polynomial given by the difference equation $x[i] = x[i-2] \oplus x[i-5]$.

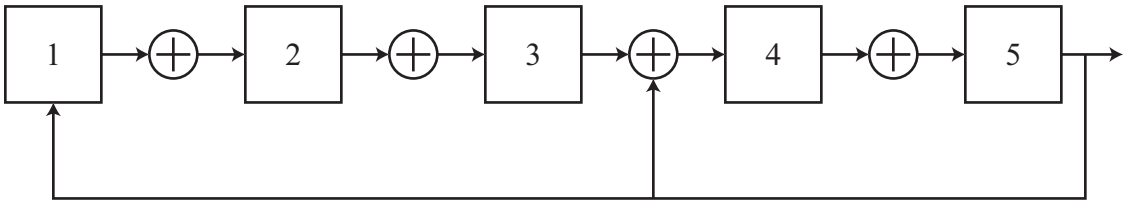

Figure 2.4: Modular LFSR. Modular linear feedback shift register realization of a polynomial given by the difference equation $x[i] = x[i-2] \oplus x[i-5]$.

representing the LFSR, while the $[\quad]_M$ notation indicates the quotients of a primitive polynomial that is the reciprocal of the primitive polynomial representing the LFSR.[11] The construction used by Sarwate in [32] is similar to the simple LFSR but the representing polynomial is the reciprocal of the one representing the construction of simple LFSR in Fig. 2.3. The ETSI proposal for WCDMA standard [63] uses the notation of Sarwate [32]. Therefore, for our simulations, we implement the reciprocals of the polynomials given in proposed standards [63] using the structures of Fig. 2.3 and Fig. 2.4.

2.4.2 Gold Sequences

The m-sequences have excellent autocorrelation properties but their cross-correlation properties do not follow any particular rules [40, 64] and typically exhibit undesirably high values [22]. Furthermore, the number of m-sequences for a given number of registers in an LFSR is limited. Gold sequences address these problems, and are

[11] The reciprocal of a polynomial is obtained by reversing the quotients; if $p(x)$ is a polynomial of degree n, its reciprocal is given by $x^n P(1/x)$. The reciprocal of a primitive polynomial is also primitive [32, 40].

derived by combining the m-sequences from two LFSRs [65, 66].[12] In comparison to m-sequences, Gold sequences provide larger sets of sequences and exhibit better cross-correlation properties [22, 40].

Gold sequences are generated from two equal length m-sequences that form a so-called *preferred pair*. The cross-correlation of two m-sequences that form a preferred pair is tri-valued [67] and it takes the values from the set $\{-1, -t(m), t(m) - 2\}$, where $t(m) = 1 + 2^{\lfloor (m+2)/2 \rfloor}$, and m is the number of binary shift registers in the LFSR. A requirement for the generation of Gold sequences is that m should be equal to 2 Modulo 4. Under this condition, $GCD\,(t(m), 2^{m-1}) = 1$, i.e $t(m)$ and 2^{m-1} are relatively prime [32]. Thus, if u is an m-sequence, a $t(m)$-decimated version of u, denoted by $v = u\,[t(m)]$ is also an m-sequence, and u and v form a preferred pair [32]. A set of $2^m + 1$ Gold sequences can be generated from u and v as given by the set $\{u, v, u \oplus T^i\{v\}\}$, where $T^i\{v\}$ indicates the right (or left) shift of sequence v by i bits, and i varies from 0 to $L - 1$, where L is the length of sequences that form the preferred pair.

2.4.3 Kasami Sequences

Kasami sequences also address the two undesirable properties of the m-sequences: smaller sets of sequences and potentially higher cross-correlation values. Kasami sequences can be generated either as a small set or as a large set. The small set has better cross-correlation properties, while the large set provides more sequences to choose from. Generation of Kasami sequences involves a method similar to the one used to generate the Gold sequences, as given below.

2.4.3.1 Small Set

To generate the small set Kasami sequences, an m-sequence, denoted as u, is first generated. Let the length of the sequence u be L, and m be the number of binary registers in the LFSR, such that $L = 2^m - 1$. One period of the sequence u is

[12] Combining two m-sequences refers to performing Modulo 2 addition of the two sequences.

decimated by $2^{m/2}+1$ to generate a sequence w of length $\{2^m-1\}/\{2^{m/2}+1\}$; the length of w simplifies to $2^{m/2}-1$. Next, $2^{m/2}+1$ repetitions of w are concatenated to form a sequence v of length L. The small set Kasami sequences are then given by the set $\{u, u \oplus T^i\{v\}\}$, where $T^i\{v\}$ indicates the right (or left) shift of sequence v by i bits, and i varies from 0 to $2^{m/2}-1$.

2.4.3.2 Large Set

The large set Kasami sequences are generated either from the Gold set or from the Gold-like set.[13] Large set Kasami sequences includes the Gold set and the small set Kasami sequences as the subsets. The procedure to generate large set Kasami sequences can be found in the literature, e.g., [32] and is not discussed here.

2.5 CDMA Uplink Signal Model

A baseband model of a CDMA uplink is shown in Fig. 2.5. The signal received at the base station is the summation of signals from all users, multipath components for each user's signal, and additive white gaussian noise (AWGN). Figure 2.5 also includes channel encoders for each transmitter. For simulations performed without channel encoding, the encoder has no effect. For simulations that use channel encoding a convolutional encoder of constraint length 5 is used [22].

There are N_u users in the system and the data signals from these users are designated as $d_1(t), d_2(t), \ldots, d_{N_u}(t)$. The data symbols within the data signals are spread by multiplying with respective spreading sequences $K_1(t), K_2(t), \ldots, K_{N_u}(t)$. The channel introduces delays $\tau_1, \tau_2, \ldots, \tau_{N_u}$ to signals from different users, and $A_1(t), A_2(t), \ldots, A_{N_u}(t)$ are the fading coefficients for the single resolvable path of each user.[14] The spreading sequences are the periodic extensions of single periods

[13] Large set Kasami sequences can be generated for all even values of m, the number of binary registers in LFSR. When m is equal to 2 Modulo 4, large set Kasami sequences are generated by first generating Gold sequences. When m is equal to 0 Modulo 4, it is not possible to generate Gold set and large set Kasami sequences are generated by first generating Gold-like sequences [32].

[14] The product with fading coefficients in Fig. 2.5 is equivalent to a time varying convolution with

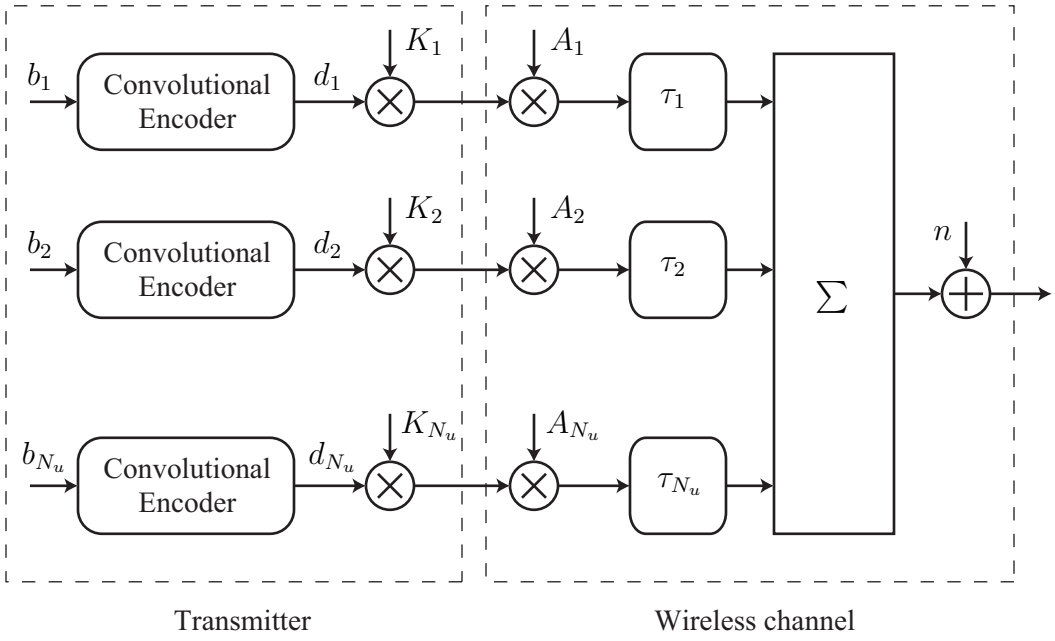

Figure 2.5: CDMA Uplink. Demonstrating a typical CDMA transmitter and a generic channel in the CDMA uplink. The received signal is the sum of signals from individual users modified by the respective channel.

$\tilde{K}_1(t), \tilde{K}_2(t), \ldots, \tilde{K}_{N_u}(t)$, given by:

$$\tilde{K}_i(t) = \sum_{m=1}^{N} c_{im} p(t - (m-1)T_c) \tag{2.12}$$

where c_{im} denotes the *m-th* chip of the spreading sequence $\tilde{K}_i(t)$, N is the length of spreading sequence, and $p(t)$ is the chip pulse shape that is assumed to be rectangular for our simulations. No assumption is made regarding the length of the spreading sequences for the description of the new scheme. The spreading sequences may potentially be one symbol long (short code system) or they may span hundreds of symbols (long code system). At this point, it is convenient to define the symbol-period correlation matrix for the time-aligned spreading sequences of the active mobile users.

a single tap filter response and corresponds to a single resolvable path. For multiple resolvable paths, the product operation is replaced by more general time-varying convolution with multiple taps, where each tap fades individually and corresponds to one resolvable path.

Therefore,

$$R_{ij}(t) = \int\limits_{\substack{\text{symbol} \\ \text{period}}} K_i(t)K_j(t) \tag{2.13}$$

is the element of symbol-period correlation matrix in the *i-th* row and *j-th* column.

The signal at the receiver front end is the sum of signals transmitted by individual mobile users, modified by the channel gain for each user and contaminated by additive white gaussian noise, as depicted in Fig. 2.5. Therefore, the received signal $r(t)$ can be written as:

$$r(t) = \sum_{j=1}^{N_u} \Big(K_j(t-\tau_j)A_j(t-\tau_j)d_j(t-\tau_j) \Big) + n(t) \tag{2.14}$$

where $n(t)$ is additive white gaussian noise (AWGN) with variance σ_n^2. The received signal in the above expression is the one present at the front end of any CDMA system receiver. The signal at the output of the receiver depends upon the receiver structure. Various receiver types, conventional and more advanced, are discussed in subsequent chapters.

Chapter 3

Linear Synchronous Receivers

This chapter introduces some of the receivers[1] employed for the DS-CDMA systems. The received signal model used in these receivers is as derived in Chapter 2. A single user matched filter receiver, described in Sec. 3.1, is the simplest of all DS-CDMA receivers. 'Zero forcing' and 'minimum mean squared error' detectors are described in Sec. 3.2. The remainder of this chapter is dedicated to the algorithms used in more advanced linear multiuser detectors.

3.1 Single User Matched Filter

The basic CDMA receiver, popularly known as a conventional detector [37], employs a single user matched filter (SUMF) which is often implemented as a correlator. In SUMF detection, the signal from each user is demodulated individually without any knowledge of signals from other users. There is one SUMF detector at the base station for each active user, and the output of each detector is determined independently of the output of any other detector. The description, construction, and performance of the SUMF detector are explained in what follows.

The SUMF detector is a maximum-likelihood detector in the sense of maximizing the signal-to-noise ratio (SNR) for a particular user without regard to the signals from other users. Thus, it is the optimal detector (see [22] and [68] for details) if

[1]The terms receiver and detector are used interchangeably.

the despread and demodulated signal for each user contains only additive white noise (AWN). This detector also minimizes the probability of error for the single user in case of additive white gaussian noise (AWGN) [36]. The assumption that signals from other users sharing the channel can be neglected is valid only when the spreading sequences of all the users are orthogonal[2] to each other and remain so when the signal is received at the base station after passing through the wireless propagation environment. However, non-zero cross-correlations among spreading sequences lead to multiple access interference (MAI) which, in general, increases with the number of users [36]. Even if the spreading sequences are chosen to be orthogonal to each other to start with, the orthogonality is lost when the signals pass through the multipath environment and arrive at the base station with random delays [33, 46].

This section details the construction of the single user matched filter. For this purpose, we utilize the channel and received signal model as described in Chapter 2. Because a signal received at the front end of any CDMA receiver depends in part upon the channel through which the received signal has propagated, we first describe synchronous and asynchronous classes of DS-CDMA channels. Next, we describe the SUMF receivers for these two DS-CDMA channel classes.

3.1.1 CDMA Channel Classification

CDMA systems are classified as either synchronous or asynchronous on the basis of the timing method for signals received from different users. In the synchronous channel, the basic assumption is that the users' transmission times are controlled in a way that the signals received from different users coincide at the bit boundaries observed at the base station receiver.[3] Since the users are geographically separated

[2]Orthogonality of two spreading sequences in the received signal means that the portion of the signal from one user results in zero output from the receiver of the other user. That is, the receiver for first user will have zero output, except for the AWGN, if the signal transmitted from the first user is cut off, irrespective of the signal from the second user.

[3]Strictly speaking, in a synchronous CDMA system, signals received from different users coincide in time at the chip boundaries as well as the bit boundaries. Asynchronous systems do not pose such requirement. Simulation results presented in this thesis use one sample per chip, therefore, the requirement of chip alignment is implicit for synchronous and asynchronous CDMA systems.

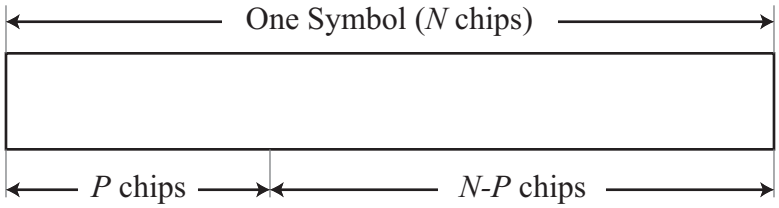

Figure 3.1: QS-CDMA Symbol. Depicting a typical symbol in a QS-CDMA system. The spreading gain of the system is N and symbol boundaries from various users are allowed to fall within the first P chips of the symbol.

from one another and often are in motion, a synchronous system requires timing control for each and every user.

An asynchronous system does not require the received symbols from different users to be time aligned at symbol boundaries at the base station. It is a more general CDMA system, and most commercial systems fall in this category. Specifically, the reverse links in commercial CDMA systems are asynchronous due to a lack of accurate control on user transmission instants.

An asynchronous CDMA system with approximately aligned symbols is sometimes referred to as a quasi-synchronous code division multiple access (QS-CDMA) system. In QS-CDMA, the uncertainty in symbol alignment lies within a small fraction of the total number of chips in the spreading sequence. For example, as shown in Fig. 3.1, if N is the total number of chips in one symbol and P is the smallest number such that any symbol start time at the receiver does not fall within $N - P$ chips, then the uncertainty in symbol alignment for such a system is P chips. The signal in the period of uncertainty may be blanked out by appending blank chips to the actual spreading sequence [69], thereby increasing the symbol time.[4] For our example, where P is the period of uncertainty and N is the number of chips per original symbol, the symbol period is extended to $N+P$ chips per symbol. There are QS-CDMA systems, however, in which the period of uncertainty in alignment is not blanked out. In this case, the system is exactly the same as an asynchronous system with a smaller degree of asynchronism [70].

[4]The period of uncertainty is blanked out by a decrease in symbol rate rather than an increase in chip rate because actual dependence of uncertainty is on time and not the number of chips.

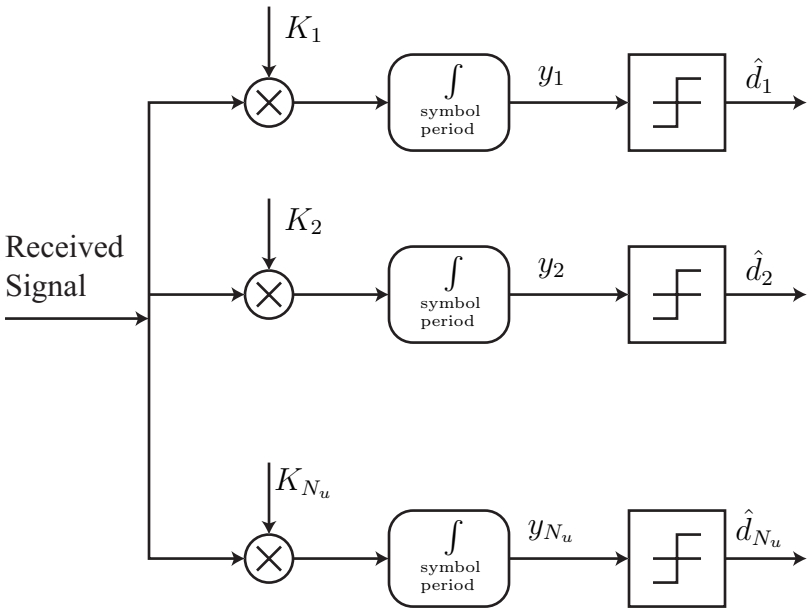

Figure 3.2: SUMF Receiver. A typical CDMA uplink model with single user matched filter for N_u distinct users; time-dependence of the parameters have been omitted for simplicity. For synchronous case, the delays τ are made the same.

3.1.2 SUMF for Synchronous CDMA Systems

Currently deployed DS-CDMA receivers use SUMF detection. The detection is performed by correlating a locally generated replica of the spreading sequence of the user of interest with the incoming signal, as shown in Fig. 3.2. The correlation is performed over a symbol period and it is assumed that the symbol-long portion of the locally generated spreading sequence correlates weakly with spreading sequences of the other users. For a particular symbol, the output of the SUMF is given by:

$$y_i(t) = \int_{\substack{\text{symbol} \\ \text{period}}} r(t) K_i(t - \tau_j) \tag{3.1}$$

where $r(t)$ is given by Eq. 2.14 and τ_j is the channel delay for the *j-th* user. For a synchronous system, Eq. 3.1 reduces to

$$y_i(t) = \sum_{j=1}^{N_u} \Big(R_{ij}(t) A_j(t) d_j(t) \Big) + n_i(t) \tag{3.2}$$

where $n_i(t)$ is the noise $n(t)$ in Eq. 2.14 processed by the *i-th* matched filter. That is, $n_i(t)$ is the gaussian noise with variance $R_{ii}(t)\sigma_n^2$. Equation 3.2 can also be written as:

$$y_i(t) = R_{ii}(t)A_i(t)d_i(t) + \sum_{\substack{j=1 \\ j\neq i}}^{N_u}\Big(R_{ij}(t)A_j(t)d_j(t)\Big) + n_i(t) \tag{3.3}$$

It can be seen from the above expression that $y_i(t)$ has three components: the desired signal $R_{ii}(t)A_i(t)d_i(t)$, the additive gaussian noise $n_i(t)$, and the remainder terms that arise as a result of non-zero cross correlation between spreading sequences. The undesired terms in $y_i(t)$ comprise the additive noise and the multiple access interference (MAI) which are neglected by the SUMF detector that performs the slicing or decision operation on $y_i(t)$.[5]

MAI degrades the system performance and limits the capacity of CDMA systems [71]. It depends on other users' signals, as demonstrated by Eq. 3.3, and does not change with signal-to-noise ratio (SNR). This leads to a BER floor that is always exhibited by the SUMF detector regardless of whether the system is synchronous or asynchronous.

3.1.2.1 Orthogonal Sequences

When the DS-CDMA system can be guaranteed to be synchronous,[6] it is preferable to use orthogonal sequences for spreading. This results in the complete elimination of MAI, so that the SUMF detector actually achieves the AWGN performance.[7] From Eq. 3.2 the demodulated signal[8] for the *i-th* user can, therefore, be written as:

$$y_i(t) = R_{ii}(t)A_i(t)d_i(t) + n_i(t) \tag{3.4}$$

[5]Slicing or decision operation for digital signals produces the data from the transmitted alphabet. For equiprobable binary signals transmitted as +1 and -1, slicing operation at the output of a receiver produces +1 when the receiver output is greater than 0 [22].

[6]Accurate control over transmission instants of all the users is required to guarantee that the system will be synchronous.

[7]Orthogonal sequences in a synchronous system will eliminate the local cell MAI. Interference from other cells may still cause the performance to be deteriorated.

[8]Signal that appears at the output of SUMF is regarded as the demodulated signal.

which is obtained by setting all the cross-correlation terms, $R_{ij}(t), i \neq j$, equal to zero. When the additive noise is gaussian, the error probability in detecting $y_i(t)$ is given by the tail of the gaussian distribution [68] and can be derived as $Q(\sqrt{\text{SNR}})$ [22], where SNR is the ratio of the signal power to the noise power, and the Q-function is the tail of the 'standard' gaussian probability distribution.[9] Thus, the error probability, $P_{e,1}$ in the detection of $y_i(t)$ is given by:

$$P_{e,1} = Q\left(\frac{\sqrt{R_{ii}(t)}A_i(t)}{\sigma}\right) \tag{3.5}$$

which is the same as that for a single user in AWGN channel [22].

3.1.2.2 Semi-orthogonal sequences

Semi-orthogonal sequences do not exhibit zero cross-correlation, but their cross-correlation properties are generally better than those of orthogonal sequences [22,33]. When the transmission instants of individual users can not be controlled accurately, symbols from users will be received asynchronously at the base station. In such a case, spreading sequences generally are chosen such that the cross-correlation and hence the MAI is minimized. The Gold and Kasami sequences discussed in Sec. 2.4 are examples of sequences that exhibit good cross-correlation properties [22]. For example, Kasami sequences exhibit a tri-valued cross-correlation function [32]. Semi-orthogonal sequences limit the MAI in an asynchronous system at the expense of producing some MAI when the system happens to be synchronous.

MAI under synchronous operation can be directly computed from Eq. 3.2. To perform a quantitative analysis of MAI, consider a system with two users, so that the

[9] A standard gaussian probability distribution is defined as having zero mean and unit variance [55]. Q-function is defined as $Q(x) = \frac{1}{\sqrt{2\pi}}\int_{-\infty}^{x} e^{-u^2/2}du$ and is related to the complementary error function as $Q(x) = \frac{1}{2}\text{erfc}(\frac{x}{\sqrt{2}})$.

SUMF outputs from Eq. 3.2 can be written as:

$$y_1(t) = R_{11}(t)A_1(t)d_1(t) + R_{12}(t)A_2(t)d_2(t) + n_1(t) \tag{3.6}$$

$$y_2(t) = R_{21}(t)A_1(t)d_1(t) + R_{22}(t)A_2(t)d_2(t) + n_2(t) \tag{3.7}$$

Equation 2.13 dictates that $R_{11}(t) = R_{22}(t)$ and $R_{12}(t) = R_{21}(t)$. Thus, by symmetry, the probability of error in the detection of $y_1(t)$ is the same as the probability of error in the detection of $y_2(t)$. Conditioning on the symbol of the second user, this error probability $P_{e,2}$ can be derived from the above equations and is given by [36]:

$$P_{e,2} = \frac{1}{2}Q\left(\frac{R_{11}A_1 - R_{12}A_2}{\sqrt{R_{11}}\sigma}\right) + \frac{1}{2}Q\left(\frac{R_{11}A_1 + R_{12}A_2}{\sqrt{R_{11}}\sigma}\right) \tag{3.8}$$

where the time dependence of variables has been removed for the sake of simplicity. The equation above assumes that the data symbol from the interfering users takes on each of the possible binary values with 50% probability. Since the Q-function is monotonic, it can be seen that $P_{e,2}$ is greater than $P_{e,1}$ and reduces to $P_{e,1}$ when the cross-correlation R_{12} is set to zero: probability of error in detection for a two-user system is greater than the corresponding probability for a single user system. The analysis can be extended to an arbitrary number of users in a similar fashion (see Chapter 3 of [36] for details). In summary, for the synchronous DS-CDMA channel, the error probability depends on the following parameters:

i) Relative magnitudes of the received signals.

ii) Cross-correlation values of the spreading sequences.

iii) Power of the additive noise.

3.1.3 SUMF for Asynchronous CDMA Systems

Asynchronous systems, in which received symbols from different users are not time-aligned, respond to the SUMF in the same way as do synchronous systems [36]. In

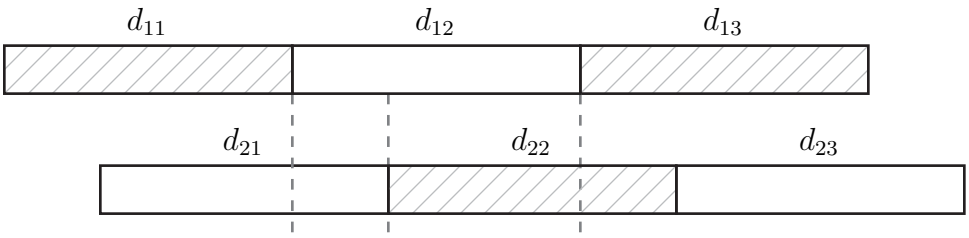

Figure 3.3: Interfering Symbols. Depicting the MAI for the case of two asynchronous users. Each symbol from a user is contaminated by two different symbols from the other user.

an asynchronous system, one symbol of each user is "contaminated" by at most two symbols from each of the other users. Thus, in a K-user system, where there are $(K-1)$ interfering users, the are $(K-1)$ interfering symbols in the synchronous case and up to $2(K-1)$ interfering symbols in the asynchronous case. Figure 3.3 depicts the interfering symbols in an asynchronous system with two users. An increase in the number of interfering symbols from $(K-1)$ to $2(K-1)$ does not imply an increase in MAI in an asynchronous system compared with the synchronous system, because the cross-correlation products are computed only over the overlapping portion of the symbols. In this case, the MAI and the bit error probability are dependent upon the following parameters:

i) Relative magnitudes of the received signals.

ii) Partial cross-correlation values of the spreading sequences.

iii) Power of the additive noise.

Partial cross-correlation values among the spreading sequences are dependent upon how much one symbol overlaps with the other symbol, which in turn depends upon the transmission instants of the individual users and their distances from the base station. It may be probable that the partial cross-correlation values between two sequences exceed the full-period cross-correlation.

When data signals and spreading sequences are purely random, the signal value within each chip interval from each user is completely random. In this instance,

interfering portions of two symbols from each interfering user can be thought of as just one symbol. For example, in Fig. 3.3, portions of d_{21} and d_{22} that interfere with d_{12} can be regarded as a single interfering symbol. Thus, with random spreading sequences, the asynchronous and the synchronous systems will exhibit the same average bit error rate.

3.1.4 SUMF in Rayleigh Fading Environment

The error probabilities discussed in the above sections assume that the received signal amplitudes $A_i(t)$ are deterministic. In a fading environment, however, these coefficients are random and we need to average the error probabilities over the fading distribution [36, 43]. In widely accepted models, as discussed in Sec. 2.3.3, the fading coefficients usually follow the Rayleigh distribution. Averaging the error probabilities according to a Rayleigh distribution results in much higher bit error rates [36, 71], as compared with those obtained in the case of deterministic amplitudes. For a single user, the error probability in Rayleigh fading environment falls linearly with SNR, whereas in AWGN, the error probability falls exponentially with SNR [22,72,73]. Simulation results for bit error rates with SUMF in Rayleigh faded channels are shown in Sec. 3.2, where a comparison with linear multiuser detectors is made.

3.1.5 SUMF for Resolvable Multipath: RAKE Receiver

A RAKE receiver combines independently fading paths in a DS-CDMA receiver. Thus a RAKE receiver implements multipath diversity combining. It consists of a number of SUMF receivers, each of which detects one fading path. The resulting paths are then combined using one of the three algorithms for diversity combining: Selection, Equal-gain, and Maximal Ratio. A thorough analysis of selection diversity combining algorithms is given in [74] and maximal ratio combining is discussed in [75]. A textbook treatment of diversity combining algorithms is provided in [43].

DS-CDMA systems are well-suited for diversity reception because spreading renders the channel wideband, thereby making it easier to resolve multiple path at the

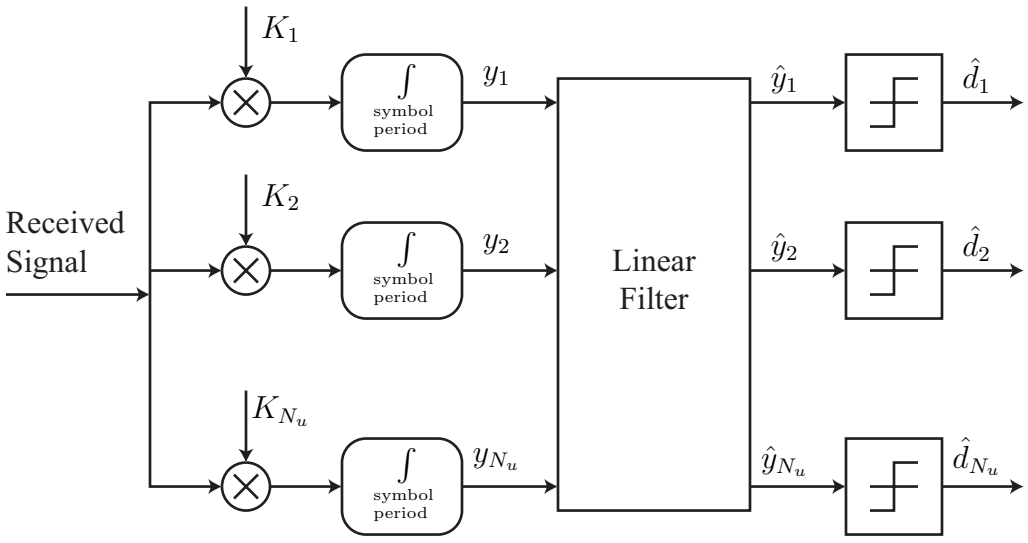

Figure 3.4: Linear Multiuser Detector. A generic linear multiuser detector consists of a linear filter applied at the outputs of a set of single user matched filters. The objective is to reduce the MAI that appears at the output of single user matched filters.

receiver [46]. In fact, multipath resolution and combining is one of the major benefits of DS-CDMA system over other multiaccess wireless communication systems. Diversity combining is a powerful technique to mitigate the effects of fading, the idea being that if the signal along one path fades, other independent fading paths are less likely to experience fading at the same time.

3.2 Receivers with Linear Multiuser Detection

This section describes the analysis and simulation results of linear multiuser receivers employing a single receive antenna; linear multiuser detectors with multiple antennas will be discussed in chapter 5.

Figure 3.4 depicts a generic linear MUD receiver. A comparison of linear MUD with SUMF of Fig. 3.2 indicates that signals from SUMFs are passed through a linear filter before performing the slicing or decision operation. The design of linear filter depends on the specific signal processing algorithm implemented by the detector. Linear MUDs can be based on either the zero forcing (ZF) criterion or the minimum

mean squared error (MMSE) criterion. Both of these designs are discussed in the following sections.

3.2.1 Zero Forcing Linear Multiuser Detector

A ZF linear MUD, or simply ZF MUD, attempts to completely eliminate the MAI in a DS-CDMA system without regard to AWGN. For the purpose of this section, we consider a synchronous CDMA system. The ZF linear MUD for an asynchronous system is considered in Sec. 3.3.

Using Eq. 3.2 for all the users, we write the received signal after despreading in matrix form :

$$\vec{y} = \mathbf{R}\mathbf{A}\vec{d} + \vec{n} \tag{3.9}$$

where $\mathbf{R}$ is the Kasami[10] correlation matrix whose elements are defined by Eq. 2.13, $\mathbf{A}$ is a diagonal matrix that contains Rayleigh fading coefficients for each user, and $\vec{d}$ is the vector of transmitted symbols, which may or may not be coded.[11] Since $\mathbf{R}$ is not a diagonal matrix in general, it reflects the MAI introduced due to non-zero cross-correlations. For a synchronous system that uses orthogonal sequences $\mathbf{R}$ is a diagonal matrix indicating that no MAI exists in the system.

For the derivation of zero forcing (ZF) linear multiuser detector filter, we set the additive gaussian noise term to be equal to zero in Eq. 3.9. Then, by setting the required response to be equal to $\mathbf{A}\vec{d}$, the ZF linear filter is given by $\mathbf{R}^{-1}$. To eliminate MAI, ZF MUD performs the $\mathbf{R}^{-1}$ operation on the received signal $\vec{y}$ [37], as depicted in Fig. 3.5. Thus the vector signal, $\vec{y}_{decor}$, at the output of ZF linear MUD can be written as:

$$\vec{y}_{decor} = \mathbf{R}^{-1}\vec{y} = \mathbf{A}\vec{d} + \mathbf{R}^{-1}\vec{n} \tag{3.10}$$

[10] In general, $\mathbf{R}$ is the cross-correlation matrix of the spreading sequences. Since we use Kasami sequences for the simulation results reported in this thesis, we specialize $\mathbf{R}$ to denote Kasami correlation matrix.

[11] Communication systems generally employ channel encoding prior to transmission; this involves generating a coded bit sequence from the uncoded bit sequence [22]. We consider $\vec{d}$ as a generic data vector: it contains coded symbols if any encoding is used on the channel, otherwise $\vec{d}$ simply contains the raw data.

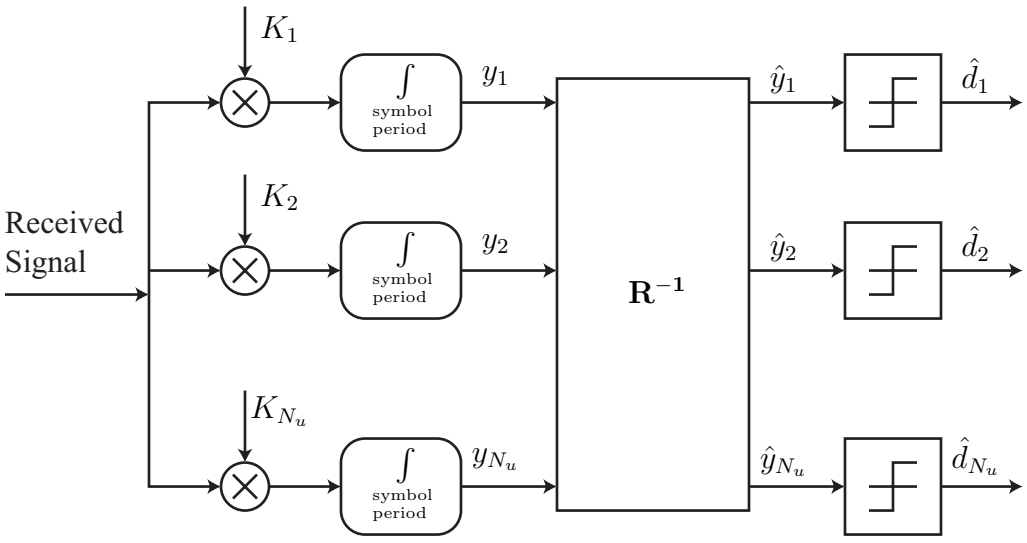

Figure 3.5: ZF Linear MUD. Depicting the zero forcing linear multiuser detector filter applied at the outputs of a set of single user matched filters. The resulting signal contains no MAI if the CDMA system is synchronous.

Decisions made on signs of $\vec{y}_{decor}$, at the output of ZF MUD, are always correct if additive noise term is neglected. However, for low SNRs, the $\mathbf{R}^{-1}\vec{n}$ term becomes significant, resulting in poor performance. The BER performance of a ZF MUD is compared with a single user matched filter detector in Fig. 3.6. Simulation results shown in Fig. 3.6 are obtained using parameters specified in the WCDMA standard proposal submitted by ETSI [63] and are summarized in Table C.1.

Figure 3.6 indicates that the single user matched filter exhibits a BER floor at an SNR of approximately 30 dB: increasing SNR beyond this value does not impact the BER. This error floor, as indicated in Sec. 3.1.2, results from MAI that is not affected by an increase in SNR. ZF MUD eliminates the MAI and, therefore, does not exhibit a BER floor. i.e. an increase in SNR results in a decrease in BER. Also shown in Fig. 3.6 is the graph indicating the performance of the ZF MUD with channel encoding, where a Viterbi decoder (VD) is employed. For this case, a rate $\frac{1}{2}$ encoder of constraint length 5 is used at the transmitter, while a Viterbi decoder employing soft decision decoding is used at the output of ZF MUD [22]. As with the wireline channels, channel encoding and Viterbi decoding brings an SNR gain to the system.

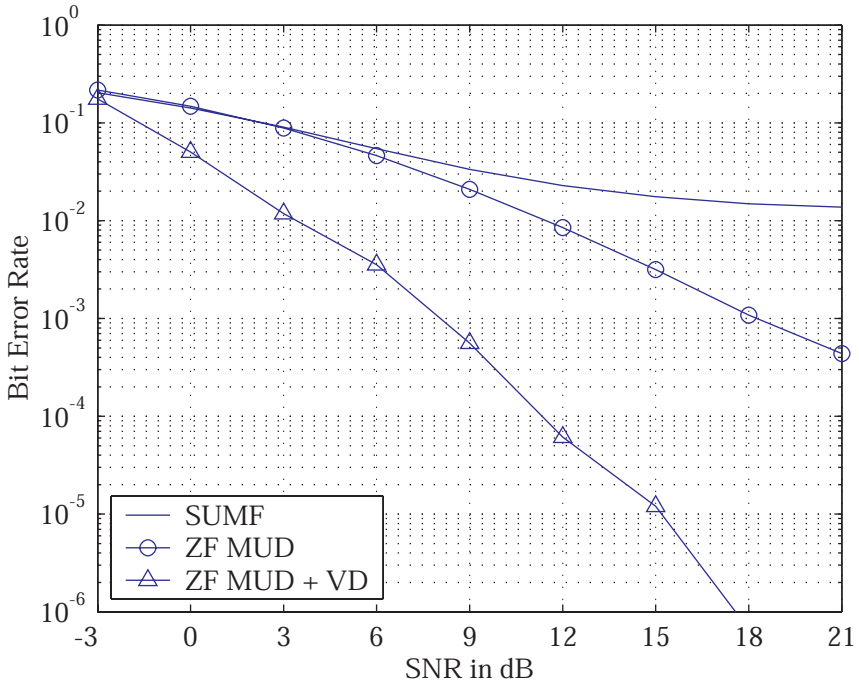

Figure 3.6: ZF MUD Performance. Performance comparison of zero forcing multiuser detector with and without channel encoding. In case of channel encoding, a soft decision Viterbi decoder (VD) is used at the output of multiuser detector.

3.2.2 MMSE Linear Multiuser Detector

Minimizing the mean squared error is an approach to linear multiuser detection that performs as well as or better than the ZF MUD for all SNRs. The zero forcing solution works on the principle of channel inversion and, therefore, leads to poor BER performance at very low signal-to-noise ratios [22]. It is shown in [76] that ZF MUD is the most near-far resistant detector, since it completely eliminates MAI. This point was corroborated in Sec. 3.2.1, where it was shown that ZF MUD doesn't exhibit a BER floor. However, the BER performance of ZF detector is not optimal because the $\mathbf{R}^{-1}$ decorrelating filter merely aims to eliminate MAI without regard to AWGN, which results in additive colored gaussian noise in the detector output $\vec{y}_{decor}$.

MMSE linear MUD performs better than the ZF linear MUD at low and moderate SNRs since it accounts for AWGN [77]. In the case of ZF MUD, the linear filter is given by $\mathbf{R}^{-1}$, whereas for the MMSE MUD, it is given by $(\mathbf{R} + \sigma_n^2 \mathbf{A}^{-2})^{-1}$ as derived

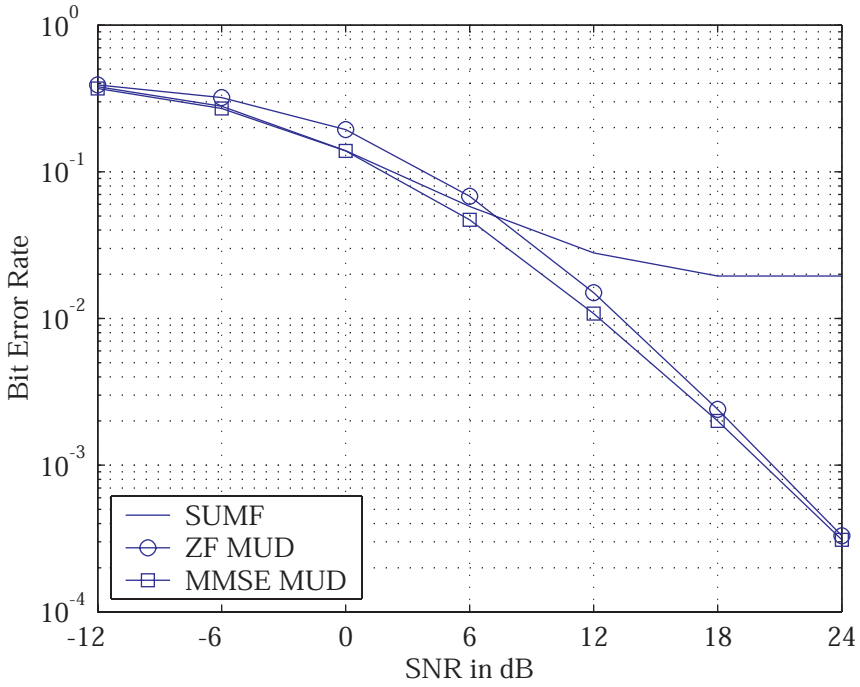

Figure 3.7: ZF versus MMSE Detector. Performance comparison of ZF and MMSE linear multiuser detectors for the case of 15 users using short set Kasami sequences.

in Appendix A. At high SNRs, performance of MMSE linear MUD converges to that of ZF linear MUD, whereas at low SNRs, the difference in performance depends on the following two parameters [22, 78]:

- Effective power in the second term of MMSE linear MUD filter given by Eq. A.1.
- The condition number—ratio of the max to min singular values—of the correlation matrix $\mathbf{R}$.

Figure 3.7 compares the BER performance of MMSE MUD with that of ZF MUD for 15 users. For 12 or fewer users, the performance difference between the two detectors is not noticeable because, for fewer users, the condition number of Kasami correlation matrix $\mathbf{R}$ is not sufficient to cause a performance disparity between ZF and MMSE detectors. For Kasami sequences, $\mathbf{R}$ exhibits a higher condition number as more sequences are selected from the set. Figure 3.7 also indicates that for very low SNRs, ZF MUD performs worse than a SUMF detector, whereas MMSE MUD

performs as well as SUMF. Thus, at low SNRs, MMSE MUD outperforms ZF MUD, whereas at high SNRs, their performance becomes comparable.

Since MMSE linear MUD requires channel estimation [36, 77], and maximum likelihood (ML) MUD is prohibitively complex to implement [79], ZF MUD offers a viable alternative. This thesis thus uses the ZF MUD as the basis for further development of multiuser detection methods.

3.3 Existing Multiuser Detectors

Various MAI reduction schemes, for synchronous and asynchronous systems, have been developed and studied and are discussed in references [36], [37], and [38].

An optimum MUD for asynchronous systems has been derived previously by Verdú [36, 79], but is too complex to implement. A number of sub-optimum low-complexity schemes have since been proposed and analyzed extensively. For asynchronous systems, a linear multiuser detector based on the zero forcing principle was developed by Lupas [80]. This section deals only with linear multiuser detectors, which form the basis for the novel detector presented in the next chapter.

As is evident from Eq. 3.10, the decorrelating matrix required by a ZF MUD is an $N_u \times N_u$ matrix, where N_u is the total number of active users. However, Eq. 3.10 assumes a synchronous CDMA system with flat fading (no multipath). Commercial CDMA systems are asynchronous in nature and require multiuser detection to be performed in an asynchronous environment; such systems differ from synchronous flat-faded systems in two respects:

- Random distances of mobile users from the base station and random transmission instants of mobile users cause the symbols from different users to be received at the base station at different times, thus resulting in an asynchronous system.

- Multiple resolvable paths from each user cause the fading to be frequency-selective (or time-dispersive), also leading to an asynchronous system.

For asynchronous systems, the ZF MUD becomes significantly complex even with flat fading, as an $N_sN_u \times N_sN_u$ matrix is needed for decorrelation, where N_s is the number of symbols in the whole duration of transmission [80]. The technique of discontinuous transmission or isolation bit insertion (IBI) [81] can be used to limit the size of the decorrelating matrix to $N_uN_i \times N_uN_i$ where N_i is the number of symbols after which an isolation bit is inserted. The IBI method not only reduces the effective data rate by a factor $(1 + N_i)/N_i$ but also requires moderate synchronism between the users. Furthermore, it results in a detection delay of N_i symbols.

For frequency-selective synchronous CDMA channels, a ZF MUD proposed in [82], requires an $N_rN_u \times N_rN_u$ decorrelating matrix, where N_r is the number of resolvable paths in the multipath channel. The fact that all of the resolvable paths in a multipath channel have underlying symbols belonging to the same constellation point can be exploited to reduce the decorrelating matrix size to $N_u \times N_u$ for a frequency-selective synchronous CDMA channel, as developed in [83]. Both of these schemes for frequency-selective fading channels work on a single-shot basis; i.e., they consider just one symbol duration and hence intrinsically neglect the multipath from previous symbols contaminating the current symbol.

In conclusion, modelling of frequency-selective channels requires the consideration of asynchronous systems because—although one resolvable path from each user may be synchronized—the multipath scenario that arises from frequency-selective behavior distorts synchronism in a way that can not be controlled. Therefore, commercial CDMA systems, which are frequency-selective, can not be modelled as synchronous systems. Commercial systems fit the asynchronous model and are treated in the next chapter.

Chapter 4

Asynchronous Multiuser Detectors

This chapter presents a new multiuser detector for the CDMA uplink. Unlike previously proposed detectors that employ full period correlations, the scheme proposed here is based on computing partial-period correlations and combining them properly to obtain optimal system performance. We explore several diversity combining algorithms and comment on their applicability in Sec. 4.3. We also show that the new approach represents a generalized implementation of the RAKE receiver [11, 84] that is popular in CDMA systems with multiple resolvable paths.

Although the new approach improves the BER performance, it does not permit increasing the number of simultaneous users significantly in a totally asynchronous CDMA environment. The system capacity, however, can be improved by restricting the system to a quasi-synchronous mode of operation. We analyze the capacity improvements achievable by using such techniques in Sec. 4.7.2

4.1 Desirable Properties of a Detector

A good detection scheme should meet the following requirements:

i) Accommodate asynchronous users

ii) Avoid the BER floor to achieve near-far resistance

iii) Accommodate resolvable multipath gracefully

iv) Match the ZF MUD performance for a synchronous system with flat-fading

v) Match and preferably exceed the RAKE receiver performance

vi) Avoid dependence on the number of symbols in transmission without degrading symbol rate

vii) Allow simplified implementation

viii) Exhibit low detection delay

The novel approach presented in this chapter addresses all of these requirements. It employs a new form of diversity called sub-symbol diversity to achieve multiuser detection in an asynchronous CDMA system with a plurality of resolvable paths from each user.

4.2 The New Approach: Sub-Symbol Scheme

Linear multiuser detection—introduced in Sec. 1.3 and detailed in Chapter 3—consists of SUMF detectors followed by a linear filter. Previously considered methods for linear multiuser detection assume that the only signals available for further filtering are the demodulated signals at the output of SUMF. This assumption leads to a focus on the design of the linear filter at the output of SUMFs. As shown in Fig. 4.1, an additional degree of freedom is possible in the design of linear multiuser detectors when a jointly optimized design of correlators and linear filter is considered.

Previously developed linear MUD designs are based on symbol-period correlation detectors. We propose a partial-symbol correlation detector which is equivalent to joint design of the correlation detectors and the linear filter, as shown in Fig. 4.1. We show that by first performing partial-period correlations according to a specific algorithm causes an asynchronous system behave like a synchronous system with variable length symbols. The ZF MUD for synchronous systems, given in Sec. 3.2.1, can then be applied to such a system. Partial-symbol or sub-symbol correlations,

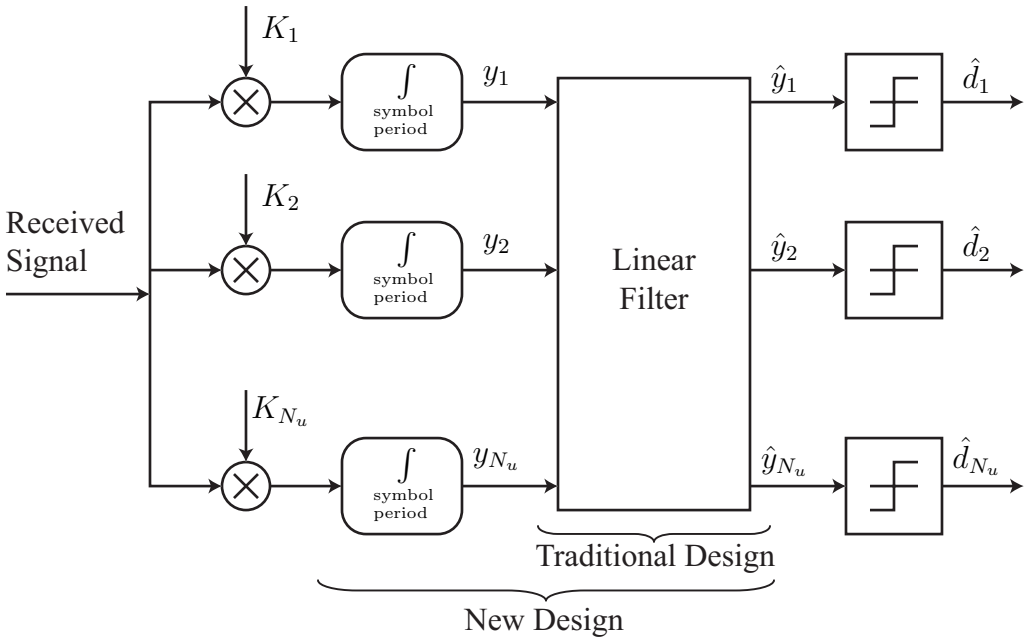

Figure 4.1: Jointly Optimized Design. Depicting the additional degree of freedom introduced as a result of jointly optimized design of linear filter and correlation detectors. Previously developed linear MUD addressed the design of linear filter alone, without consideration of design modification in correlation detectors.

instead of full symbol correlations, result in a reduction in processing gain, however. This reduction is characterized in terms of SNR penalty and can be compensated for by using a combiner within the detector, as explained in the following sections.

4.2.1 Architecture

The sub-symbol scheme operates by dividing each symbol into at most N_u sub-symbols, where N_u is the total number of active users in the system. This partitioning requires knowledge of the symbol boundaries of all other users.[1] For four asynchronous users, the process of sub-symbol formation is illustrated in Fig. 4.2, where each symbol is broken into four sub-symbols. Multiple resolvable paths from each user are initially treated as separate users and then combined after sub-symbol processing.

[1]Symbol boundaries are typically obtained by "Search and Acquisition" algorithms.

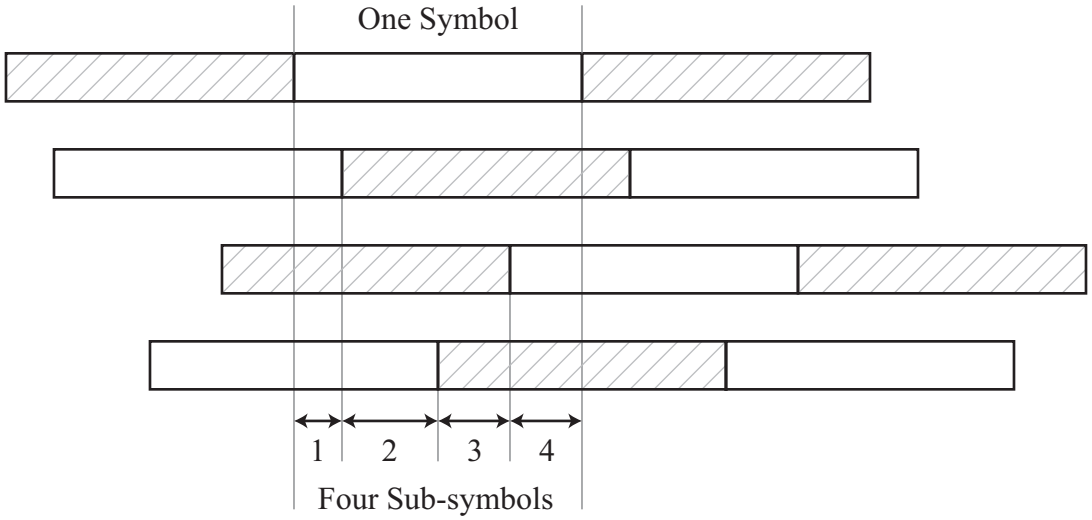

Figure 4.2: Formation of Sub-symbols. Depicting the division of symbols from different users into sub-symbols. A sub-symbol is delimited by the symbol boundaries of any two consecutive users. That is, a sub-symbol does not cross the symbol boundary for any symbol.

Every sub-symbol for a particular user is delimited by boundaries that mark the start of new symbols for any two consecutive users.[2] This makes the asynchronous system behave as a synchronous one with variable length symbols. The correlation operation is performed on a sub-symbol-by-sub-symbol basis, and the result is stored to be combined later with the other sub-symbols originating from the same symbol.

Figure 4.3 considers an example with two users to illustrate the process of decorrelation or zero forcing linear detection in which each symbol is divided into two sub-symbols. This illustration is similar to that of Fig. 3.3 used to describe the MAI in asynchronous systems. Here, the correlation product is computed for each sub-symbol and then dumped at the appropriate time instant, i.e, at the instant where sub-symbol ends. As shown in Fig. 4.3, from $t = t_0$ to $t = t_2$, each of the four demodulated sub-symbols—two from each user—can be mathematically represented as:

$$y_1^1 = \int_{t_0}^{t_1} r(t) K_1(t - \tau_1) dt \tag{4.1}$$

[2]Two users are said to be consecutive if there exist two symbols s_1 and s_2—one from each of these users—with start times t_{s_1} and t_{s_2} at the receiver such that $t_{s_1} < t_s < t_{s_2}$ is not satisfied for any t_s, where t_s is the start time of a symbol from any other user.

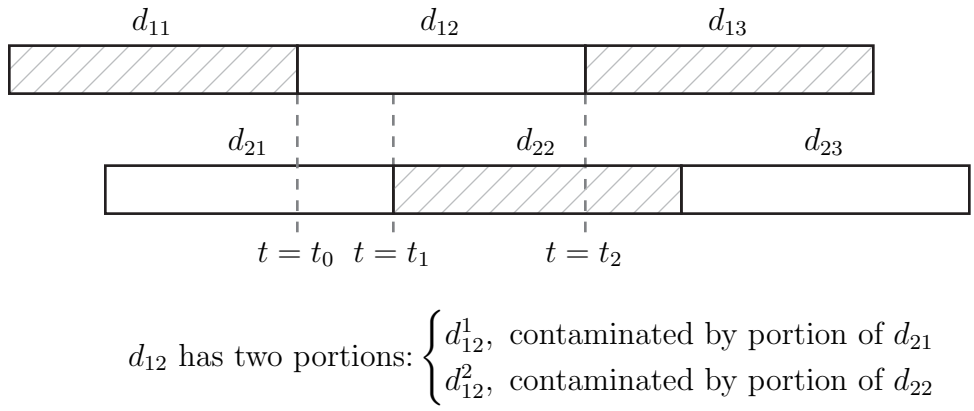

Figure 4.3: Two-User Case. Depicting the MAI in sub-symbols for the case of two asynchronous users. Every symbol is divided into two sub-symbols each of which is contaminated by portions of different symbols from the other user.

$$y_1^2 = \int_{t_1}^{t_2} r(t)K_1(t-\tau_1)dt \tag{4.2}$$

$$y_2^1 = \int_{t_0}^{t_1} r(t)K_2(t-\tau_2)dt \tag{4.3}$$

$$y_2^2 = \int_{t_1}^{t_2} r(t)K_2(t-\tau_2)dt \tag{4.4}$$

where in this instance y_1^1 and y_1^2 belong to the *same* symbol of first user and y_2^1 and y_2^2 belong to *different* symbols of the second user. It is important to note that y_1^1 and y_2^1 contaminate each other as do y_1^2 and y_2^2. Therefore, the decorrelation operation is accordingly performed within each sub-symbol as indicated in Fig. 4.4. The decorrelating matrices $\mathbf{R}_1$ and $\mathbf{R}_2$ are given as follows:

$$\mathbf{R}_1 = \begin{bmatrix} \int_{t_0}^{t_1} K_1K_1 & \int_{t_0}^{t_1} K_1K_2 \\ \int_{t_0}^{t_1} K_2K_1 & \int_{t_0}^{t_1} K_2K_2 \end{bmatrix} \tag{4.5}$$

$$\mathbf{R}_2 = \begin{bmatrix} \int_{t_1}^{t_2} K_1K_1 & \int_{t_1}^{t_2} K_1K_2 \\ \int_{t_1}^{t_2} K_2K_1 & \int_{t_1}^{t_2} K_2K_2 \end{bmatrix} \tag{4.6}$$

The inputs to each ZF decorrelating filter are generated at the same time and no delay is required to perform the decorrelating operation within each sub-symbol.

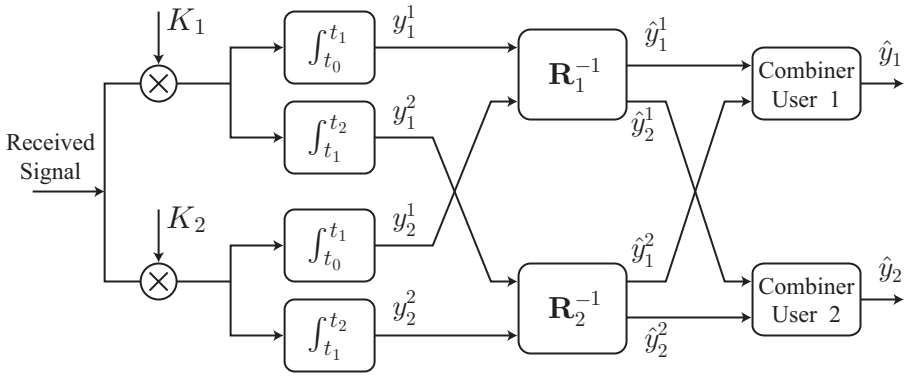

Figure 4.4: New Detection Scheme. Depicting the new sub-symbol based linear multiuser detection scheme for two users. In each sub-symbol, correlations are followed by zero forcing operation. The sub-symbols belonging to a particular symbol are combined in the last stage.

However, the two decorrelating filters $\mathbf{R}_1$ and $\mathbf{R}_2$, in the above case, are not synchronous with each other in that $\mathbf{R}_1$ acts on outputs available at $t = t_1$ while $\mathbf{R}_2$ requires data that are not available until $t = t_2$. Thus, a memory unit is required in the final stage of detection where sub-symbols belonging to a particular symbol are combined using some diversity-based combining algorithm. The inputs to each combiner are offset in time from each other as they come from different decorrelating filters and are, therefore, combined in an asynchronous fashion. Various algorithms used in the combiner are described in Sec. 4.3.

The sub-symbol scheme causes each symbol to undergo multiple decorrelations—one in each underlying sub-symbol—but the size of decorrelating matrices in each sub-symbol is just $N_u \times N_u$. Furthermore, the decorrelating matrices for each sub-symbol belonging to same symbol can be computed in parallel. Thus, with this new approach, ZF multiuser detection can be performed with a much smaller decorrelating matrix and with no increase in bandwidth.[3]

4.2.2 Modified Architecture

The architecture presented in Fig. 4.4 can be simplified by noting that sub-symbols belonging to a particular symbol are non-overlapping. Thus, only one circuit is needed

[3]Isolation bit insertion (IBI) increases the decorrelating matrix size and reduces bandwidth [81].

to compute the correlation product. Figure 4.5 depicts the modified architecture for any number of users. In this case, only one integrator is used for each user and the correlation product is dumped to the appropriate location at the end of each sub-symbol. The switches used to dump the correlation products are controlled by the acquisition and tracking circuit, which is assumed to have acquired correct symbol timing. Furthermore, delay units are incorporated within the final combiner in order to synchronize the inputs coming from different zero forcing decorrelators. The amount of delay induced in each input of a combiner is again determined by the acquisition and tracking block.

4.2.3 RAKE Implementation

RAKE receivers employ multiple detection fingers where each finger is a complete SUMF detector [11], as described in Sec. 3.1.5. Signals at the output of different RAKE fingers are combined using multipath diversity combining algorithms [43]. The new architecture described in Sec. 4.2.1 can be changed to represent a RAKE receiver by simply removing the inverse filter blocks from Fig. 4.5 while considering different RAKE fingers as individual users. The sum of signals generated as a result of multiple sub-symbol correlations over a symbol is exactly the same as the signal generated by one finger of a traditional RAKE. The combiner simply sums the signals at its input and generates a signal corresponding to the signal at the output of one RAKE finger. Thus, the new approach implements the RAKE receiver by removing ZF decorrelating filters, $\mathbf{R}_1^{-1}, \mathbf{R}_2^{-1}, \ldots, \mathbf{R}_{N_u}^{-1}$ from Fig. 4.5. Furthermore, different combiners corresponding to a symbol and its multipath can jointly process the information now available at the granularity of sub-symbols. Although the processing described above may lead to a better performance than that exhibited by a RAKE receiver, it is beyond the scope of this thesis.

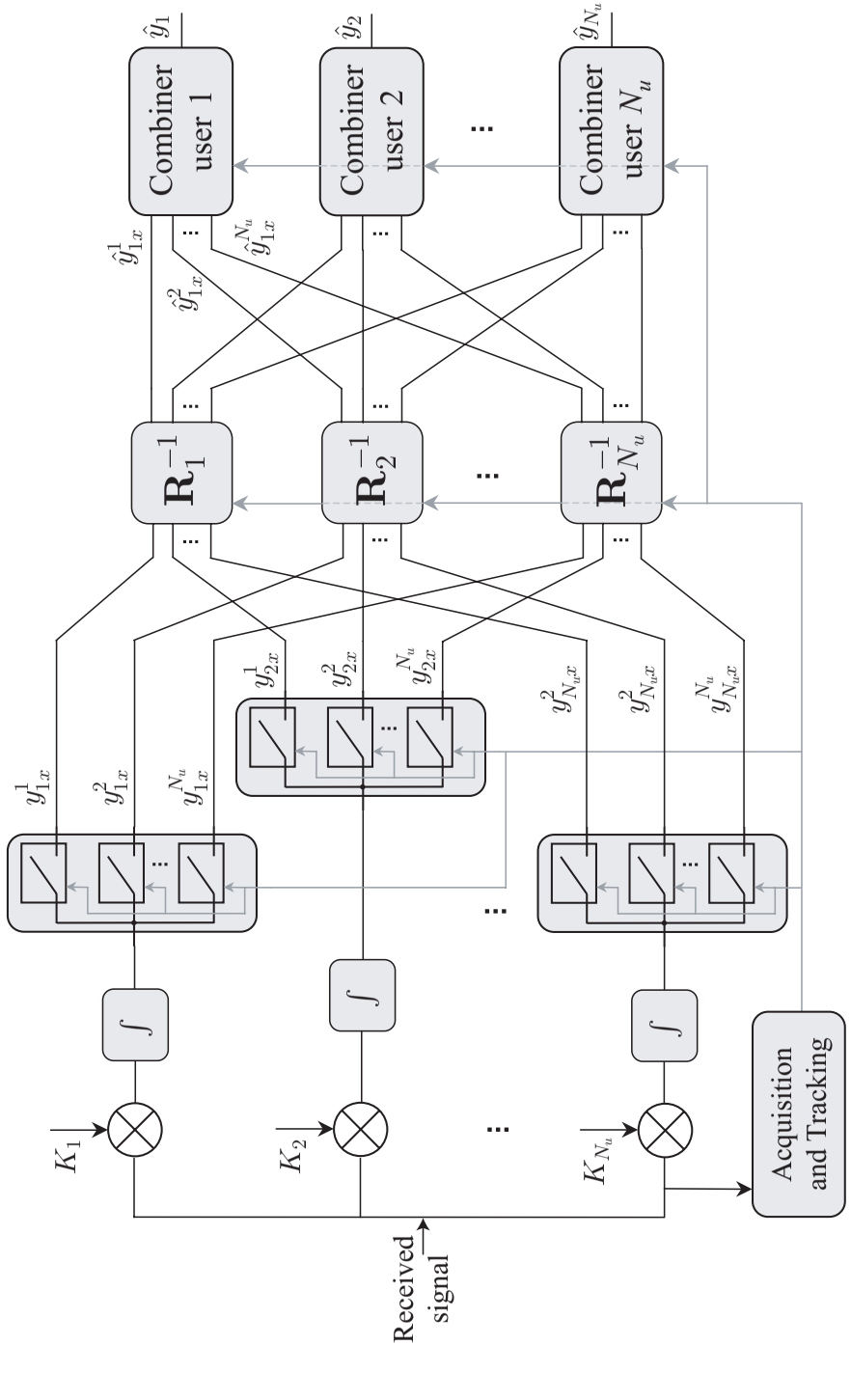

Figure 4.5: Sub-symbol Detection and Combining. Depicting the modified architecture for sub-symbol decorrelation and combining for N_u users. The outputs of the integrators are dumped at each sub-symbol boundary. Inputs to each decorrelating filter $\mathbf{R}_i^{-1}$ come from those dump circuits whose outputs are available at the same time. The subscript "x" in the outputs indicates that the value is computed every symbol period. Inputs to each combiner are available at different times and are synchronized by using delay units within the combiners.

4.2.4 Stability

The decorrelation matrix to perform the zero forcing operation is obtained by taking the Moore-Penrose generalized inverse of the correlation matrix such as the ones given in Eq. 4.5 and Eq. 4.6 [76]. If the correlation matrix is not badly scaled, the ZF MUD remains optimally near-far resistant and the signals from different users can be decorrelated successfully. In the case of badly scaled correlation matrix, however, zero forcing operation can't be performed and the performance reaches that of a single user matched filter. Further, we note that a correlation matrix with high condition number results in inferior BER performance of the ZF MUD as compared to an MMSE MUD [78]. The proposed scheme is thus based on two thresholds as follows:

i) *Chip Threshold* (γ_c) which indicates that a sub-symbol should be processed only if the size, in number of chips, of that sub-symbol exceeds this threshold. This threshold is used to eliminate all instances in which the number of users is greater than or equal to the number of chips in a sub-symbol.

ii) *Condition Number Threshold* (γ_n) which indicates that a particular sub-symbol should not be processed if the correlation matrix during that sub-symbol is badly scaled. This is used to avoid the cases of correlation matrix accidentally becoming ill-conditioned even with large number of chips over which correlation is performed.

As previously mentioned, asynchronism arises in wireless CDMA for two reasons: random transmission instants and distances of users, and frequency selective fading. The former is controllable while the latter has to be accounted for by the detection scheme. Since the proposed scheme depends on the chip threshold, at those times when, by chance, the symbols from some users are synchronous, the more chips are likely to be in a sub-symbol and the better the scheme works. It is shown in Sec. 4.7 that the sub-symbol scheme needs only one "long" sub-symbol with an easily invertible correlation matrix to essentially eliminate MAI. In the simulation of a general CDMA system, we consider the worst case scenario for asynchronous users. That

is, no effort is made to synchronize the symbol starting instants which are taken as independent and uniformly distributed over the symbol period. When the system is synchronous with flat fading, there is just one sub-symbol per symbol, and the scheme achieves the performance of the ZF MUD.

4.3 Combining algorithms

We now consider two sets of sub-symbol diversity combining algorithms: *simple* algorithms, and *condition number based* algorithms.[4] Simple algorithms are similar to the ones used in RAKE receivers [11,43], the difference being that RAKE combining algorithms operate on signals from different resolvable paths, while in the new scheme, the combining is done for sub-symbols. Three simple algorithms for sub-symbol diversity combining are as follows:

i) *Select-best*: In this algorithm the sub-symbol with maximum amplitude is selected.

ii) *Weighted*: In this case, each sub-symbol is weighted by the strength of the signal within that sub-symbol.

iii) *Accumulate*: This algorithm simply sums the signal in all the sub-symbols belonging to a particular symbol and the decision is made on the accumulated result.

In addition to the simple combining algorithms, the sub-symbol architecture lends itself to the definition of a new family of algorithms since the signals are obtained from different sub-symbols which, unlike RAKE fingers, are obtained by performing correlations over different numbers of chips. For example, in condition number based combining algorithms, the three simple algorithms described above are modified such

[4] Another set of algorithms has been identified which uses the lengths of the sub-symbols while performing the combining. It was not pursued further due to inferior performance.

that each sub-symbol is weighted by the inverse condition number of the decorrelation matrix during that sub-symbol. This idea is based on the result presented in [78] where it is shown that the BER performance of ZF MUD deteriorates with the increasing condition number of the correlation matrix.[5] Such algorithms exhibit better BER performance than simple combining algorithms as indicated by the results given in Sec. 4.5.

4.4 Computational Complexity

The sub-symbol scheme allows detection of signals from various users in an asynchronous CDMA channel with lower complexity than is required to implement previously known schemes. As stated earlier in the chapter, the scheme can also implement a generalized RAKE receiver without requiring any matrix inversion. At first it may appear that the scheme would require inverting a number of matrices per symbol as large as the total number of users. In fact, simulations show that the addition of more users to the system does not produce a linear increase in the number of matrices to be inverted, but may actually decrease this number, at the cost of a BER penalty. This occurs because adding a user to the system may cause a sub-symbol to be divided into two sub-symbols such that none of them passes the chip threshold criteria. While the complexity of many previously known schemes can be computed exactly, the complexity of sub-symbol diversity combining scheme greatly depends upon the thresholds selected and the relative asynchronism among users. Evaluation of the exact value of computational complexity is not a performance-related issue and has been scoped out of this thesis.

4.5 Performance Analysis and Results

Zero forcing linear MUD is known to completely suppress MAI and is optimally near-far resistant [36, 70, 76, 78]. Because the sub-symbol scheme presented in the

[5] This result is also explained in Sec. 3.2.2.

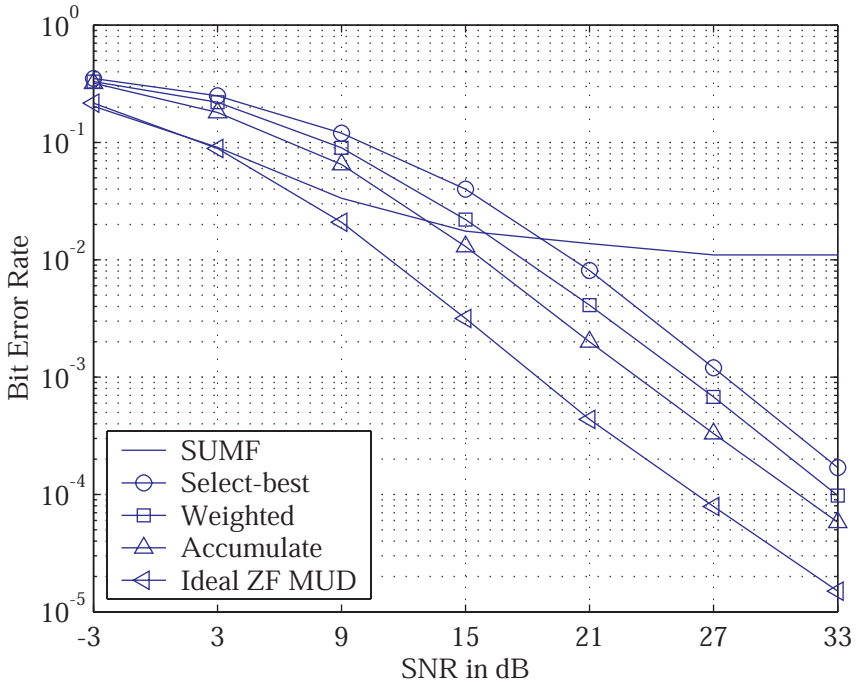

Figure 4.6: Simple Combining Algorithms. Performance comparison of three simple combining algorithms with the SUMF and ideal synchronous ZF MUD.

previous sections employs the zero forcing principle in each sub-symbol to eliminate MAI, it performs significantly better than a single user detector. The performance margin between the new scheme and the single user detector depends upon the specific combining algorithm used.

Figure 4.6 depicts the BER performance results for simple sub-symbol diversity combining algorithms. These algorithms are similar to the ones used in combining multipath diversity [11]. Of the three simple combining algorithms, the accumulate algorithm exhibits the best BER performance, because it tends to average the noise over the whole symbol. Since ZF MUD is known to perform poorly at low SNRs, the three simple combining algorithms also show poor performance at low SNRs because they are based on the zero forcing principle. Furthermore, Fig. 4.6 indicates that the simple combining algorithms perform 4 dB to 8 dB worse than an ideal ZF MUD used in completely synchronous system for uncoded BERs of 10^{-2} or better. That is, the three algorithms require 4 dB to 8 dB higher SNR than that required by an ideal

ZF MUD to realize the same bit error rates.

An approximate expression for the performance loss with respect to ideal ZF MUD can be derived for each of the simple combining algorithms. The derivation is greatly simplified by assuming that fading imposes a fixed penalty[6] in both cases: the ideal ZF MUD case, and the case of simple combining algorithms. The fixed fading penalty assumption allows the use of non-faded systems to compute the relative degradation in BER for different receivers. The details of this computation are given in Appendix B.

Since the ZF MUD performance is dependent on the condition number of the decorrelating matrix [78], it is possible to do better than the simple algorithms. This is accomplished by using an algorithm that weighs the sub-symbols in inverse proportion of the condition numbers of correlation matrices within those sub-symbols. Figure 4.7 compares the BER performance of such an algorithm with that of a simple accumulate combining algorithm. It can be seen that the condition number based algorithm provides an approximate gain of 3 dB over the simple accumulate combining algorithm for 10^{-2} or better BERs. Condition number based algorithms exhibit superior performance since they suppress those sub-symbols that lower the BER performance due to badly scaled correlation matrices.

4.6 Near-Far Resistance with Sub-Symbol Scheme

The near-far problem arises when signals from mobile users reach the base station with unequal powers. When this occurs, the signal from the user with the lowest power is swamped out by the stronger interfering signals and thus suffers the highest BER. It is well known that full symbol correlation based ZF MUD is the most near-far resistant detector [36, 76]. To quantify the near-far resistance in terms of BER, we performed simulations by placing one user, with weak signal, far from the base station, and then noting the BER for this user while other users move progressively closer to the base station. Average received power from the "far user" is fixed while

[6]Fixed penalty means that fading degrades the BER performance of each receiver in the same way.

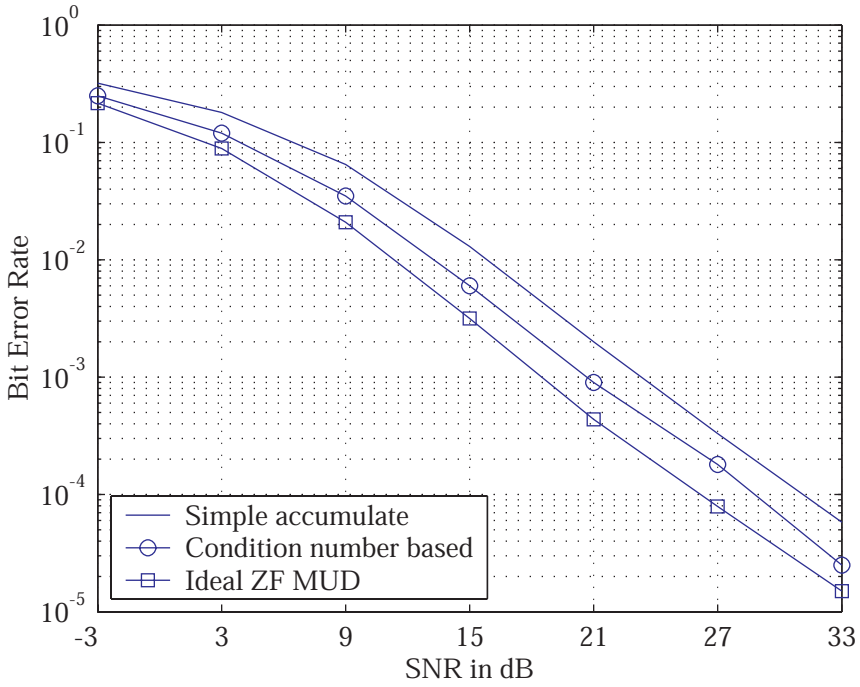

Figure 4.7: Condition Number Combining. Depicting performance improvement by doing condition number based combining rather than simple combining. The curve for ideal ZF MUD is also shown for comparison purposes. At a bit error rate of 10^{-3}—typical for voice applications—condition number based accumulate algorithm performs 3 dB better than simple accumulate algorithm. For the simulations shown here, a condition number threshold of 200 is used.

the average received power from other users is increased as those users move towards the base station. It can be seen from Fig. 4.8 that SUMF is not near-far resistant and results in an increase in the BER of the weak user as other users move towards the base station. Since the combining schemes presented here are based on performing a ZF MUD in each sub-symbol, these schemes show extremely good near-far properties, as depicted in Fig. 4.8.

All combining schemes that are based on sub-symbol diversity, whether simple combining or condition number based combining, show a nearly constant BER for the user with a weak signal, if the average received power from other users is allowed to change. This verifies that the sub-symbol scheme is, in fact, near-far resistant. Figure 4.8 shows that the condition number based combining scheme offers the best

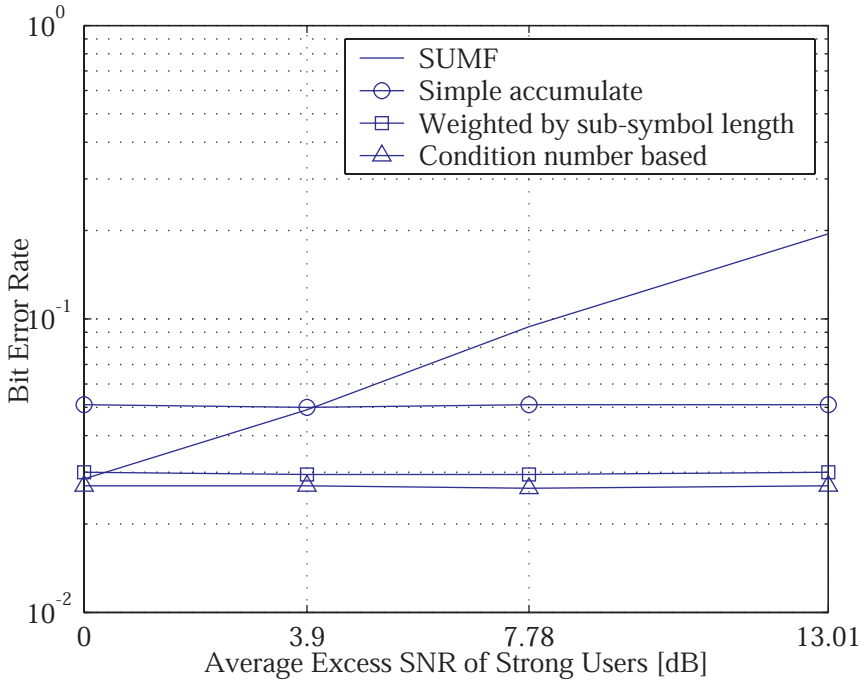

Figure 4.8: Near-Far Resistance. Comparing the near-far resistance of SUMF with various sub-symbol combining methods. A constant BER indicates that sub-symbol combining methods are near-far resistant, while an increase in BER when interfering signals become stronger indicates that SUMF is not near-far resistant. Excess average SNR is the difference between average SNR in interfering signals and the SNR in desired signal from the far user.

(i.e., lowest) BER and is completely near-far resistant. The simulations were performed when the average SNR of strong interfering users exceeded the average SNR of the far user by as much as 13 dB.

4.7 Maximizing System Capacity

This section focusses on fine tuning the sub-symbol technique to maximize the number of simultaneous users for the combining algorithms described in Sec. 4.3. Here we assume that moderate synchronism is achieved, as in a QS-CDMA system, by issuing downlink commands to the users to adjust their transmission instants.

In previous sections it is assumed that user transmission is uncontrolled, which implies that the starting instants of symbols received at the base station are uniformly

distributed over the entire symbol period. For a small number of users, the sub-symbol intervals are long enough to allow easy decorrelation. But as the number of users increases, the expected size of the sub-symbols becomes smaller, and it becomes more difficult to perform ZF decorrelations within sub-symbols. When the number of chips in a sub-symbol falls below the number of users, it is impossible to decorrelate the signals of all the users in that sub-symbol successfully because the decorrelation matrix always has one or more zero eigenvalues. In particular, if N_c is the number of chips in a given sub-symbol, the maximum number of linearly independent users in that sub-symbol is also N_c.[7] When the actual number of users is greater than N_c, the correlation matrix is singular and the signals within that sub-symbol can not be completely decorrelated.

4.7.1 Types of Sub-Symbols

When the number of chips in a symbol is smaller than the total number of active users, a regular inverse of the correlation matrix does not exist [76]. The same is true for sub-symbols. In such cases, a generalized inverse or pseudo inverse has to be used, while the condition number threshold γ_n is set to infinity. Towards this end, we distinguish between two types of sub-symbols for a given user: a *clean* sub-symbol indicating that the signal from this particular user has been successfully decorrelated in this particular sub-symbol, and a *corrupted* sub-symbol which corresponds to one of the zero eigenvalues of the correlation matrix.

When the correlation matrix is not of full rank, the maximum number of clean sub-symbols is equal to the rank of the correlation matrix. Although one "long" sub-symbol in which decorrelation can be performed is sufficient to bring the BER down by a significant amount (see performance of select-best type simple combining algorithm in Sec. 4.3), combining many clean sub-symbols brings down the SNR penalty.[8] Combining the corrupted sub-symbols with the clean sub-symbols, however,

[7] See [76] for details.

[8] SNR penalty results from reduced processing gain; it is computed in Appendix B.

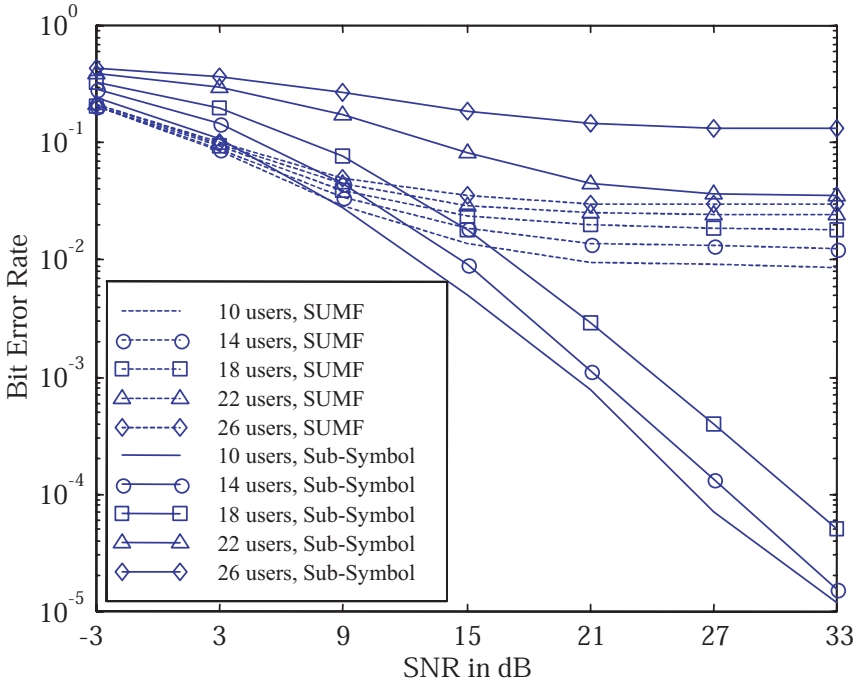

Figure 4.9: Maximum Allowable Number of Users. Indicating the BERs for SUMF and sub-symbol scheme for various number of users; for sub-symbol combining, condition number based accumulate algorithm is used with $\gamma_c = 1.25N_u$ and $\gamma_n = \infty$, where N_u is the total number of active users in the system.

degrades the BER, so that it is preferable not to combine corrupted sub-symbols at all.

For an asynchronous CDMA system, where transmission instants are uncontrolled, we simulated the sub-symbol scheme for a relatively low value of γ_c that is less than 5% of the spreading gain. In this instance, combining all sub-symbols—clean or corrupted—with the simple combining algorithms results in the allowable number of users only up to 8–9% of the spreading gain. A higher value of γ_c further reduces the allowable number of users because sub-symbols become smaller with an increase in the number of users, and none of them is used in combining. This is also indicated in Fig. 4.9 for a spreading gain of 255 with Kasami sequences. As more and more users are packed, sub-symbols become smaller and smaller. For a given user, many of the sub-symbols become corrupted thereby affecting the BER performance significantly.

4.7.2 Sub-Symbol Scheme for QS-CDMA Systems

QS-CDMA systems, introduced in Sec. 3.1.1, reflect a moderately controlled environment in which users are instructed[9] to adjust their transmission instants such that their symbol arrival times at the base station fall within some fraction of the symbol period. This kind of moderate synchronization is easier to implement than a fully synchronized system.

For a QS-CDMA system employing sub-symbol detection, the thresholds for sub-symbol decorrelation play an important role in determining the maximum number of users that can be simultaneously accommodated in a QS-CDMA system employing the sub-symbol scheme. The chip threshold γ_c is set sufficiently high such that only one sub-symbol is used for demodulation. Use of such values for γ_c further reduces the processing gain resulting in an SNR penalty, but if the signals from users can be decorrelated successfully, simulations indicate that a significant improvement is seen in BER for medium to high SNRs. For a QS-CDMA system with large number of users, the sub-symbol combining system becomes the one that only uses selection sub-symbol diversity since we consider only one dominant sub-symbol per symbol. Thus, in this case, all the sub-symbol diversity combining algorithms converge to the select-best sub-symbol combining algorithm. In this case, it is further known which sub-symbol is selected for decorrelation in the select-best algorithm.

4.7.3 SNR Penalty for QS-CDMA Systems

The SNR penalty is defined as the degradation in SNR that results from partial-period correlations instead of full period correlations. It is, therefore, the result of reduced processing gain of the sub-symbol scheme. The SNR penalty for select-best algorithm is derived in Appendix B and is given by $\frac{N}{M}$, where N is the total number of chips per symbol and M is the number of chips used to perform partial-period or sub-symbol correlation. This penalty can be reduced if fewer users are present and more sub-symbols can be combined. If the system is moderately synchronized, as in

[9]Sending commands on the downlink can accomplish this.

	$P = 64$	$P = 128$	$P = 192$
$N_u = 10$	196.86	139.26	81.65
$N_u = 30$	192.66	130.77	68.90
$N_u = 50$	191.83	129.08	66.35
$N_u = 70$	191.50	128.37	65.27
$N_u = 90$	191.32	127.98	64.67

Table 4.1: Expected number of chips in a sub-symbol.

case of QS-CDMA, and the users are allowed to have their transmission instants lie within the first P chips of a reference symbol,[10] then the expected value of M is given by:

$$\begin{aligned} E[M] &= (N-P) + \sum_{i=0}^{P-1} \left\{ i(\alpha^i - \alpha^{i+1}) \right\} + P\alpha^P \\ &= (N-P) + \frac{\alpha - \alpha^{P+1}}{1-\alpha} \end{aligned} \tag{4.7}$$

where α is defined as:

$$\alpha \equiv \left(\frac{P-1}{P} \right)^{N_u} \tag{4.8}$$

For practical reasons, P is a large fraction of N, typically ranging from 50% to 80%. In such cases, the expected value of M for a large number of users is approximately given by $N - P$; for $N = 255$, exact expected value of M is listed in Table 4.1.

4.8 Threshold Optimization

For the decorrelation process in each sub-symbol, either the regular inverse, which we will denote by $\Im$, or the generalized inverse, denoted by $\wp$, is used. We consider the effect of thresholds in each case. The condition number threshold γ_n is important only if the $\Im$ operation is performed and does not have any significance for the $\wp$ operation. As long as the number of chips in a sub-symbol is less than the number of users in that sub-symbol, the $\Im$ operation can not be performed. Thus, the performance of the $\Im$

[10] Also see Sec. 3.1.1.

operation becomes independent of γ_c when γ_c is less than the number of users. As the number of users increases, it may not be possible to perform the $\Im$ operation at all and the $\wp$ operation is the only recourse. In such a case, a small value of γ_c results in more and more sub-symbols being considered for decorrelation, which increases the probability of contamination of clean sub-symbols by the corrupted sub-symbols.

For a given γ_c, increasing the number of users brings two benefits: more users are accommodated, and there is less chance for a corrupted sub-symbol being considered for combining with closely packed users. Therefore, when transmission instants of users can be bound within a small region, a value of γ_c exceeding the length of that region is desirable. Otherwise, with fewer users, it is better to use the $\Im$ operation.

When the $\wp$ operation is used, it is ensured that in each sub-symbol there are enough chips to decorrelate the signals from various users. If there are many corrupted sub-symbols and fewer clean sub-symbols in a sub-symbol interval, it is advantageous to isolate all the sub-symbols in that interval without using them in sub-symbol combining. Obviously, the ideal situation is to be able to pick the sub-symbols for only those users that have been decorrelated successfully. If it is not possible to selectively pick users from within a sub-symbol, the chip threshold γ_c should be selected such that there is a good chance for most of the users to be decorrelated. Thus as the number of users increases, a larger value of γ_c is needed, up to a certain limit, after which it should be set to a constant value such that we have at least one sub-symbol to carry out the decorrelation process.

An alternate measure for performance adjustment is the rank threshold γ_r, which indicates that the decorrelation operation is performed in a sub-symbol if the corresponding correlation matrix has a rank that exceeds γ_r. We consider following two cases for a QS-CDMA system:

i) Number of users is small such that $N_u \ll N_c$ for all sub-symbols. In this case, γ_r is made equal to the number of active users. Furthermore, either γ_c or γ_n is used in conjunction with γ_r. The possibility of combining corrupted sub-symbols is reduced by using one of the following two strategies:

	Pseudo Inverse ($\wp$)	Regular Inverse ($\Im$)	
		$\gamma_n = 200$	$\gamma_n = 500$
$P = 128; \gamma_c = 0.25N_u$	117	97	110
$P = 192; \gamma_c = 1.00N_u$	62	51	53

Table 4.2: Maximum number of supported users. The numbers shown are determined when the conditions in the table result in a BER that is an order of magnitude less than the BER exhibited by an SUMF at an SNR of 30 dB.

(a) Choose γ_c slightly larger than N_u; by using much higher values for γ_c, we run the risk of not considering an interval in which all the sub-symbols are clean. For $\gamma_c < N_u$, we do not avoid combining of corrupted sub-symbols.

(b) Choose γ_n in the medium range; lower values run the risk that clean sub-symbols will not be combined, and higher values do not avoid combining of corrupted sub-symbols.

ii) Number of users is very large. Under this condition, we have only one sub-symbol available that needs to be decorrelated and a value of γ_r slightly smaller than the number of users would be the right choice.

Table 4.2 depicts the maximum number of users in a moderately synchronized system with a spreading gain of 255. The maximum number of supported users shown in this table is determined by the criteria that the sub-symbol detector results in a BER that is at least an order of magnitude better than the single user matched filter receiver at a signal-to-noise ratio of 30 dB.

4.9 Recap

This chapter presents a sub-symbol based computational scheme for linear multiuser detection in a DS-CDMA system. This scheme facilitates decorrelating the undesired signals from the received signal at the base-station receiver. Further, it keeps the linear decorrelating filter computationally tractable while accommodating the asynchronicity of users created by random transmission instants and multiple resolvable

paths. Unlike previous multiuser detection schemes for asynchronous systems, this scheme does not depend on the number of symbols in the duration of transmission and it does not reduce the symbol transmission rate.

The sub-symbol scheme uses a new kind of diversity which we call sub-symbol diversity. Algorithms for diversity combining of sub-symbol are also presented in this chapter. Simulations confirm that the sub-symbol scheme is near-far resistant and performs significantly better than a SUMF detector.

The new scheme also represents an alternate construction of the RAKE receiver where reduction in multiple access interference (MAI) is not the primary objective. In such a case, signals from users are not decorrelated within sub-symbols and the sub-symbol diversity combiner is used as a multipath diversity combiner.

Though the application of sub-symbol method to asynchronous systems improves the BER for all users, it still limits the maximum number of users and, therefore, does not improve the system capacity significantly. When the sub-symbol method is applied to a QS-CDMA system, however, system capacity improves and the total number of users accommodated in such a system is given roughly by the length, in number of chips, of the longest sub-symbol. In QS-CDMA systems, when the appropriate values for the chip and condition number thresholds are used, the "select-best" sub-symbol scheme can support a maximum number of users that is approximately given by the maximum number of chips in any sub-symbol. For example, if the longest sub-symbol is 63 chips long, irrespective of the spreading factor, the maximum number of users supported is approximately 63. In this case, for each user, the sub-symbol based MUD yields a BER that is at least an order of magnitude better than a SUMF detector.

Chapter 5

Multiple Antenna Systems

This chapter presents signal processing and communication techniques that make use of multiple antennas at the transmitter and the receiver. The use of multiple antennas for wireless communications produces significant performance improvements, including the reduction of bit error rates and the increase of capacity. These improvements allow more users to access the system with higher data rates for the same bit error rates than is the case of single antenna. How multiple antenna systems can be combined with linear multiuser detectors to enhance the performance of a DS-CDMA system is the subject of this chapter.

"Beamforming" and "adaptive array processing" are terms used primarily to refer to the use of multiple receiving antennas in a mobile communication system. To avoid confusion, however, it should be noted that beamforming is used to also refer to the use of multiple transmitting antennas at the base stations in fixed wireless systems.[1] For the purpose of the discussion of the mobile DS-CDMA environment, we restrict the use of these terms to a system with multiple receiving antennas.

While beamforming (BF) with multiple receiving antennas significantly improves the BER performance, it fails to suppress multiple access interference, resulting in an irreducible BER floor. Adding channel encoding at the transmitter and soft-decision Viterbi decoding (VD) at the receiver further lowers the BER floor. Furthermore,

[1]Fixed wireless systems can be cellular or non-cellular and have the constraint that the end users are not mobile.

a combination of BF and linear MUD results in effective elimination of MAI while maintaining better BERs at low SNRs.

This chapter provides the vector channel model that characterizes a wireless system with multiple antennas. It also presents simulation results for the case of multiple receiving antennas with one dominant path from each mobile user. Such results depict the effect of using multiple receiving antennas in a wireless communication systems. The simulations performed are for a DS-CDMA system with specifications as given in some of the proposed WCDMA standards [63]. We demonstrate that it is preferred to define the "performance gain" achieved by multiple antenna system in terms of improvement in BER rather than as a decrease in required SNR. We further argue that such definition of performance gain is applicable to most communication systems that exhibit a BER floor.

5.1 Background

All multiple access systems employ some form of filtering at the receiver to recover the desired signal. In an FDMA system, a receiver rejects the undesired signals and recovers the desired signal by passing the composite signal through a narrowband filter. In TDMA, time selection is achieved based on the knowledge of time frames during which signals from different users are received. In CDMA, "code-matched" filtering or correlation detection is performed to recover the desired signal whilst attenuating the other undesired signals. Multiple antennas (or an antenna with multiple elements) provide a means of performing spatial filtering which offers increased signal-to-interference-plus-noise ratio (SINR) by increasing the relative antenna gain in the direction of the desired user. The notion of spatial filtering is, therefore, synonymous with beamforming, where the tap weights dictate the antenna gain pattern.

5.1.1 Classification of Multiple Antenna Systems

From a signal processing point of view, systems using multiple antennas can be broadly classified into three different categories:

i) Systems in the first category use multiple receiving antennas with one path from each transmitting handset in a multiple access channel. In such systems, array signal processing algorithms are used to combine signals from different receiving antennas. These algorithms and the conditions under which they are applicable are specified later in the chapter.

ii) In the second category, the receiver has multiple antennas with the possibility of multiple paths from each mobile user. In this case, array signal processing needs to be combined with processing in time—the combination is referred to as space-time (ST) processing. Although ST processing can be used at the transmitter as well as at the receiver, the term is generally used to describe the processing at the receiver. The ultimate goal is to equalize the multiuser channel thereby combating channel impairments that include multipath fading, co-channel interference (CCI), delay spread, and thermal noise.

iii) The third category of systems uses multiple antennas at both the transmitter and the receiver. This enables the use of ST processing at the receiving end and *space-time coding* at the transmitting end. This is the most common situation of using multiple antennas in a mobile communication system.

Another important, and sometimes overlooked, way of classifying the multiple antenna systems is by considering the spacing between antenna elements. This spacing between the elements is very important for ST processing (at the receiver) or ST coding (at the transmitter) as it gives an idea of the correlation between the signals at different antenna elements. The farther the elements are spaced, the lower is the correlation between the signals received at each antenna element. When the elements are sufficiently spaced, the signal decorrelates from one element to the other. That

is, signals at different elements undergo uncorrelated fading. In such an instance, signals from different elements can be combined to realize a form of diversity called *antenna diversity*. Therefore, multiple antenna systems can be viewed as providing one or both of the following gains:

i) Diversity gain, which is achieved if individual elements are widely spaced and undergo uncorrelated fading. Diversity gain allows a reduction in average output SNR per antenna for a given bit error rate.

ii) Directional gain, which is achieved when the elements are closely placed. This gain, also called directive gain, signifies the reduction in required received signal power for a given output SNR.

Element spacing that achieves uncorrelated fading is generally a complex function of the signal frequency and propagation environment [85]. The most important environmental factor that effects the required element spacing for signal decorrelation is the angular spread:[2] the smaller the angular spread, the farther the elements need to be placed for the received signals to fade independently [87]. Thus, the requirement for signal decorrelation at different elements leads to large antenna sizes in such environments that exhibit small angular spread (for example, base stations mounted on the top of the buildings). In such instances, where angular spread is small and antenna size is limited, diversity gain may not be realized because of correlated fading on individual antenna elements. Still, the directional gain makes use of multiple antennas an attractive choice. In fact, smaller angular spread results in larger directional gain by using multiple antennas, so that the two types of gains realized by multiple antenna systems tend to compensate for one another's deficiencies.

[2]Estimation of angular spread is accomplished by means of super resolution techniques. See [86] for details.

5.2 Beamforming Mechanism

The beamforming mechanism is described by means of an *array response vector* and a beamformer tap *weight vector* (i.e., tap weights in the spatial filter). In order to appreciate the benefits of spatial filtering, consider two users and a receiving antenna with two elements. If v_{11} and v_{21} are the antenna gains for user-1 at the two elements while v_{12} and v_{22} are those for user-2, then the array response vectors for the two users are expressed as $[v_{11} \quad v_{21}]^T$ and $[v_{12} \quad v_{22}]^T$, where $[\cdot]^T$ denotes the transpose.

For the two user and two antenna example, there is one beamformer for each user. The beamformer for the $1st$ user simply provides a beamformer tap weight vector $\vec{w}_1^* = [w_{11}^* \quad w_{21}^*]$, where asterisk in the superscript denotes the conjugate of a scalar. For the two users, overall gains obtained from this beamformer are:

$$\text{For user-1: Gain is } g_{11} = w_{11}^* v_{11} + w_{21}^* v_{21}$$
$$\text{For user-2: Gain is } g_{12} = w_{11}^* v_{12} + w_{21}^* v_{22}$$

To suppress the signal from user-2, we need $g_{11} > g_{12}$, which can be achieved by a judicious choice of $\vec{w}_1^*$. Specifically, consider a user whose angle of arrival (AOA) is θ at a uniform linear array, as shown in Fig. 5.1. The array is assumed to have N_m similar elements with element spacing d. In the case of a planar wavefront, the path difference between two consecutive elements is $d \sin\theta$, such that the corresponding phase difference is as follows [88]:

$$\phi = d \sin\theta \Big(\frac{2\pi f_c}{c}\Big) = 2\pi \sin\theta \Big(\frac{d}{\lambda}\Big) \tag{5.1}$$

where f_c is the carrier frequency, λ is the wavelength, and c is the velocity of the incident wave.

The array response vector is an indication of how an array responds to a signal. For a single AOA, the array response vector is given by:

$$\Big[v_0 \; v_0 e^{-j\phi} \; v_0 e^{-j2\phi} \; \ldots \; v_0 e^{-j(N_m-1)\phi}\Big]^T \tag{5.2}$$

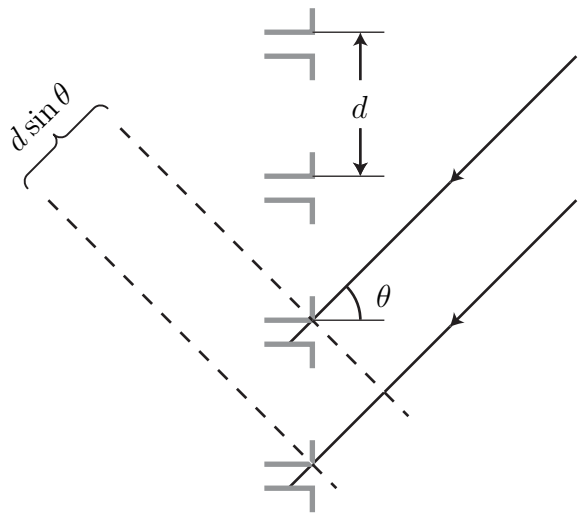

Figure 5.1: Single AOA at Multiple Receiving Antennas. A uniform linear array is demonstrated here on which radio signal falls from a single angle. Generally, the signal received at the array comes with some angular spread, even when there is a single transmission source; the amount of angular spread depends upon the propagation environment.

which indicates that the array response vector is a function of d, λ, and θ: the array response vector can be evaluated by determining the antenna spacing and the frequency and AOA of the incident wave. In the above expression, taking $v_0 = 1$ without loss of generality, the array response vector becomes:

$$\left[1 \; e^{-j\phi} \; e^{-j2\phi} \; \cdots \; e^{-j(N_m-1)\phi}\right]^T \tag{5.3}$$

If $\vec{v}_1$ is the array response vector for the $1st$ user and $\vec{v}_2$ for the $2nd$ user, then the beamformer for user-1 selects $\vec{w}_1^*$ such that:

$$|\vec{w}_1^* \vec{v}_1| \geq |\vec{w}_1^* \vec{v}_2| \tag{5.4}$$

5.2.1 Beamforming Algorithms

Various beamforming algorithms exist for choosing the tap *weight vector* and each of these algorithms are based on different criteria. The simplest algorithm, in which the

weight vector is selected to be the conjugate transpose of the array response vector, is called the delay-and-sum algorithm [89]. It simply compensates for the different delays incurred by the impinging signal at different antenna elements. While it is the simplest of all algorithms, it is not optimal in all the situations. Other beamforming techniques, based on more sophisticated algorithms, exist and have been discussed in [88] and [89].

In our simulations, an array with $N_m = 4$ and $d = \lambda$ is used. We assume a narrow angle of arrival that can be estimated fairly accurately, such that the spatial fading over the antenna elements can be neglected [86, 88]. Under such conditions, another beamforming algorithm, the max-SINR algorithm, can be used effectively. In the max-SINR algorithm, the conjugate transpose of tap weight vector is selected such that the SINR is maximized. The tap weight vector for SINR maximization is derived in [88] and is given by the following:

$$\vec{w}_i = \mathbf{R}_{uu,i}\vec{v}_i \tag{5.5}$$

where $\vec{v}_i$ is the array response vector as before, and $\mathbf{R}_{uu,i}$ is the correlation matrix of the undesired signal for *i-th* user. Therefore, $\mathbf{R}_{uu,i}$ can be written as [88]:

$$\mathbf{R}_{uu,i} = \sum_{\substack{j=1 \\ j\neq i}}^{N_u} \left(\sigma^2_{\text{BPSK}} R^2_{ij} E[A_j A_j^*] \vec{v}_j \vec{v}_j^* \right) + N\sigma_n^2 \mathbf{I} \tag{5.6}$$

5.2.2 Transmitter Analysis and Vector Channel

Let us now consider modelling a system with single transmitting antenna. The transmitter model, which is independent of the number of receiving antennas, is essentially the same as described in Chapter 2. The channel model, however, changes with the number of receiving antennas. Let the *i-th* user be incident with angle θ_i. From Eq. 5.3 and Eq. 5.1, the array response vector for the *i-th* user, denoted as $\vec{v}_i$, can be written as:

$$\vec{v}_i = \left[1 \; e^{-j2\pi \frac{dSin\theta_i}{\lambda}} \; e^{-j4\pi \frac{dSin\theta_i}{\lambda}} \; \cdots \; e^{-j(N_m-1)2\pi \frac{dSin\theta_i}{\lambda}} \right]^T \tag{5.7}$$

Using the notation such that v_{ij} denotes the elements of $\vec{v}_i$, the array response vector for the *i-th* user can be written as:

$$\vec{v}_i = \begin{bmatrix} v_{1i} & v_{2i} & \cdots & v_{N_m i} \end{bmatrix}^T \tag{5.8}$$

The vector channel or the array response matrix $\mathbf{V}$ for all the users is, therefore, given by:

$$\mathbf{V} = \begin{bmatrix} v_{11} & v_{12} & \cdots & v_{1N_u} \\ v_{21} & v_{22} & \cdots & v_{2N_u} \\ \vdots & \vdots & \ddots & \vdots \\ v_{N_m 1} & v_{N_m 2} & \cdots & v_{N_m N_u} \end{bmatrix} \tag{5.9}$$

where N_u is the number of active users as before.

5.2.3 Receiver Analysis

The receiver is assumed to have N_m antenna elements and the signal received is a vector signal with N_m dimensions. The "signal+interference" portion of the received signal given in Eq. 2.14 passes through the vector channel and is scaled by the array response vectors. The gaussian "noise" portion, however, remains intact because noise is assumed to be added at the antenna elements.

If r_i is the signal received from antenna-i, then the received vector signal is:

$$\vec{r} = \begin{bmatrix} r_1 \\ r_2 \\ \vdots \\ r_{N_m} \end{bmatrix} = \begin{bmatrix} v_{11}K_1A_1d_1 + v_{12}K_2A_2d_2 + \cdots + v_{1N_u}K_{N_u}A_{N_u}d_{N_u} \\ v_{21}K_1A_1d_1 + v_{22}K_2A_2d_2 + \cdots + v_{2N_u}K_{N_u}A_{N_u}d_{N_u} \\ \vdots \\ v_{N_m 1}K_1A_1d_1 + v_{N_m 2}K_2A_2d_2 + \cdots + v_{N_m N_u}K_{N_u}A_{N_u}d_{N_u} \end{bmatrix} + \vec{n}_{ant} \tag{5.10}$$

where the correlation matrix of $\vec{n}_{ant}$ is $\mathbf{R}_{n_{ant}n_{ant}} = \sigma_n^2 \mathbf{I}_{N_m}$.

At the receiver, there are two options: "beamform" first and then "despread", or despread first and then beamform.[3] In linear systems, these options are equivalent

[3]The term despread is used to denote the process of correlating the received spread spectrum

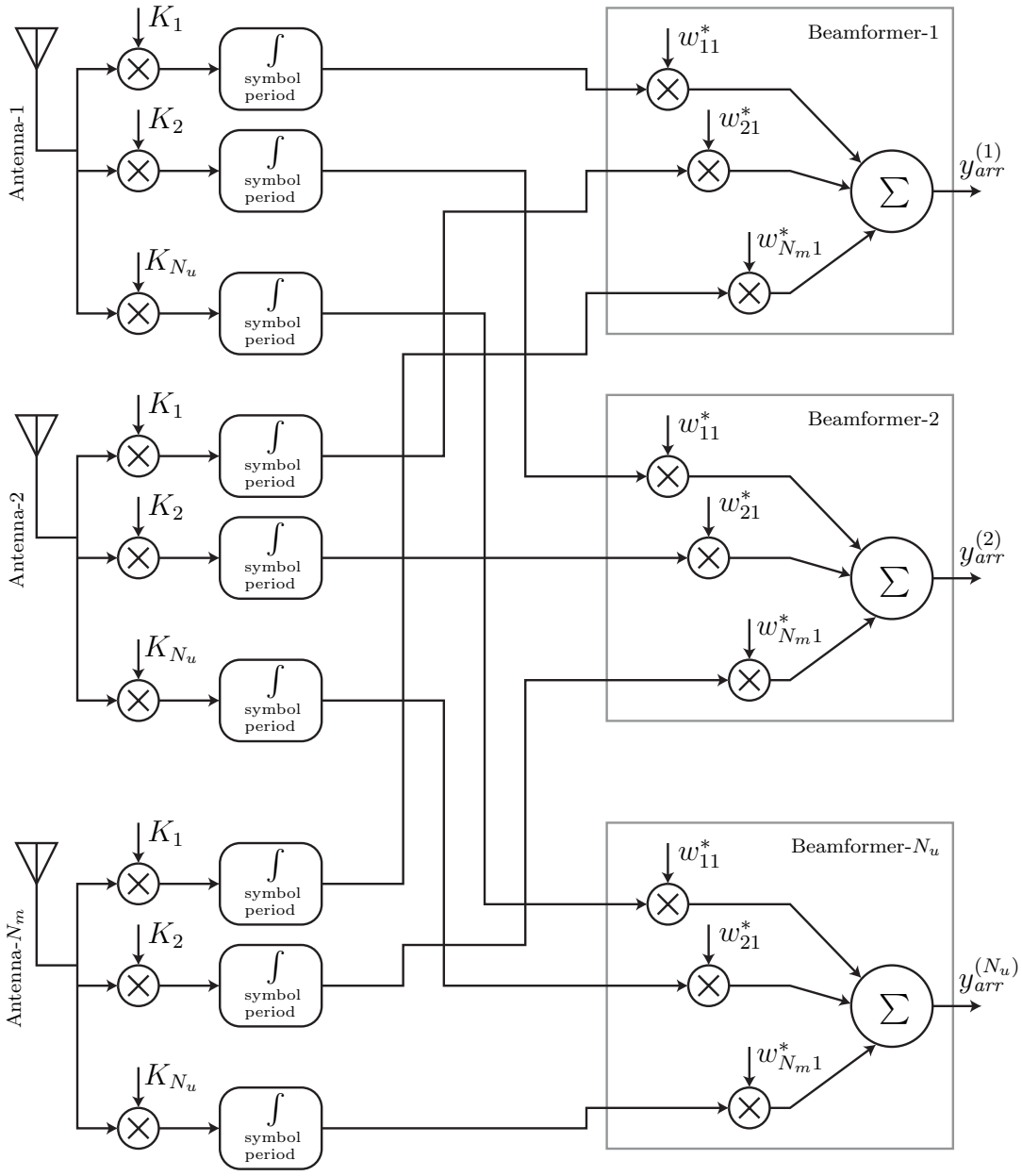

Figure 5.2: Multiple Antenna Receiver-I. Despreading prior to beamforming.

to one another. Two schemes based on these options are shown in Fig. 5.2 and Fig. 5.3. It is more cost-effective to despread first and then beamform, since in this case beamforming is performed at the symbol rate instead of at the chip rate.

CDMA signal with the spreading sequence. The term beamform denotes the process of combining the signals from multiple antennas.

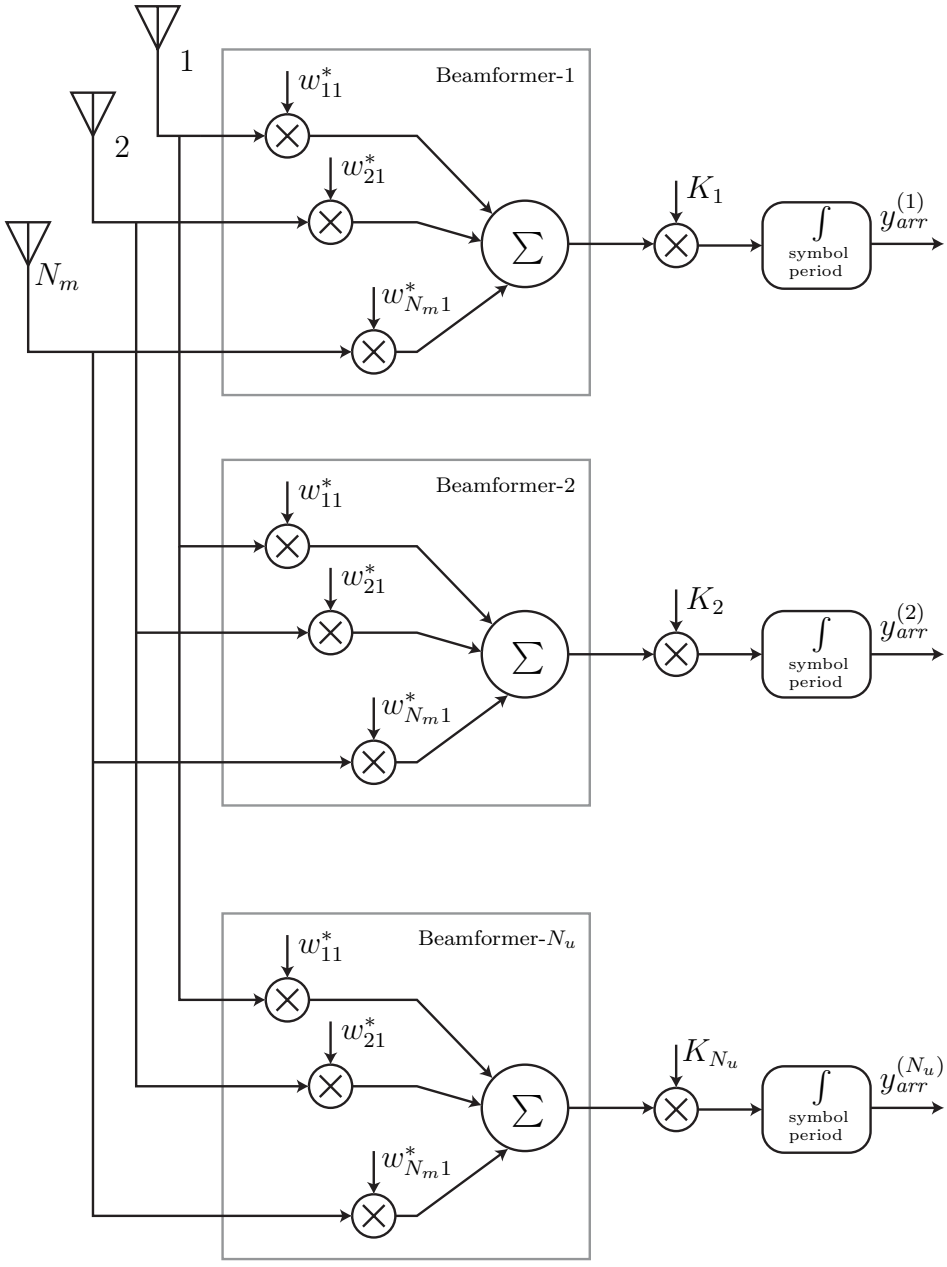

Figure 5.3: Multiple Antenna Receiver-II. Beamforming prior to despreading.

The gain provided by the *i-th* beamformer to the signal of the *j-th* user is given by:

$$g_{ij} = \vec{w}_i^* \vec{v}_j \tag{5.11}$$

where $\vec{w}_i^*$ is the conjugate transpose of $\vec{w}_i$. The objective is to select $\vec{w}_i^*$ such that:

$$g_{ii} \geq g_{ij}, \quad \forall j \neq i \tag{5.12}$$

After despreading and beamforming, the received signal for the *i-th* user can be written as:

$$y_{arr}^{(i)} = g_{ii} R_{ii} A_i d_i + \sum_{\substack{j=1 \\ j \neq i}}^{N_u} \Big(g_{ij} R_{ij} A_j d_j \Big) + n_{arr}^{(i)} \tag{5.13}$$

Comparing Eq. 5.13 with Eq. 3.3 and neglecting the additive noise terms, we observe a significant improvement in $\vec{y}_{arr}$ over $\vec{y}$ since a judicial choice of $\vec{w}_i^*$ ensures $g_{ii} \geq g_{ij}, \ \forall j \neq i$. Furthermore, the spreading sequences are selected such that $R_{ii} \gg R_{ij}, \forall j \neq i$. Hence:

$$g_{ii} R_{ii} \gg g_{ij} R_{ij}, \quad \forall j \neq i \tag{5.14}$$

Equation 5.14 indicates that the undesired or MAI components are attenuated as compared to the desired component. Simulation results, assuming random AOAs for each user's signal, are given in Fig. 5.4. These results demonstrate that multiple antenna systems perform significantly better than a single antenna system. Though a BER floor is still observed, it is lower for systems with multiple antennas than it would be for a single antenna system.

The use of channel encoding with multiple antennas results in further improvement in performance, as indicated in Fig. 5.5. However, a BER floor is again noticed since channel encoding is not designed to mitigate the MAI.

The two beamforming algorithms stated in Sec. 5.2.1—delay-and-sum and max-SINR—perform equally well for uniformly distributed users. This is because uniformly distributed users appear approximately spatially "white", and thus the correlation matrix of the undesired signal, $\mathbf{R}_{uu,i}$, is also approximately uniform. Under this condition, the weight vector obtained from SINR maximization criterion is the same as the one obtained from delay-and-sum criterion [88].

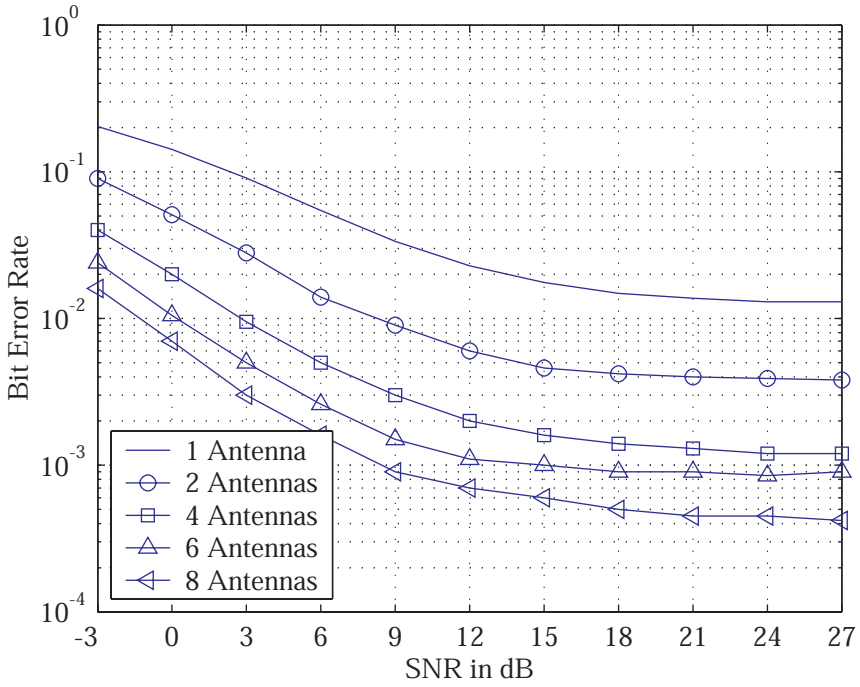

Figure 5.4: BER Performance with Multiple Antennas. Performance Improvement with Multiple Antennas for $N_u = 12$ users and Flat Rayleigh Fading. Delay-and-sum beamforming is used with SUMF to obtain these curves.

When the angular distribution of users is not spatially uniform, as is the case for a 30° sector, max-SINR beamformer performs better than the delay-and-sum beamformer. Simulation results shown in Fig. 5.6 confirm this.

5.3 Multiple Transmitting Antennas

Beamforming at the receiver is well understood and several researchers have addressed the topic of ST processing at the receiver [87, 88]. Furthermore, diversity techniques using multiple receiving antennas are also discussed in several textbooks [11, 22, 43]. Use of multiple transmitting antennas and ST coding at the transmitter, however, represent a relatively new research area. In this section, we summarize the performance gains achieved by using multiple transmitting antennas. When both transmitter and receiver use multiple antennas, the performance improvement depends upon the number of receiving antennas used in the system.

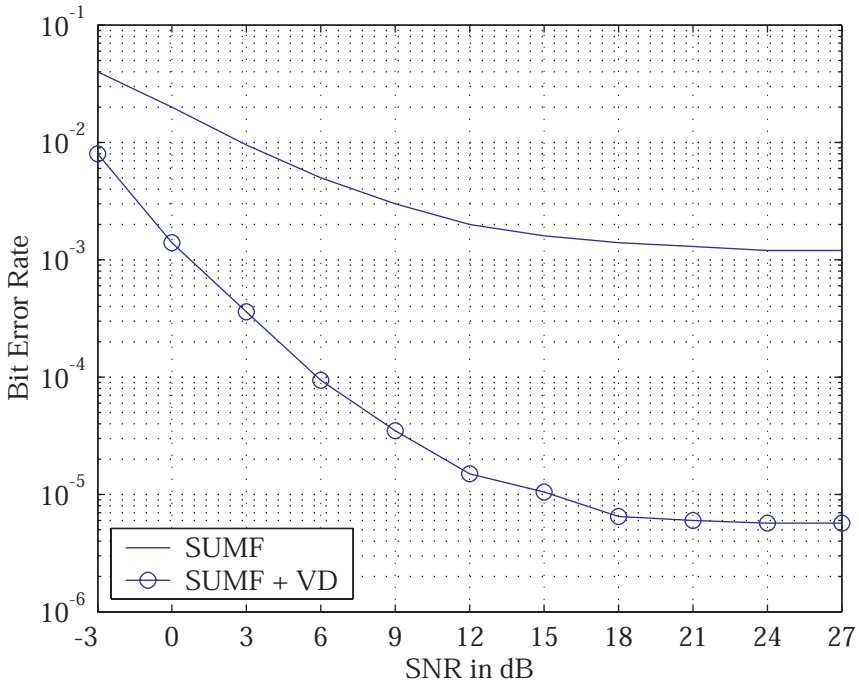

Figure 5.5: Multiple Antennas with Channel Encoding. Performance improvement with channel encoding in a four-antenna receiver (i.e., $N_m = 4$) for $N_u = 12$ users. The results with channel encoding are obtained by using a Viterbi decoder at the receiver and an encoder at the transmitter. The encoder used is a convolutional encoder with rate $\frac{1}{2}$ and constraint length 5.

Multiple transmitting antennas provide a form of diversity known as space diversity.[4] There are situations when space diversity is the only choice because it is not possible to use other types of diversity under all conditions. For example, the presence of small values of delay spread prohibits RAKE combining (or multipath diversity) in DS-CDMA systems. Similarly time diversity can not be used in slowly fading channels, especially if the data are delay constrained [90].

Beamforming using multiple transmitting antennas is based on the same vector channel model described in Sec. 5.2.2 for multiple receiving antennas. Transmit diversity schemes can be of three types: feedback assisted, training assisted, and blind. The capacity regions using transmit diversity have been discovered previously [90], but practical schemes are still being investigated. The delay diversity scheme [91] is a very simplified form of transmit diversity in which two transmitting antennas are

[4]In the literature, space diversity is also referred to as transmit diversity.

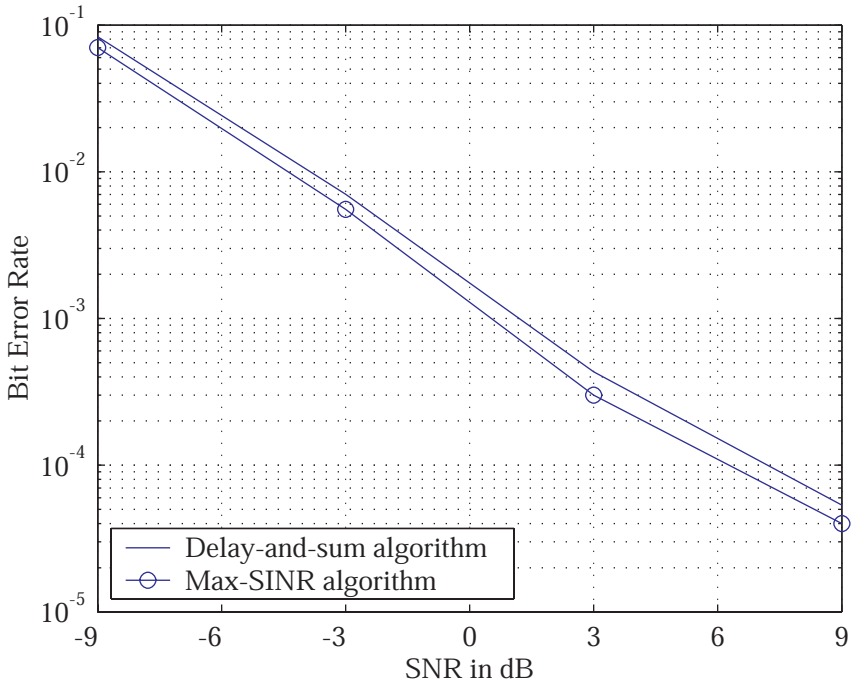

Figure 5.6: Comparison of Beamforming Algorithms. Two beamforming algorithms, delay-and-sum and max-SINR, are compared for a 30° sector. The curves are obtained for a system with $N_m = 4$ antennas and $N_u = 12$ users in flat Rayleigh fading.

used and the same symbol sequence is transmitted from each with a delay of one symbol between the two antennas. As a consequence, this scheme prevents the loss of data rate while providing a dual branch diversity reception at the receiver using maximum likelihood sequence estimation (MLSE). It can be demonstrated that the capacity grows linearly with the number of transmitting antennas under the condition that the number of transmitting antennas remains less than the number of receiving antennas [90]. Considering n transmitting antennas and m receiving antennas, where the gain from antenna i to antenna j is assumed to be slowly varying, then for BPSK in Rayleigh fading, the average probability of symbol error is given by [90]:

$$\bar{P}_e \leq \left(\frac{1}{\prod_{i=1}^{n}(1 + \lambda_i E_s/4N_o)} \right)^m \tag{5.15}$$

where λ_i denotes the *i-th* eigenvalue of error covariance matrix [90]. If the error covariance matrix has r non-zero eigenvalues (that is, it has a rank r), then the above

inequality can be written as:

$$\bar{P}_e \leq \left(\prod_{i=1}^{r} \lambda_i\right)^{-m} \left(\frac{E_s}{4N_o}\right)^{-rm} \tag{5.16}$$

Comparing this with the standard expressions for error probability as given in [22] and [43], a diversity gain of mr and a coding gain of $(\lambda_1\lambda_2\cdots\lambda_r)^{1/r}$ is achieved. The criterion for the selection of ST codes for transmit diversity in Rayleigh and Rician fading have been reported in [90].

ST coding, which fundamentally addresses transmit diversity, can be combined with array processing in order to reduce the decoding and encoding complexity of the transmitter and receiver that results by using ST codes. Decoding complexity exponentially increases with the decoding rate for a fixed number of transmitting antennas [92]. A linear array processing technique at the receiver, described in detail in [92], can be used in conjunction with ST coding. This technique, called the group interference suppression method, works by assuming that the signals transmitted from *other* groups of antennas are interference and tries to cancel out such interference.

5.4 Performance Gain

In this section, we provide a definition of the performance gain of multiple antenna system over single antenna system. This definition is applicable to any communication system that exhibits BER floor, such as a wireless DS-CDMA system.

Figure 5.4 shows that the DS-CDMA system exhibits BER floor like many other communication systems. The reasons for BER floor for different communication systems are quite different. For example, TDMA systems exhibit an error floor due to ISI. But systems using differential modulation exhibit a BER floor due to doppler spread [43]. The BER floor in DS-CDMA systems is the result of multiple access interference. This floor is observed irrespective of the number of receiving antennas because beamforming with multiple receiving antennas can not completely eliminate

multiple access interference for the DS-CDMA systems. However, use of multiple receiving antennas results in a reduction in BER floor.

The performance gain for any performance improvement scheme is usually defined as the reduction in required SNR for a given BER. Referring to Fig. 5.4, this definition can not be applied to beamforming performance gain because a specified BER may never be achieved by the system if the number of antennas is too small. An alternate measure of equal significance is the reduction in BER at a given SNR. This definition is most effective in the floor region. Thus, we define the performance gain of a beamforming scheme as the ratio of BER floor for multiple antennas to the BER floor for single antenna. That is, if $G(m)$ is the gain by using m antennas, we can write:

$$G(m) = \frac{\text{BER floor with } m \text{ antennas}}{\text{BER floor with one antenna}} \tag{5.17}$$

We also note from Fig. 5.4 that $G(m)$ does not increase linearly with m, and increasing the number of receiving antennas brings diminishing returns in gain.

5.5 Linear MUD with Multiple Antennas

In Chapter 3, we demonstrate that use of linear multiuser detectors improves system performance. Furthermore, as given in earlier sections, use of multiple antennas in a DS-CDMA systems results in a reduction in BER floor, a second improvement. When multiple antennas are used with linear multiuser detectors, the resulting system enables further improvements in system performance. This section describes a combination of multiantenna systems and linear multiuser detectors.

It has been established in previous chapters that beamforming and linear multiuser detection combat multiple access interference, but perform poorly in certain SNR regions. Specifically, ZF linear MUD performs poorly for low SNRs, while a multiple antenna system with SUMF exhibits a BER floor at high SNRs. In Chapter 3, we demonstrated that linear multiuser detectors are extremely near-far resistant and robust against MAI originated within local cell. Further, Sec. 5.2 depicts that

beamforming is more robust against unknown MAI that originates from other cells. Thus, a combination of the two schemes, namely linear MUD with beamforming, offers substantial gains, as pointed out in [93] based on architecture proposed in [94].

Simulation results suggest that for various voice and data applications, a combination of linear multiuser detector and beamformer outperforms either the beamformer or the multiuser detector alone. Voice applications generally require a BER of 10^{-3} or better, while BER requirements for data applications are more stringent, lying in the range of 10^{-6} or better. A receiver that uses ZF linear MUD with BF is shown in Fig. 5.7. At each element of the antenna array, individual users are first despread, then decorrelated via the $\mathbf{R}^{-1}$ filter, and then beamformed individually. Such an approach completely eliminates MAI at high SNRs while affording an adequate performance at lower SNRs, as shown in Fig. 5.8.

5.5.1 ZF MUD with Beamforming

In a multiple antenna receiver system, performing the decorrelation operation at each antenna renders the statistical signal spatially white at the input of the beamformer. To prove this, it suffices to show that when ZF or decorrelator MUD is used at each antenna element then the correlation matrix of the *undesired signal* present at the input of each beamformer is spatially white [93], irrespective of the sector size.

The heuristics of the proof are as follows: Since the beamformer for a particular user receives the input signals from different antennas, the unwanted signal that causes non-zero spatial correlation is MAI and not the additive gaussian noise.[5] In Fig. 5.8, without decorrelating operation at each antenna, we would expect spatial correlation due to the presence of MAI in the signals coming from each of the antenna. However, the use of a decorrelating filter leaves only additive gaussian noise as the unwanted signal uncorrelated with the additive gaussian noise on any other antenna element, thereby rendering the unwanted signal spatially white. The formal proof is provided

[5]This follows from the assumption that the additive gaussian noise at one antenna is uncorrelated with the noise at any other antenna.

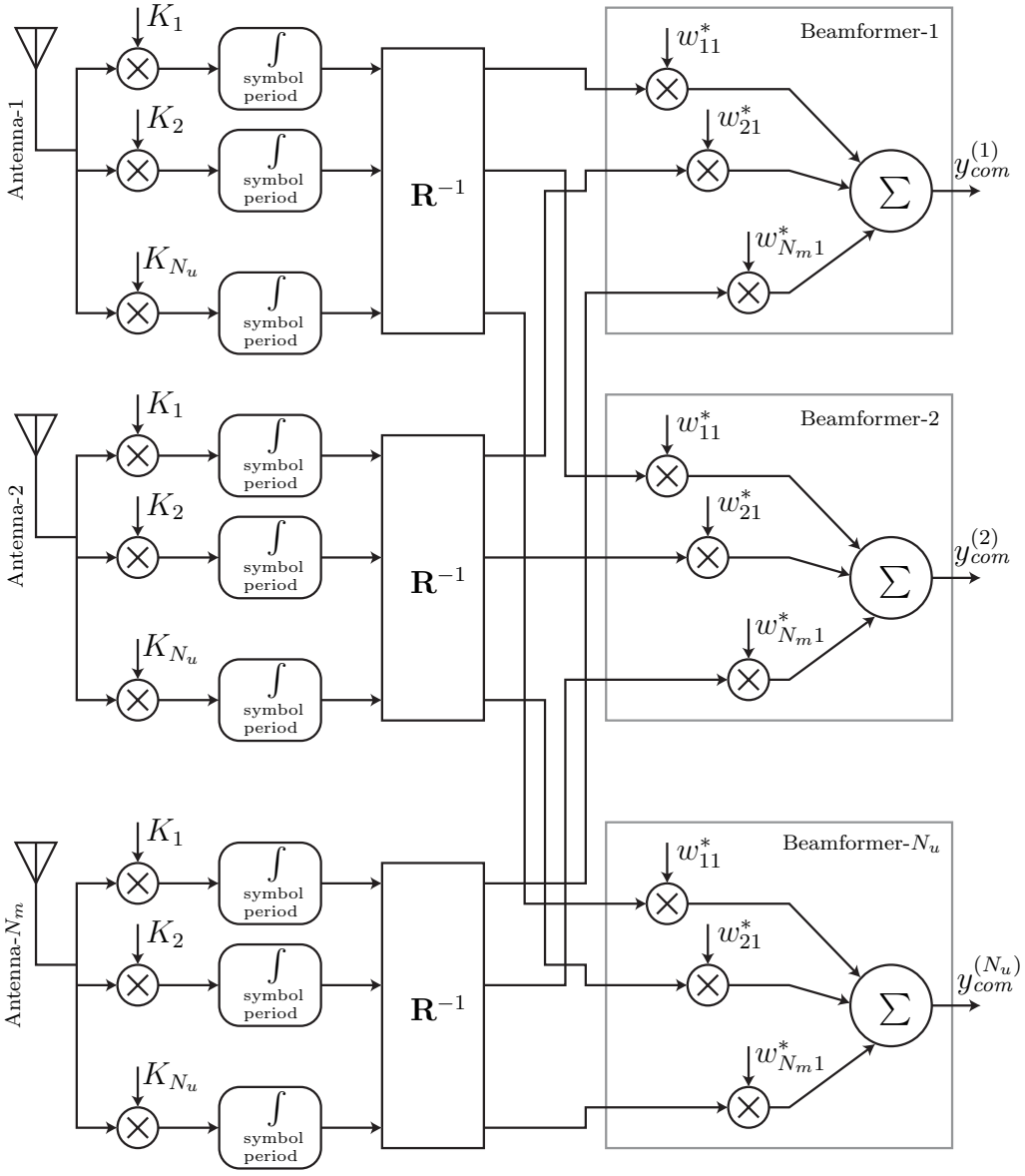

Figure 5.7: Multiantenna with linear MUD. A multiantenna ZF multiuser detector. The zero forcing or decorrelation operation is performed at each antenna individually and the signals are combined later using a beamformer for each user.

below:

The received vector signal from Eq. 5.10 is written as:

$$\vec{r} = K_1 A_1 d_1 \vec{v}_1 + K_2 A_2 d_2 \vec{v}_2 + \cdots + K_{N_u} A_{N_u} d_{N_u} \vec{v}_{N_u} + \vec{n}_{ant} \tag{5.18}$$

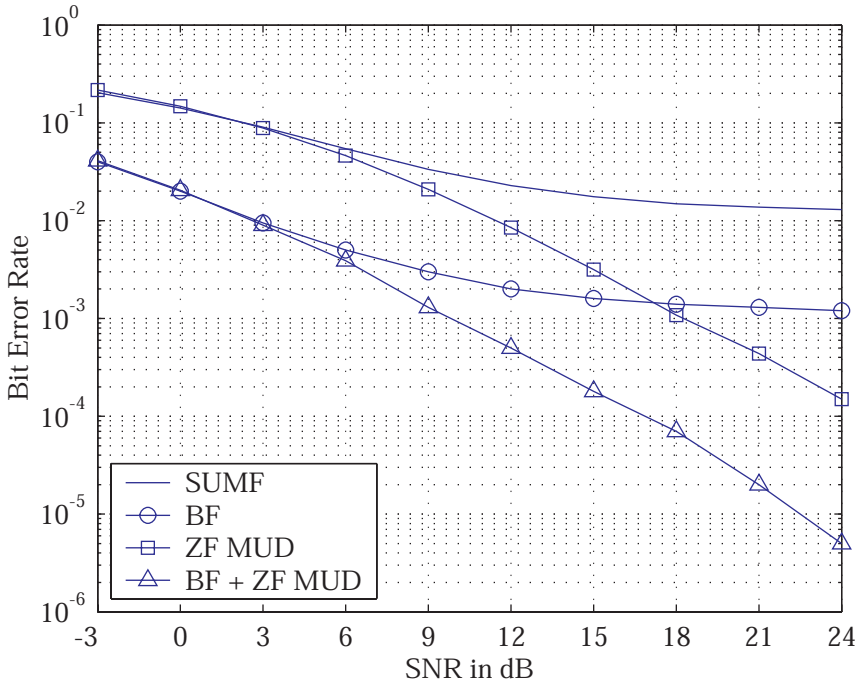

Figure 5.8: Combined Performance of BF and ZF MUD. Demonstrating the impact of BF and ZF MUD—combined and separately—on the performance of SUMF. ZF MUD effectively eliminates the BER floor while BF ensures better BER at low SNRs; the combination offer the best performance by providing lower BER at low SNRs while avoiding error floors at high SNRs.

where $\vec{n}_{ant}$ is AWGN with correlation matrix $\mathbf{R}_{\mathbf{n}_{ant}\mathbf{n}_{ant}} = \sigma_n^2 \mathbf{I}_{N_m}$. Note that each component of $\vec{n}$ is the noise generated per chip for all the users on a particular antenna. From Eq. 5.18, the despread vector signal at the *i-th* antenna can be written as:

$$\vec{y}_{pre}^{(i)} = \begin{bmatrix} v_{i1}R_{11}A_1d_1 + v_{i2}R_{12}A_2d_2 + \cdots + v_{iN_u}R_{1N_u}A_{N_u}d_{N_u} \\ v_{i1}R_{21}A_1d_1 + v_{i2}R_{22}A_2d_2 + \cdots + v_{iN_u}R_{2N_u}A_{N_u}d_{N_u} \\ \vdots \\ v_{i1}R_{N_u1}A_1d_1 + v_{i2}R_{N_u2}A_2d_2 + \cdots + v_{iN_u}R_{N_uN_u}A_{N_u}d_{N_u} \end{bmatrix} + \begin{bmatrix} \tilde{n}_{i1} \\ \tilde{n}_{i2} \\ \vdots \\ \tilde{n}_{iN_u} \end{bmatrix} \quad (5.19)$$

where $\tilde{n}_{ij}$ denotes the noise at *i-th* antenna in the *despread* signal of *j-th* user; this

noise can be represented in terms of input noise as:

$$\tilde{n}_{ij} = \int_{\substack{\text{symbol} \\ \text{period}}} K_j n_{ant}^{(i)} = \sum_{m=1}^{N} c_{jm} n_m^{(i)} \tag{5.20}$$

where c_{jm} denotes the *m-th* chip value of the *j-th* user, and n_{im} denotes the input noise generated in the *m-th* chip received at the *i-th* antenna. Noting that the noise generated in different chips are uncorrelated, we get:

$$R_{\tilde{n}_{ij}\tilde{n}_{kl}} = \sigma_n^2 \delta_{ik} R_{jl} \tag{5.21}$$

which indicates that the noise embedded in the despread signal of a user at one antenna is uncorrelated with the noise embedded in the despread signal of any other user at any other antenna.

After ZF decorrelation, MAI is effectively eliminated and additive noise is the *only* unwanted signal for a particular user at each antenna. Let u_{ij} be the unwanted signal for *i-th* user at the output of ZF filter at the *j-th* antenna, then:

$$u_{ij} = \left\langle i\text{-}th \text{ row of } \mathbf{R}^{-1}, \vec{\tilde{n}}_j{}^T \right\rangle \tag{5.22}$$

which clearly indicates that:

$$R_{u_{ij}u_{ik}} = 0, \quad \forall j \neq k \tag{5.23}$$

Thus the unwanted signals for the *i-th* beamformer are spatially uncorrelated. Had a decorrelating filter not been used at each antenna, spatial correlation would have existed for undesired signals at the input of each beamformer because of MAI that is correlated with itself over the antennas. Since the decorrelating filter removes MAI completely irrespective of the sector size, the unwanted signals into a particular beamformer must consist of additive gaussian noise only.

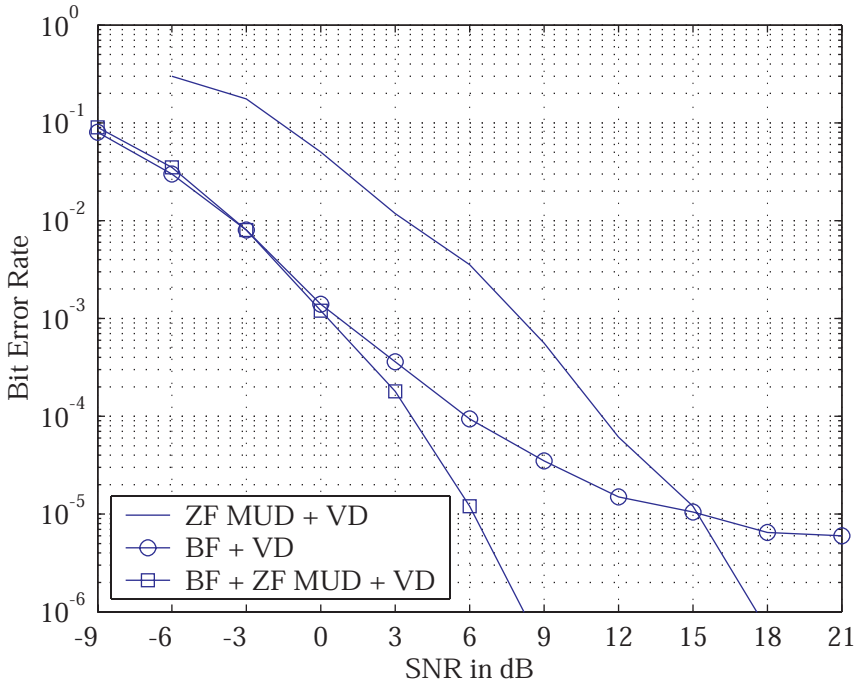

Figure 5.9: Performance Comparison: BF + ZF MUD + VD. Comparing the performance of Beamformer and ZF MUD combined with VD.

5.5.2 The Received Signal

We have shown that performing the $\mathbf{R}^{-1}$ decorrelation operation at each antenna causes the undesired signal to appear as spatially white at the input of the beamformer regardless of the sector's angular size. Under these conditions, max-SINR algorithm reduces to the delay-and-sum algorithm [88] which is used to generate the plots in Fig. 5.8 and Fig. 5.9.

The received vector signal, from Eq. 5.10, can be represented as:

$$\vec{r} = \begin{bmatrix} v_{11}K_1A_1d_1 + v_{12}K_2A_2d_2 + \cdots + v_{1N_u}K_{N_u}A_{N_u}d_{N_u} \\ v_{21}K_1A_1d_1 + v_{22}K_2A_2d_2 + \cdots + v_{2N_u}K_{N_u}A_{N_u}d_{N_u} \\ \vdots \\ v_{N_m1}K_1A_1d_1 + v_{N_m2}K_2A_2d_2 + \cdots + v_{N_mN_u}K_{N_u}A_{N_u}d_{N_u} \end{bmatrix} + \vec{n_{ant}} \qquad (5.24)$$

After despreading at each antenna with $K_1, K_2, \cdots, K_{N_u}$, the pre-MUD signal at

the first antenna is given by:

$$\vec{y}_{pre}^{(1)} = \begin{bmatrix} v_{11}R_{11}A_1d_1 + v_{12}R_{12}A_2d_2 + \cdots + v_{1N_u}R_{1N_u}A_{N_u}d_{N_u} \\ v_{11}R_{21}A_1d_1 + v_{12}R_{22}A_2d_2 + \cdots + v_{1N_u}R_{2N_u}A_{N_u}d_{N_u} \\ \vdots \\ v_{11}R_{N_u1}A_1d_1 + v_{12}R_{N_u2}A_2d_2 + \cdots + v_{1N_u}R_{N_uN_u}A_{N_u}d_{N_u} \end{bmatrix} + \vec{\tilde{n}}_1 \qquad (5.25)$$

which, for the *m-th* user, can be written as:

$$\vec{y}_{pre}^{(m)} = \mathbf{R}\ diag(v_{mi}; 1 \leq i \leq N_u)\mathbf{A}\vec{d} + \vec{\tilde{n}}_m \qquad (5.26)$$

Thus by using $\mathbf{R}^{-1}$ filter, the decorrelation operation can be performed at each antenna individually. Once the decorrelation is performed at each antenna, the signals corresponding to individual users are routed to their respective beamformers, as indicated in Fig. 5.7.

5.6 Performance Results

Figure 5.8 compares all the schemes discussed in this chapter without any channel encoding. It clearly indicates that for BER specifications for voice and data transmission (i.e., 10^{-3} and 10^{-6} respectively), ZF MUD combined with BF outperforms the other receivers.

Results with channel encoding are shown in Fig. 5.9. In this case, beamforming appears to perform significantly better than multiuser detection prior to reaching a BER floor of about 10^{-5}. These results, however, are obtained for equal power users, while a realistic comparison of BF and ZF MUD requires consideration of a scenario in which users transmit unequal powers. Near-far resistance of a detector is a direct indication of how well that detector can handle the users transmitting unequal powers. Simulations results for BER of a far user with low SNR are shown in Fig. 5.10. These results indicate that linear MUDs are extremely near-far resistant while BF is not.

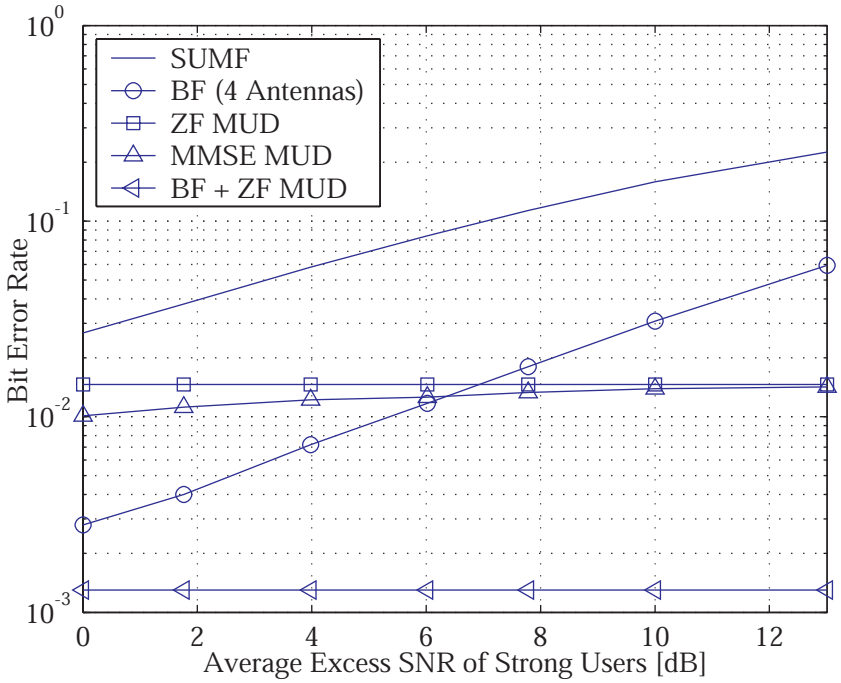

Figure 5.10: Near-Far Resistance. Depicting the Near-Far Resistance of various receivers with 15 active users. The plot shows the BER of a far user whose SNR is kept at 12 dB. SNR of all other users is increased progressively as indicated on the x-axis.

On the other hand, BF is robust against unknown MAI while MUDs are not. Thus a combination offers the best performance. For voice applications requiring BER of 10^{-3} or lower, the gain of ZF MUD+BF is approximately 8 dB more than a single-antenna ZF MUD (see Fig. 5.8). A comparison of Fig. 5.8 with Fig. 5.9 indicates that with channel encoding, an additional gain of 9 dB is obtained.

Chapter 6

Summary and Conclusions

The capacity of practical DS-CDMA systems is normally limited by the allowable level of multiple access interference (MAI). The MAI problem is more severe in the uplink where the transmissions originate from spatially distributed handsets than in the downlink where transmissions originate from a single point—the base station. In a DS-CDMA downlink, the transmitted signal is the sum of signals intended for all users. Thus, for each user, the desired and interfering signals all follow the same propagation path.

This thesis explores the use of detection techniques to mitigate the effects of the uplink MAI. These techniques reduce the BER for the individual users in addition to improving the overall system capacity. Specifically, two broad classes of multiuser detection techniques were studied. These classes are differentiated by the use of:

i) Linear filtering.

ii) Multiple antennas.

Both these techniques have improved performance compared with the single user, single antenna detector. But there are certain regions of SNR where the individual techniques, i) and ii) above, suffer some performance deterioration while the combination of the two yields remarkable improvements in BER and an increase in system capacity.

Systems using linear filters for multiuser detection result in effective elimination of MAI. Thus, a BER floor is avoided rendering the system near-far resistant. For low SNRs, however, the linear filter suffers from poor BER characteristics. For a practical system, which is usually set up in a near-far environment, the use of a linear filter results in a significant improvement in BER for medium to high SNRs.

Beamforming (BF)using multiple receiving antennas reduces the BER of a user by suppressing the signals from other users without eliminating them completely. Since the interfering signals can not be completely removed, there exists an error floor for the BER performance of these systems. This error floor, however, is lower than that exhibited by a single antenna system. The use of multiple receiving antennas generally yields better performance at low SNRs and moderate performance at high SNRs.

Linear MUD attempts to eliminate the local-cell MAI. In contrast, a system using multiple receiving antennas is more robust against unknown MAI that originates from other cells. Thus, a combination of BF and linear filter is near-far resistant with improved performance at high as well as at low SNRs.

Linear MUD uses a linear filter at the base station. Implementation of such filtering is simplified when the signals are synchronous at the symbol level. For an asynchronous systems, however, linear MUD is far too complex to implement. The sub-symbol scheme, discussed in this thesis, simplifies implementation of the linear MUD in an asynchronous system.

For completely asynchronous systems, the use of sub-symbol based linear MUD results in a significant reduction in the BER without any decrease in the system capacity. Furthermore, when applied to a QS-CDMA system, this MUD results in a remarkable increase in the capacity of the system.

6.1 Contributions to Knowledge

The following are the principal contributions of the research presented in this thesis:

i) Proposal for a novel multiuser detector using sub-symbols. This approach offers simplified implementation and is based on dividing the symbols into segments called sub-symbols.

ii) Proposal for diversity combining algorithms for the sub-symbol scheme. Diversity is achieved by virtue of the fact that each constituent sub-symbol of a particular symbol contains the same user data.

iii) Demonstration by simulation that the bit error rates of condition number based combining algorithms outperform all the other combining algorithms.

iv) Rules for maximizing the number of users in the sub-symbol scheme using proper thresholds. The rules are defined in terms of the chip threshold, the condition number threshold, and the rank threshold.

v) Discovery that use of a single sub-symbol is sufficient to outperform the conventional detector in the sub-symbol scheme for large number of users in a moderately synchronous QS-CDMA system.

vi) Demonstration that the performance difference between ZF MUD and MMSE MUD for a synchronous CDMA system depends on the condition number of the correlation matrices of spreading sequences. This performance disparity leads to the invention of condition number based algorithms for sub-symbol combining.

vii) Approach to combine linear multiuser detectors with multiple antennas resulting in improved BER performance at all SNRs. This involves performing linear multiuser detection at each antenna and combining the outputs from these antennas.

The first five contributions in the above list were addressed in Chapter 4, and the last one is detailed in Chapter 5. The contribution regarding performance disparity of ZF MUD and MMSE MUD is explained in Chapter 3.

6.2 Future Directions

During the development of this thesis, a number of promising research avenues were discovered. Some of them are as below.

i) *RAKE combining using sub-symbols.* As explained in Sec. 4.2.3, the sub-symbol receiver reduces to a RAKE receiver when the inverse filters are eliminated. Yet, more information on demodulated signals is available in a sub-symbol scheme than in a RAKE receiver. While the RAKE receiver provides the correlation product for the full symbol, partial products are available when the sub-symbol scheme is employed. Availability of additional information in the sub-symbol case may be explored to obtain levels of performance better than those shown by standard RAKE receivers.

ii) *Optimal algorithm for sub-symbol combining.* While the "simple" combining algorithms treat all sub-symbols in the same way, condition number based algorithms weigh the sub-symbols before combining. The latter are improvements over simple algorithms but their optimality is not proved. Obtaining an optimal algorithm for sub-symbol combining is an important and interesting future research area.

iii) *Combining only "clean" sub-symbols.* Inversion of correlation matrix in a sub-symbol period results in a set of sub-symbols, some of which are clean. Simulation results presented in this thesis considered combining all sub-symbols, whether clean or not. An algorithm that considers only clean sub-symbols is expected to provide better performance and is also an interesting research area.

iv) *Code acquisition based on linear MUD.* The use of MUDs results in lower BERs. Thus, the data signal actually transmitted can be constructed at the receiver with higher probability which may help in solving the code acquisition problem.

v) *Consideration of synchronization errors.* Our simulations, which use the parameters recommended by WCDMA proposals, also assume ideal synchronization.

These assumptions allowed us to use a single sample per chip for the simulations. Use of multiple samples per chip is expected to be more robust when timing and synchronization errors are present, especially in a fast fading system. These considerations also indicate an area that can be researched further.

vi) *Different methods of modulation.* Results in this thesis are based on the use of BPSK modulation. While these results are applicable to QPSK and QAM modulation schemes, consideration of effects of other modulation methods such as differential modulation and continuous phase modulation is an important area that can be explored in future.

Appendix A

MMSE Linear MUD Derivation

We show that the linear filter for MMSE MUD is given by:

$$\mathbf{W}_{\text{MMSE}} = \left(\mathbf{R} + \sigma_n^2 \mathbf{A}^{-2}\right)^{-1} \tag{A.1}$$

where $\mathbf{R}$ is the correlation matrix of the spreading sequences, $\mathbf{A}$ is a diagonal matrix containing Rayleigh fading amplitudes for all users and σ_n^2 is the input noise variance per sample. From Eq. 3.9, the signal at the output of SUMFs is:

$$\vec{y} = \mathbf{R}\mathbf{A}\vec{d} + \vec{n} \tag{A.2}$$

Let $\vec{x}$ be the faded data signal defined as $\vec{x} = \mathbf{A}\vec{d}$, and $\mathbf{W}$ is the linear filter through which the SUMF output $\vec{y}$ is processed. The MMSE filter $\mathbf{W}_{\text{MMSE}}$, by definition, minimizes the mean squared value of the difference signal $\vec{x} - \mathbf{W}\vec{y}$ and is given by:

$$\mathbf{W}_{\text{MMSE}} = \arg\min_{\mathbf{W}} E\left[(\vec{x} - \mathbf{W}\vec{y})(\vec{x} - \mathbf{W}\vec{y})^*\right] \tag{A.3}$$

where * in the superscript denotes conjugate transpose. Solving, we get [95]:

$$\mathbf{W}_{\text{MMSE}} = \mathbf{R}_{xy}\mathbf{R}_{yy}^{-1} \tag{A.4}$$

where $\mathbf{R}_{xy}$ is the cross-correlation matrix of $\vec{x}$ and $\vec{y}$ while $\mathbf{R}_{yy}$ is the autocorrelation matrix of $\vec{y}$. These matrices can be evaluated as follows:

$$\begin{aligned}
\mathbf{R}_{xy} &= E[\vec{x}\vec{y}^*] \\
&= E[\mathbf{A}\vec{d}(\vec{d}^*\mathbf{A}^*\mathbf{R}^* + \vec{n}^*)] \\
&= \sigma^2_{BPSK}\mathbf{A}\mathbf{A}^*\mathbf{R}^* \\
&= \mathbf{A}\mathbf{A}^*\mathbf{R} \qquad \text{(A.5)} \\
\mathbf{R}_{yy} &= E[\vec{y}\vec{y}^*] \\
&= E[(\mathbf{R}\mathbf{A}\vec{d} + \vec{n})(\vec{d}^*\mathbf{A}^*\mathbf{R}^* + \vec{n}^*)] \\
&= \mathbf{R}\mathbf{A}\mathbf{A}^*\mathbf{R} + \sigma_n^2\mathbf{R} \qquad \text{(A.6)}
\end{aligned}$$

Using Eq. A.5 and Eq. A.6 in Eq. A.4, the MMSE linear filter is given as:

$$\begin{aligned}
\mathbf{W}_{\text{MMSE}} &= \mathbf{A}\mathbf{A}^*\mathbf{R}(\mathbf{R}\mathbf{A}\mathbf{A}^*\mathbf{R} + \sigma_n^2\mathbf{R})^{-1} \\
&= \left(\mathbf{R} + \sigma_n^2\mathbf{A}^{-2}\right)^{-1} \qquad \text{(A.7)}
\end{aligned}$$

The term $\sigma_n^2\mathbf{A}^{-2}$ represents inverse SNR for a unit amplitude vector signal. Thus, the linear filter for an MMSE multiuser detector is given by $\left(\mathbf{R} + \frac{1}{\text{SNR}}\right)^{-1}$.

Appendix B

Computation of SNR Penalty

The SNR penalty of a sub-symbol multiuser detection scheme is defined as the difference in input SNRs of the sub-symbol scheme for an asynchronous system and the ideal ZF detector for a synchronous system when both systems exhibit the same BER. Thus, it is also equivalent to the reduction in output SNR for a sub-symbol scheme; this reduction is a result of reduced processing gain. In this appendix, we derive an expression for the SNR penalty when a sub-symbol scheme is used in a DS-CDMA system. We assume a spreading factor of $N = 255$ chips per symbol and a sampling rate of one sample per chip; these values are used in all the simulations performed to obtain the results presented in this thesis.

To characterize the SNR penalty, we compute the output SNR in two cases: ideal full-symbol synchronous case, and the sub-symbol case. For sub-symbol case, the "select-best" simple combining algorithm, as described in Sec. 4.3, is used. We further assume that the fading imposes a fixed penalty for each receiver such that the performance of any two receivers is affected by fading in the same way. This assumption allows comparing non-fading systems and extending the results to those fading systems that undergo similar kind of fading. For comparing different receivers, these assumptions are generally valid as the receivers are used in the same environment and the change in sampling rate has similar effects on each receiver considered.

Let S denote the total output signal and X the total output noise in the same interval. We use subscript "f" to refer to the case of full-symbol synchronous system,

and subscript "s" for the case of sub-symbol synchronous receiver. For the *i-th* user, the SNR for the two cases is computed as follows:

Full-symbol correlation: In this case, the decorrelation is performed over one full symbol, such that the output signal and output noise are given by:

$$S_f = \sum_{m=1}^{N} c_{im} c_{im} = N \tag{B.1}$$

$$X_f = \sum_{m=1}^{N} c_{im} X_m = c_{i1} X_1 + c_{i2} X_2 + \cdots + c_{iN} X_N \tag{B.2}$$

where X_m's are i.i.d. Normal$(0, \sigma_n^2)$ random variables that indicate the additive noise per sample at the input of the receiver and c_{im} is the *m-th* chip value in the spreading sequence for the *i-th* user.

The output SNR can be computed from $\sigma_{S_f}^2$ and $\sigma_{X_f}^2$ as follows:

$$\sigma_{S_f}^2 = N^2 \tag{B.3}$$

$$\sigma_{X_f}^2 = \sum_{m=1}^{N} {c_{im}}^2 \sigma_{X_1}^2 = N\sigma_n^2 \tag{B.4}$$

$$SNR_f = \frac{\sigma_{S_f}^2}{\sigma_{X_f}^2} = \frac{N}{\sigma_n^2} \tag{B.5}$$

Sub-symbol correlation: Let M be the number of chips in the best sub-symbol,[1] used by the select-best algorithm. Using a similar procedure as in the case of full-symbol correlation, we can write the expressions for output signal and noise as:

$$S_s = \sum_{i=1}^{M} 1 = M \tag{B.6}$$

$$X_s = X_1 + X_2 + \cdots + X_M \tag{B.7}$$

$$\sigma_{X_s}^2 = M\sigma_{X_1}^2 = M\sigma_n^2 \tag{B.8}$$

[1]Best sub-symbol is the one used in select-best combining and is described as the one in which the sum of signal, noise, and MAI is largest. See Sec. 4.3 for details.

and the output SNR is, therefore, computed as:

$$\sigma_{S_s}^2 = M^2 \tag{B.9}$$

$$\sigma_{X_s}^2 = \sum_{m=1}^{M} {c_{im}}^2 \sigma_{X_1}^2 = M\sigma_n^2 \tag{B.10}$$

$$SNR_f = \frac{\sigma_{S_s}^2}{\sigma_{X_s}^2} = \frac{M}{\sigma_n^2} \tag{B.11}$$

SNR Penalty: The SNR penalty δ_s can be computed from expressions for SNR_f and SNR_s, as follows:

$$\delta_s = \frac{SNR_f}{SNR_s} = \frac{N}{M} \tag{B.12}$$

We may assume that M is approximately equal to the expected number of chips in the longest sub-symbol within a symbol, the accuracy of the result mostly dependenpt on this approximation. In a slow fading environment, this approximation is reasonably good since the longest sub-symbol would yield the best amplitude when integrated over its own length. We can compute M analytically. The analysis, however, becomes cumbersome for a large number of sub-symbols. In such a case, we compute M by simulations.

For 12 asynchronous users with uniformly distributed random transmission instants, M is found to be approximately 55. SNR penalty for the select-best algorithm is, therefore, approximated by $\frac{255}{55} = 4.64 = 6.7$ dB which agrees with the results depicted in Fig. 4.6. For condition number based accumulate combining, an SNR penalty of 2 dB is observed from Fig. 4.7; this corresponds to the use of approximately 161 chips to perform correlation in a sub-symbol scheme employing select-best simple combining algorithm. Thus, combining many sub-symbols, weighted by the inverse condition numbers of corresponding correlation matrices, results in a reduction in SNR penalty.

Appendix C

Simulation Parameters

For the simulations, we use parameters recommended in proposed WCDMA standards [63]. Following table summarizes the system parameters used in the simulations presented in this thesis:

Common System Parameters	
Carrier Frequency	1.9 GHz
Spreading Sequences	Kasami (small set)
Spreading gain (chips per bit)	255
Sampling Rate	1 sample/chip
Modulation	BPSK
Convolutional code Rate	$\frac{1}{2}$
Constraint Length	5
Maximum Mobile Speed	120 Km/hr
Maximum doppler	211 Hz
Environment	Outdoor
Angular Spread	Narrow
Number of Receive Antennas	1 (unless specified otherwise)
Fading	Flat Rayleigh
Number of Users	12 (unless specified otherwise)

Table C.1: WCDMA simulation parameters.

Bibliography

[1] G. C. Di Piazza, A. Plitkins, and G. I. Zysman, "The Cellular Concept," *Bell Systems Technical Journal*, vol. 58, no. 1, pp. 215–48, January 1979.

[2] R. Nelson and D. Westin, "The Evolution of the North American Cellular Network," *Telecommunications (International Edition)*, vol. 26, no. 9, pp. 24–28, September 1992.

[3] V. H. MacDonald, "The Cellular Concept," *Bell Systems Technical Journal*, vol. 58, no. 1, pp. 15–42, January 1979.

[4] F. H. Blecher, "Advanced Mobile Phone Service," *IEEE Transactions on Vehicular Technology*, vol. VT-29, no. 2, pp. 238–244, May 1980.

[5] E. S. K. Chien, "AT&T Cellular System-System Description and System Trial Results," in *Proceedings of the ICC*, vol. 3, pp. 1207–1213, May 1984.

[6] D. C. Cox, "A Radio System Proposal for Widespread Low Power Tetherless Communications," *IEEE Transactions on Communications*, vol. 39, no. 2, pp. 324–335, February 1991.

[7] D. L. Huff, "AT&T Cellular Technology Review," in *Proceedings of MILCOM 1985*, vol. 2, pp. 490–494, October 1985.

[8] J. E. Padgett, C. G. Günther, and T. Hattori, "Overview of Wireless Personal Communications," *IEEE Communications Magazine*, pp. 28–41, January 1995.

[9] L. R. Maciel and H. L. Bertoni, "Cell Shape for Microcellular Systems in Residential and Commercial Environments," *IEEE Transactions on Vehicular Technology*, vol. 43, no. 2, pp. 270–278, May 1994.

[10] M. Gustafsson, K. Jamal, and E. Dahlman, "Compressed Mode Techniques for Interfrequency Measurements in a Wide-band DS-CDMA System," in *Proc. of PIMRC '97*, pp. 23–35, Helsinki, Finland, September 1997.

[11] T. S. Rappaport, *Wireless Communications: Principles and Practice*, Prentice-Hall, NJ, 1996, ISBN:0133755363.

[12] A. Andreadis, G. Benelli, G. Giambene, and B. Marzucchi, "Performance analysis of the WAP protocol over GSM-SMS," in *Proceedings of the ICC*, vol. 2, pp. 467–471, June 2001.

[13] W. C. Y. Lee, "Smaller Cells for Greater Performance," *IEEE Communications Magazine*, vol. 29, no. 11, pp. 19–23, November 1991.

[14] W. C. Y. Lee, "Cellular Telephone System," U.S. Patent 4,932,049, June 1990, Patent Assigned on June 05, 1990.

[15] M. Schwartz, *Telecommunication Networks: Protocols, Modeling, and Analysis*, Addison-Wesley Pub. Co., Reading, MA, August 1986, ISBN:020116423X.

[16] D. A. Harvey and R. Santalesa, "Wireless Gets Real," *BYTE*, vol. 19, no. 5, pp. 90–96, May 1994.

[17] TIA/EIA IS-54, "Cellular System Dual-Mode Mobile Station-Base Station Compatibility Standard," Standard Document, April 1992, Telecommunication Industry Association Standard.

[18] TIA/EIA IS-95, "Mobile Station-Base Station Compatibility Standard for Dual-Mode Wideband Spread-Spectrum Cellular Systems," Standard Document, July 1993, Telecommunication Industry Association Standard.

[19] G. Keiser, *Local Area Networks*, McGraw-Hill, New York, 2nd edition, 2002, ISBN:0072393432.

[20] N. Abramson, "Multiple Access in Wireless Digital Networks," *Proceedings of the IEEE*, vol. 82, no. 9, pp. 1360–1370, September 1994.

[21] L. Kleinrock, "On Some Principles of Nomadic Computing and Multi-Access Communications," *IEEE Communications Magazine*, pp. 46–50, July 2000.

[22] J. G. Proakis, *Digital Communications*, McGraw-Hill, New York, 3rd edition, 1995, ISBN:0070517266.

[23] ETSI, "GSM Specifications, Series 01-12," Standard Document, ETSI Standard.

[24] G. Brasche and B. Walke, "Concepts, Services, and Protocols of the New GSM Phase 2+ General Packet Radio Service," *IEEE Communications Magazine*, vol. 35, no. 8, pp. 94 –104, August 1997.

[25] J. Cai and D. J. Goodman, "General Packet Radio Service in GSM," *IEEE Communications Magazine*, vol. 35, no. 10, pp. 122–131, October 1997.

[26] R. V. Nobelen, N. Seshadri, J. Whitehead, and S. Timiri, "An adaptive radio link protocol with enhanced data rates for GSM evolution," *IEEE Personal Communications*, pp. 54–64, February 1999.

[27] B. Jabbari, "Cost-effective Networking via Digital Satellite Communications," *Proceedings of the IEEE*, vol. 72, no. 11, pp. 1556–1563, November 1984.

[28] M. Rahnema, "Overview of the GSM System and Protocol Architecture," *IEEE Communications Magazine*, vol. 31, no. 4, pp. 92–100, April 1993.

[29] W. Stallings, *Data and Computer Communications*, Prentice-Hall, Englewood Cliffs, NJ, 6th edition, November 1999, ISBN:0130843709.

[30] A. S. Tanenbaum, *Computer Networks*, Prentice-Hall, Englewood Cliffs, NJ, 3rd edition, January 1996, ISBN:0133499456.

[31] C. A. Sunshine, *Computer Network Architectures and Protocols*, Plenum Publishing Corp, New York, 2nd edition, October 1989, ISBN:0306431890.

[32] D. V. Sarwate and M. B. Pursley, "Crosscorrelation Properties of Pseudorandom and Related Sequences," *Proceedings of the IEEE*, vol. 68, no. 5, pp. 593–619, May 1980.

[33] R. Prasad, *CDMA for Wireless Personal Communications*, Artech House, Norwood, MA, 1996, ISBN:0890065713.

[34] M. K. Simon, J. K. Omura, R. A. Scholtz, and B. K. Levitt, *Spread Spectrum Communications*, Computer Science Press, MD, 1985, ISBN:0881750174.

[35] E. H. Dinan and B. Jabbari, "Spreading Codes for Direct Sequence CDMA and Wideband CDMA Cellular Networks," *IEEE Communications Magazine*, pp. 48–54, September 1998.

[36] S. Verdú, *Multiuser Detection*, Cambridge University Press, Cambridge, UK, 1998, ISBN:0521593735.

[37] S. Moshavi, "Multi-User Detection for DS-CDMA Communications," *IEEE Communications Magazine*, pp. 124–136, October 1996.

[38] A. Duel-Hallen, J. Holtzman, and Z. Zvonar, "Multiuser Detection for CDMA Systems," *IEEE Personal Communications*, pp. 46–58, April 1995.

[39] E. S. Esteves and R. A. Scholtz, "Bit Error Probability of Linear Multiuser Detectors in the Presence of Unknown Multiple Access Interference," in *Proceedings of the IEEE Globecom*, vol. 2, pp. 599–603, November 1997.

[40] M. K. Simon, J. K. Omura, R. A. Scholtz, and B. K. Levitt, *Spread Spectrum Communications Handbook*, McGraw-Hill, New York, 1994, ISBN:0071369643.

[41] B. P. Lathi, *Modern Digital and Analog Communications Systems*, McGraw-Hill, New York, 2001, ISBN:0070111278.

[42] A. B. Carlson, P. B. Crilly, and J. C. Rutledge, *Communication systems: An Introduction to Signals and Noise in Electrical Communication*, Oxford University Press, New York, 1998, ISBN:0195110099.

[43] A. J. Goldsmith, *Course Reader: Advanced Topics in Wireless Communications*, Stanford University, Stanford, CA, Spring 1999.

[44] D. C. Cox, "910 MHz urban mobile radio propagation: Multipath characteristics in New York City," *IEEE Transactions on Communications*, vol. COM-21, no. 11, pp. 1188–1194, November 1973.

[45] W. C. Jakes, *Microwave Mobile Communications*, Wiley, New York, 1974, ISBN:0780310691.

[46] G. L. Stüber, *Principles of Mobile Communication*, Kluwer Academic Publishers, MA, 2nd edition, February 2001, ISBN:0792379985.

[47] S. Ramo, J. R. Whinnery, and T. Van Duzer, *Fields and Waves in Communication Electronics*, John Wiley & Sons, New York, 1993, ISBN:0471585513.

[48] N. Amitay, "Modeling and Computer Simulation of Wave Propagation in Lineal Line-of-sight Microcells," *IEEE Transactions on Vehicular Technology*, vol. VT-41, no. 4, pp. 337–342, November 1992.

[49] J. W. McKown and R. L. Hamilton, "Ray Tracing as a Design Tool for Radio Networks," *IEEE Network*, vol. 5, no. 6, pp. 27–30, November 1991.

[50] K. Schaubach, N. J. Davis IV, and T. S. Rappaport, "A Ray Tracing Method for predicting path loss and delay spread in microcellular environment," in *IEEE Vehicular Technology Conference Records*, pp. 932–935, May 1992.

[51] M. C. Lawton and J. P. McGeehan, "The application of GTD and ray launching techniques to channel modelling for cordless radio systems," in *IEEE Vehicular Technology Conference Records*, pp. 125–130, May 1992.

[52] F. Niu and H. L. Bertoni, "Path Loss and Cell Coverage of Urban Microcells in High-Rise Building Environments," in *Proceedings of the IEEE Globecom*, vol. 1, pp. 266–270, November 1993.

[53] M. D. Yacoub, *Foundations of Mobile Radio Engineering*, CRC Press, Boca Raton, FL, 1993, ISBN:0849386772.

[54] H. L. Bertoni, W. Honcharenko, L. R. Maciel, and H. H. Xia, "UHF Propagation Prediction for Wireless Personal Communications," *Proceedings of the IEEE*, vol. 82, no. 9, pp. 1333–1359, September 1994.

[55] S. Ross, *A First Course in Probability*, Prentice-Hall, New York, 6th edition, 2001, ISBN:0130338516.

[56] F. Ikegami, S. Takeuchi, and S. Yoshida, "Theoretical prediction of mean field strength for urban mobile radio," *IEEE Transactions on Antennas and Propagation*, vol. AP-39, no. 3, pp. 299–302, March 1991.

[57] M. Hata, "Empiricla formula for propagation loss in land mobile radio services," *IEEE Transactions on Vehicular Technology*, vol. VT-29, no. 3, pp. 317–325, August 1980.

[58] M. Gudmundson, "Correlation Model for Shadow Fading in Mobile Radio Systems," *Electronics Letters*, vol. 27, no. 23, pp. 2145–2146, November 1991.

[59] R. S. Kennedy, *Fading Dispersive Communication Channels*, Wiley, New York, 1969, ISBN:0471469033.

[60] S. O. Rice, "Mathematical Analysis of Random Noise-I," *Bell Systems Technical Journal*, vol. 23, no. 7, pp. 282–333, July 1944.

[61] S. O. Rice, "Mathematical Analysis of Random Noise-II," *Bell Systems Technical Journal*, vol. 24, no. 1, pp. 46–156, January 1945.

[62] S. Glisic and B. Vucetic, *Spread Spectrum CDMA Systems for Wireless Communications*, Artech House, Norwood, MA, 1997, ISBN:0890068585.

[63] Evaluation Document Concept Group Alpha-WCDMA, "Part-1: System Description; Performance Evaluation," Tdoc SMG 905/97.

[64] H. F. A. Roefs, *Binary Sequences for Spread-Spectrum Multiple-Access Communications*, Ph.D. thesis, University of Illinois, Urbana, Illinois, 1997.

[65] R. Gold, "Optimal Binary Sequences for Spread Spectrum Multiplexing," *IEEE Transactions on Information Theory*, vol. IT-13, pp. 619–621, October 1967.

[66] J. H. Lindholm, "An Analysis of the Pseudo-Randomness Properties of Subsequences of Long m-Sequnces," *IEEE Transactions on Information Theory*, vol. IT-14, pp. 569–576, July 1968.

[67] R. Gold, "Maximal Recursive Sequences with 3-valued Recursive Cross-correlation Functions," *IEEE Transactions on Information Theory*, vol. IT-14, pp. 154–156, January 1968.

[68] A. Leon-Garcia, *Probability and Random Processes for Electrical Engineering*, Addison-Wesley, Reading, MA, 2nd edition, 1994, ISBN:020150037X.

[69] V. Heeswyk, "A Delay Independent Decorrelating Detector for Quasi-Synchronous CDMA," *IEEE Journal on Selected Areas in Communications*, vol. 14, no. 8, pp. 1619–1626, October 1996.

[70] Z. A. Uzmi and M. J. Narasimha, "Maximizing System Capacity in a Sub-symbol Based DS-CDMA Multiuser Detector," in *Proceedings of the IEEE Globecom*, vol. 1, pp. 15–19, November 2000.

[71] G. L. Turin, "The Effects of Multipath and Fading on the Performance of Direct-Sequence CDMA Systems," *IEEE JSAC*, vol. SAC-2, no. 4, pp. 597–603, July 1984.

[72] M. K. Simon and M.-S. Alouini, "A unified approach to the performance analysis of digital communication over generalized fading channels," *Proceedings of the IEEE*, vol. 86, no. 9, pp. 1860–1877, September 1998.

[73] M.-S. Alouini, M. K. Simon, and A. Goldsmith, "A unified performance analysis of DS-CDMA systems over generalized frequency-selective fading channels," in *IEEE International Symposium on Information Theory*, pp. 16–21, August 1998.

[74] M.-S. Alouini and M. K. Simon, "An MGF-based performance analysis of generalized selection combining over Rayleigh fading channels," *IEEE Transactions on Communications*, vol. 48, no. 3, pp. 401 –415, March 2000.

[75] M.-S. Alouini and M. K. Simon, "Performance of coherent receivers with hybrid SC/MRC over Nakagami-m fading channels," *IEEE Transactions on Vehicular Technology*, vol. 48, no. 4, pp. 1155–1164, July 1999.

[76] R. Lupas and S. Verdú, "Linear Multiuser Detectors for Synchronous Code-division Multiple-Access Channels," *IEEE Trans. Info. Theory*, vol. 35, no. 1, pp. 123–136, January 1989.

[77] H. V. Poor and S. Verdú, "Probability of Error in Multiuser Detection," *IEEE Trans. Info. Theory*, vol. 43, no. 3, pp. 858–871, May 1997.

[78] Z. A. Uzmi and S. A. Mujtaba, "A Novel Scheme for Linear Multiuser Detection in Asynchronous DS-CDMA Systems with Frequency Selective Fading," in *Proceedings of the IEEE Globecom*, vol. 1b, pp. 981–985, December 1999.

[79] S. Verdú, "Minimum Probability of Error for Asynchronous Gaussian Multiple-Access Channels," *IEEE Transactions on Information Theory*, vol. IT-32, no. 1, pp. 85–96, January 1986.

[80] R. Lupas and S. Verdú, "Near-Far Resistance of Multiuser Detectors in Asynchronous Channels," *IEEE Transactions on Communications*, vol. 38, no. 4, pp. 496–508, April 1990.

[81] Fu-Chun Zheng and S. K. Barton, "Near-Far Resistant Detection of CDMA Signals via Isolation Bit Insertion," *IEEE Transactions on Communications*, vol. 43, no. 2/3/4, pp. 1313–1317, Feb/Mar/Apr 1995.

[82] Z. Zvonar and D. Brady, "Suboptimal Multiuser Detector for Frequency-Selective Rayleigh Fading Synchronous CDMA Channels," *IEEE Transactions on Communications*, vol. 43, no. 2/3/4, pp. 154–157, Feb/Mar/Apr 1995.

[83] H. C. Huang and S. Verdú, "Linear Differentially Coherent Multiuser Detection for Multipath Channels," *Wireless Personal Communications*, vol. 6, no. 1-2, pp. 113–136, January 1998.

[84] Qualcomm. Inc., "Wideband Spread Spectrum Digital Cellular System," Proposed EIA/TIA Interim Standard, April 1992.

[85] J. H. Winters, "Smart Antennas for Wireless Communications," *IEEE Personal Communications*, pp. 36–48, February 1998.

[86] M. C. Vanderveen, *Estimation of Parametric Channel Models in Wireless Communication Networks*, Ph.D. thesis, Stanford University, Stanford, CA, 1998.

[87] L. C. Godara, "Application of Antenna Arrays to Mobile Communications, Part II: Beam-Forming and Direction-of-Arrival Considerations," *Proceedings of the IEEE*, vol. 85, no. 8, pp. 1195–1245, August 1997.

[88] A. F. Naguib, *Adaptive Antennas for CDMA Wireless Networks*, Ph.D. thesis, Stanford University, Stanford, CA, 1996.

[89] D. H. Johnson and D. E. Dudgeon, *Array Signal Processing: Concepts and Techniques*, Prentice-Hall, Englewood Cliffs, NJ, 1993, ISBN:0130485136.

[90] V. Tarokh, N. Seshadri, and A. R. Calderbank, "Space-Time Codes for High Data Rate Wireless Communication: Performance Criterion and Code Construction," *IEEE Transactions on Information Theory*, vol. 44, no. 2, pp. 744–765, March 1998.

[91] A. Wittneben, "A New Bandwidth Efficient Transmit Antenna Modulation Diversity Scheme for Linear Digital Modulation," in *Proceedings of the ICC*, pp. 1630–1634, 1993.

[92] V. Tarokh, A. Naguib, N. Seshadri, and A. R. Calderbank, "Combined Array Processing and Space-Time Coding," *IEEE Transactions on Information Theory*, vol. 45, no. 4, pp. 1121–1128, May 1999.

[93] J. Choi, "Beamforming for the Multiuser Detector in Synchronous CDMA Systems: Approaches and Performance Analysis," *Signal Processing, Elsevier for EURASIP*, vol. 60, no. 2, pp. 195–211, July 1997.

[94] Z. Zvonar, "Beamforming for the Multiuser Detector in Synchronous CDMA Systems: Approaches and Performance Analysis," *IEEE Transactions on Vehicular Technology*, vol. 45, no. 1, pp. 205–211, February 1996.

[95] T. Kailath, A. H. Sayed, and B. Hassibi, *Linear Estimation*, Prentice-Hall, Upper Saddle River, NJ, 2000, ISBN:0130224642.